N° d'ordre :

الجمهورية الجزائرية الديمقراطية الشعبية

République Algérienne Démocratique et Populaire

وزارة التعليم العالي والبحث العلمي

Ministère de L'enseignement Supérieur et de La Recherche Scientifique

المركز الجامعي بلحاج بوشعيب عين تموشنت

Centre Universitaire Belhadj Bouchaib-Ain Témouchent

Institut de Technologie
Departement de Genie Mécanique
Laboratoire des Structures Intelligentes

THESE

Présentée pour l'obtention du **diplôme de DOCTORAT 3eme Cycle**
Domaine : Science et Technologie
Filière : Génie Mécanique
Spécialité : Energétique

Par : El MERIAH Abderrahmane

Intitulé de la thèse

Etude thermo hydraulique d'un écoulement à moyenne température

Soutenue publiquement, le / / , devant le jury composé de :

Mr. ZIADI Abdelkader	Pr	Président	Centre Universitaire BELHADJ Bouchaib/ Ain Témouchent.
Mr. ADJLOUT Lhouari	Pr	Examinateur	Université des Sciences et de la Technologie Mohamed Boudiaf - Oran
Mr. IMINE Bachir	Pr	Examinateur	Université des Sciences et de la Technologie Mohamed Boudiaf - Oran
Mme. BENSAAD Bourassia	MCA	Examinateur	Centre Universitaire BELHADJ Bouchaib/ Ain Témouchent.
Mr. NEHARI Driss	Pr	Directeur de thèse	Centre Universitaire BELHADJ Bouchaib/ Ain Témouchent.
Mr. HAMMADI Larbi	MCA	Co-Directeur	Université des Sciences et de la Technologie Mohamed Boudiaf - Oran

Année Universitaire : 2018/2019

N° Order:

الجمهورية الجزائرية الديمقراطية الشعبية

People's Democratic Republic of Algeria

وزارة التعليم العالي والبحث العلمي

Ministry of Higher Education and Scientific Research

المركز الجامعي بلحاج بوشعيب عين تموشنت

University Center of Belhadj Bouchaib-Ain Temouchent

Institute of Technology
Departement of Mechanical engineering
Smart Structures Laboratory

THESIS

Presented for graduation in **DOCTORATE 3rd Cycle**
Domain: Science and Technology
Field : Mechanical Engineering
Speciality : Energetic

By : EL MERIAH Abderrahmane

Title of the thesis

Thermo-hydraulic study of a flow at medium temperature

Publicly supported, in / / , before the jury composed of:

Mr. ZIADI Abdelkader	Pr	President	University Center of BELHADJ Bouchaib/ Ain Témouchent.
Mr. ADJLOUT Lhouari	Pr	Examiner	University of Sciences and Technology Mohamed Boudiaf - Oran
Mr. IMINE Bachir	Pr	Examiner	University of Sciences and Technology Mohamed Boudiaf - Oran
Mrs. BENSAAD Bourassia	MCA	Examiner	University Center of BELHADJ Bouchaib/ Ain Témouchent.
Mr. NEHARI Driss	Pr	Director of thesis	University Center of BELHADJ Bouchaib/ Ain Témouchent.
Mr. HAMMADI Larbi	MCA	Co-Director	University of Sciences and Technology Mohamed Boudiaf - Oran

University year : 2018/2019

Acknowledgement

I would to direct my special thank to the crew of jury

Mr. Abdelkader ZIADI,

Mr. Lhouari ADJLOUT, Mr. Bachir IMINE and Mrs. Bourassia BENSAAD

for their participation in this scientific session and taking it into account.

Also I want to thank my supervisor Mr.Pr Driss Nehari for the efforts which has made for us throughout my PhD cycle.

Without forget Mr.Pr Abdelkader Ziadi, Mr. Dr Larbi Hammadi and Mrs. Bourassia BENSAAD to the helps that has been given to us.

My thanks and appreciation to all teachers in the Mechanical Engineering Department and fellow coworkers in the Smart Structure Laboratory.

To all the academic promotions of Mechanical Engineering.

EL MERIAH

Dedication

First, I thank Allah Almighty who lights us the right way.

I would like to thank everyone who made this possible degree. I would like to acknowledge my family and parents; specially to my mother, i want to express my appreciation for your love and support.

Without forget my PhD students friends and brothers Remlaoui ahmed, Saadaoui yacine and Ikbel ayat yala.

Finally, to all my teachers who taught me to know myself along my university studies ... Thank you.

Abderrahmane. E

Abstract

This work focuses on the thermal energy storage utilization using latent heat transfer mode, different thermo physical characteristics of phase change materials (PCMs) have been discussed by their applications. A heat transfer evaluation of a shell and tube thermal energy storage (TES) unit has been carried out numerically. This devise is filled by organic material (paraffin wax) which is considered as a phase change material (PCM). Distilled water plays a role of heat transfer fluid (HTF) that flows inside the tube by constant inlet temperatures at melting and solidification moment of PCM. All the system storage is thermally isolated with the external environment. The enthalpy formulation is used to analyze the heat transfer inside 2D planar physical model during phase change process. As a result, a good agreement is found compared to the experimental results of the literature. First, the effect of geometrical parameters (tube length and shell diameter) and Reynolds number on the charging and discharging time in terms of HTF outlet temperature are investigated. The obtained results reveal that the tube length and the shell diameter are among the most influential geometrical parameters on the melting and solidification time, similarly the Reynolds number has too much effect to speed up the charging cycle. Moreover, an improved thermal storage unit is proposed which contains two phase change materials (PCMs), separated longitudinally inward the shell space and have a close melting point and different thermal characteristics. This configuration is more stable and speeds up the charging and discharging processes compared to the first unit. In addition to that, several unit positions were examined to interpret physically the thermal demeanor of the fusion process in terms of; heat transfer modes estimation, PCM melting rate, axial and radial temperatures distribution. The obtained results clarify that the TES unit inclination according to the range angles [0-90°] makes an imbalance of the natural convection in the PCM liquid fraction which contributes to create an instability and diminution of the heat transfer during the melting process. Moreover, the vertical unit state was the favorite position to the heat transfer recirculation inward the PCM.

الملخّص

هذا العمل يركز على استخدام تخزين الطاقة الحرارية باستخدام أسلوب نقل الحرارة الكامنة، وقد تمت مناقشة الخصائص الفيزيائية الحرارية لمختلف مواد متغيرة الطور (PCMs) مع تطبيقاتها. تم إجراء تقييم رقمي لانتقال الحرارة في وحدة تخزين الطاقة الحرارية (TES) للغلاف والأنبوب. يتم ملء هذه الوحدة بواسطة المواد العضوية (شمع البارافين) الذي يعتبر مادة متغيرة الطور (PCM) ، بجانب ذلك فأن الماء المقطر يلعب دورًا كسائل نقل الحرارة (HTF) الذي يتدفق داخل الأنبوب عن طريق درجات حرارة الدخول الثابتة عند عملية الذوبان والتصلب PCM، يتم عزل نظام التخزين حراريا مع البيئة الخارجية. تستخدم صيغة المحتوى الحراري لتحليل انتقال الحرارة داخل النموذج المادي المستوي ثنائي الأبعاد أثناء عملية تغيير الطور. ونتيجة لذلك ، تم العثور على اتفاق جيد مقارنة مع النتائج التجريبية للأدب. أولاً ، تم دراسة تأثير المعلمات الهندسية (طول الأنبوب وقطر الغلاف) ورقم رينولدز على زمن الشحن والتفريغ بدلالة درجة حرارة مخرج HTF .تظهر النتائج التي تم الحصول عليها أن طول الأنبوب وقطر الغلاف هما من بين أكثر المعلمات الهندسية تأثيرًا على زمن الذوبان والتصلب ، وبالمثل فإن رقم رينولدز له تأثير كبير جدًا على تسريع دورة الشحن. علاوة على ذلك، تم اقتراح وحدة تخزين حرارية محسنة تحتوي على مادتين متغيرتا الطور PCMs، مفصولان طوليًا عن منطقة الصدفة ولهما نقطة انصهار قريبة وخصائص حرارية مختلفة. هذا التكوين أكثر استقرارًا ويسرع عمليات الشحن والتفريغ مقارنةً بالوحدة الأولى. بالإضافة إلى ذلك ، تم فحص العديد من مواقع الوحدات لتفسير السلوك الحراري لعملية الاندماج من حيث: تقدير معدلات نقل الحرارة ، معدل انصهار PCM ، توزيع درجات الحرارة المحورية والشعاعية. توضح النتائج التي تم الحصول عليها أن ميل وحدة TES وفقًا لزوايا النطاق [0-90 °] يؤدي إلى اختلال التوازن في الحمل الحراري الطبيعي في جزء السائل PCM الذي يساهم في خلق عدم استقرار ونقص في نقل الحرارة أثناء عملية الذوبان. علاوة على ذلك ، كانت الوضعية العمودية للوحدة هي المكانة المفضلة لإعادة تدوير الحرارة بداخل (PCM)

Resumé

Ce travail se concentre sur l'utilisation du stockage de l'énergie thermique en utilisant le mode de transfert par chaleur latente, différentes caractéristiques thermo-physiques des matériaux à changement de phase (PCM) ont été discutées par leurs applications. Une évaluation du transfert de chaleur d'une unité de stockage d'énergie thermique (TES) à tube et calandre a été réalisée numériquement. Ce dispositif est rempli par une matière organique (paraffine) qui est considérée comme un matériau à changement de phase (PCM), ou l'eau distillée joue un rôle de fluide

caloporteur (HTF) qui circule dans le tube par des températures d'admission constantes au moment de fusion et solidification de PCM, tout le stockage du système est isolé thermiquement avec l'environnement externe. La formulation d'enthalpie est utilisée pour analyser le transfert de chaleur à l'intérieur d'un modèle physique planaire 2D pendant le processus de changement de phase. En conséquence, un bon accord est trouvé par rapport aux résultats expérimentaux de la littérature. Tout d'abord, l'effet des paramètres géométriques (longueur du tube et diamètre de la coque) et le nombre de Reynolds sur le temps de charge et de décharge en termes de température de sortie HTF sont étudiés. Les résultats obtenus révèlent que la longueur du tube et le diamètre de la coque sont parmi les paramètres géométriques les plus influents au moment de la fusion et de la solidification, de même que le nombre de Reynolds a trop d'effet pour accélérer le cycle de charge. De plus, il est proposé une unité de stockage thermique améliorée qui contient deux matériaux à changement de phase (PCM), séparés longitudinalement vers l'intérieur de l'espace de la coquille et ayant un point de fusion proche et des caractéristiques thermiques différentes. Cette configuration est plus stable et accélère les processus de charge et de décharge par rapport à la première unité. En plus de cela, plusieurs positions unitaires ont été examinées pour interpréter physiquement le comportement thermique du processus de fusion en termes de; estimation des modes de transfert de chaleur, taux de fusion du PCM, distribution des températures axiale et radiale. Les résultats obtenus clarifient que l'inclinaison de l'unité TES selon les angles de plage [0-90°] crée un déséquilibre de la convection naturelle dans la fraction liquide PCM qui contribue à créer une instabilité et une diminution du transfert de chaleur pendant le processus de fusion. De plus, l'état de l'unité verticale était la position favorite pour la recirculation du transfert de chaleur vers l'intérieur du PCM.

Contents

Nomenclature

Q	:	Heat flux	J/s
T	:	Temperature	C°
m	:	mass	Kg
Cp	:	Heat capacity	J/Kg.K
s	:	solid	----
l	:	liquid	----
dt	:	Temperature variation	----
ρ	:	density	Kg/m^3
g	:	gravitational acceleration	m/s^2
k	:	thermal conductivity	W/m.K
μ	:	dynamic viscosity	$N.s/m^2$ or Kg/m.s
S_i & S_h	:	source terms	----
u	:	velocity	m/s
i	:	i-direction	----
j	:	j-direction	----
x	:	cartesian coordinate	----
h	:	specific enthalpy	J/Kg
h_S	:	sensible enthalpy	J/Kg
H	:	total enthalpy	J/Kg
ΔH	:	enthalpy change	J/Kg
h_{ref}	:	reference enthalpy	J/Kg
T_{ref}	:	reference temperature	C°
L	:	specific enthalpy	J/Kg
γ	:	liquid fraction	----
ε	:	infinity avoidance constant	----
C	:	constant reflecting the morphology	----
$\emptyset^*$	:	Physical properties of the fluid	----
P	:	pressure	N/m^2
v	:	volume	m^3

List of Figures

Chapter 1

Chapter 2

Chapter 3

Chapter 4

Lists of Tables

Chapter 1

Chapter 4

General Introduction

General Introduction

Solar energy is among the most promising alternative sources of energy compared to traditional fossil fuels. It is available, there are no ongoing fuel costs and its environmental impact is low. Today, many solar energy systems able to convert solar radiation directly into thermal energy have been developed for low, medium and high temperature heating applications. Solar thermal power generation and solar space heating are examples of industrial applications; domestic applications include solar water heating and solar absorption refrigeration.

The exploitation of thermal solar energy has become desired currently from the companies and even members of society as a result of its diversity utilization and application in the hybrid systems such as water heating; sea water desalination and electricity production in the same cycle which makes it the most renewable energy important especially at the researchers. This demand has driven a various experts to find a solution to aim ensure the energy cycle of this source, where their first hypothesis was to create a thermal storage system in order to provide the night cycle by the energy required. The thermal energy storage (TES) appears to be the most appropriate method for correcting themismatch that sometimes occurs between the supply and demand of energy. It is therefore a very attractive technology for meeting society's needs and desires for more efficient and environmentally benign energy use.

There are mainly two types of TES systems, that is, sensible (e.g., water and rock) and latent (e.g., water/ice and salt hydrates). For each storage medium, there is a wide variety of choices depending on the temperature range and application. TES via latent heat has received a great deal of interest. Perhaps, the most obvious example of latent TES is the conversion of water to ice.

Heating systems incorporating hot storage material have a distinct size advantage over equivalent capacity chilled water units because of the ability to store large amount of energy as latent heat. TES deals with the storing of energy, usually by cooling, heating, melting, solidifying, or vaporizing a substance, and the energy becomes available as heat when the process is reversed. The selection of a TES is mainly dependent on the storage period required, that is, diurnal or seasonal, economic viability, operating conditions, and so on. In practice, many research and development activities related to energy

have concentrated on efficient energy use and energy savings, leading to energy conservation. In this regard, TES appears to be an attractive thermal application.

Phase-change materials including organic paraffins, metallic alloys and inorganic salts undergo reversible phase transformation. Due to their isothermal behavior during the melting and solidification processes, such materials can be used in such diversified applications as latent heat storage in building or thermal control in electronic modules. A latent heat storage system is preferable to sensible heat storage in applications with a small temperature swing because of its nearly isothermal storing mechanism and high storage density, based on the enthalpy of phase change (latent heat).

In a latent heat thermal storage (LHTS) system, during phase change the solid–liquid interface moves away from the heat transfer surface. In the case of solidification, conduction is the sole transport mechanism, and in the case of melting, natural convection occurs in the melt layer and this generally increases the heat transfer rate compared to the solidification process. During the phase-change process, the surface heat flux decreases due to the increasing thermal resistance of the growing layer of the molten or solidified medium. This thermal resistance is significant in most applications and especially when the organic phase-change materials are used, because the latter have rather low thermal conductivity. The decrease of the heat transfer rate calls for the usage of proper heat transfer enhancement techniques in the LHTS systems.

According to the various thermal storage unit configurations, we have used a shell and tube TES unit model which contains two coaxial cylinders. With this unit shape we have made two numerical studies in order to evaluate the thermal behavior of the storage system during phase change process at pure conduction mode. Initially we have made a comparison between unit has a paraffin wax as phase change material and another one has paraffin wax and RT60 which has a close melting points where the numerical outcomes were in terms of the heat temperature flow (HTF). Moreover, we have assess the effect of the unit inclination from the vertical to the horizontal position on the melting process of RT35 PCM that used in another literature. Our thesis is structured as fellow:

- ✓ Chapter 1 has witnessed general information about energy storage systems such as Mechanical, chemical, electrical storage systems. All this storage fields have a specific method to ensure the continuity of the energy consumption required, where each domain is different to the other in terms of cost and function duration.

- ✓ Chapter 2 presents an overview of the thermal storage systems such as sensible, latent and thermochemical storage procedure with a concept of latent heat storage thermal energy storage system (TES), and also has clarified different commercial PCMs and PCM systems used.

- ✓ Chapter 3 introduces the concept of numerical modeling when employed in thermal energy evaluations. It also describes two conventional phase change TES models, and presents a new and validated enhanced phase change model suited specifically for thermal conduction dominant phase changes. In addition to that another study has been conducted to aim assess the effect of the unit inclination on the thermal behavior of the system. Both of studies have the same numerical solving by Ansys Fluent 17 software.

- ✓ Chapter 4 includes the results obtained for the incorporation of two PCMs in the unit and compared by a single PCM, and then we have made another physical analysis about the inclination effect on the PCM melting progress in terms of melting front rate and temperatures distributions.

The mains reason that was to conduct this modest work is to ameliorate the thermal behavior of the PCMs that have a low or average melting temperature, this kind of materials feature by a weakened thermal conductivity that hinders the heat transfer swiftness inside molten PCM. As results of that, we have chosen the first way that included the adding of the other PCM inside TES unit in order to minimize the charging time of the thermal battery. The second way has comprised the effect of the unit inclination on the phase change physical phenomena of the molten PCM during charging process through a down warding HTF passage that circulate by laminar regime.

Chapter 1

Thermal Energy Storage (TES) Methods

Thermal Energy Storage (TES) Methods

1.1 Introduction

The use of renewable energy sources and increased energy efficiency are the main strategies to reduce the dependency of fossil fuels and CO_2 emissions. However, as it is known, renewable energy sources such as solar and wind energy in particular, are not only characterized by discontinuous availability but are also affected by random variations due to local weather conditions. In this scenario, the availability of energy storage would be essential allowing a large number of solutions and combination of different technologies from already existing power generation systems. Energy storage not only reduces the mismatch between supply and demand but also improves the performance and reliability of energy systems and plays an important role in conserving the energy (Arena 2016).

As to heat storing, a brand new class of materials has been introduced and developed throughout the last decades: activity materials (PCMs). The TES is not a replacement thought, and at has been used for hundreds of years. Energy storage will scale back the time or rate couple between energy offer and energy demand, and it plays a crucial role in energy conservation. Energy storage improves performance of energy systems by smoothing offer and increasing responsibleness.

1.2 Thermal Energy Storage

The thermal energy storage (TES) is a technology that stocks thermal energy by heating or cooling a storage medium so that the stored energy can be used at alters time for heating and cooling applications and power generation. TES systems are used particularly in buildings and industrial processes. In these applications, approximately half of the energy consumed is in the form of thermal energy, the demand for which may vary during any given day and from one day to next. Therefore, TES systems can help balance energy demand and supply on a daily, weekly and even seasonal basis. They can also reduce peak demand, energy consumption, CO_2 emissions and costs, while increasing overall efficiency of energy systems. TES is becoming particularly important for electricity storage in combination with concentrating solar power (CSP) plants where solar heat can be stored for electricity production when sunlight is not available.

There are three kinds of TES systems, namely:

1) Sensible heat storage that is based on storing thermal energy by heating or cooling a liquid or solid storage medium (e.g. water, sand, molten salts, rocks), with water being the cheapest option;

2) Latent heat storage using phase change materials or PCMs (e.g. from a solid state into a liquid state),
3) Thermo-chemical storage (TCS) using chemical reactions to store and release thermal energy. Sensible heat storage is relatively inexpensive compared to PCM and TCS systems and is applicable to domestic systems, district heating and industrial needs.

1.2.1 Sensible TES

Sensible heat water storages are the foremost common TES used these days for domestic functions. In sensible heat storage systems (SHS), energy is keep or extracted by heating or cooling a liquid or a solid that will not modification part throughout the method. SHS consists of a storage medium, an instrumentation (usually a tank) and body of water and outlet devices. The quantity of energy input needed to heat a TES with a smart heat device is proportional to the distinction between the ultimate and initial temperatures of storage, the mass of the storage medium and its heat capability. As Fig 1.1 shows, heat transferred to storage medium results in a linear temperature increase of that medium. From the figure, it can be ascertained that if the temperature of storage medium will increase, its energy content (internal energy) additionally will increase.

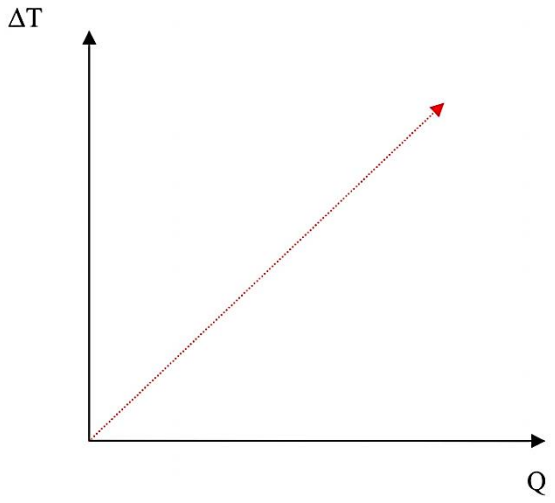

Fig 1.1 *Linear relationship between energy stored and increased temperature*

In sensible heat storage, thermal energy is stored by raising the temperature of a solid or liquid. SHS system utilizes the heat capacity and the change in temperature of the material during the process of charging and discharging. The amount of heat stored depends on the specific heat of the medium, the temperature change and the amount of storage material (Kumar and Shukla 2015).

$$Q=\int_{Ti}^{Tf} m\,Cp\,dt \qquad (1.1)$$

$$Q = m\,Cp\,(T_f - T_i) \quad (1.2)$$

Water appears to be the best SHS liquid available because it is inexpensive and has a high specific heat. However above 100°C, oils, molten salts and liquid metals, etc. are used. For air heating applications rock bed type storage materials are used (Lane 1983).

A large number of materials are available in any required temperature range therefore, the storage material is usually selected according to its heat capacity and the available space for storage. Gases have very low volumetric heat capacity and therefore are not used for sensible heat or cold storage. Table 1.1 reports some common materials used in SHS (Mehling and Cabeza 2008)

Table 1.1 *Typical materials used in sensible heat storage systems*

Material	Density [kg/m^3]	Specific heat [J/kg·K]	Volumetric thermal capacity [MJ/m^3 ·K]
Clay	1458	879	1.28
Brick	1800	837	1.51
Sandstone	2200	712	1.57
Wood	700	2390	1.67
Concrete	2000	880	1.76
Glass	2710	837	2.27
Aluminium	2710	896	2.43
Iron	7900	452	3.57
Steel	7840	465	3.68
Gravelly earth	2050	1840	3.77
Magnetite	5177	752	3.89
Water	988	4182	4.17

Water appears to be the best available liquid SHS because it is cheap and has a high specific heat and volumetric thermal capacity. However above 100 °C, materials such as oils, molten salts and liquid metals are preferred since water should be pressurized. For air heating applications rock or metal bed type storage materials are used (Sharma et al. 2009).

1.2.2 Latent TES

Latent heat storage system LHS use the energy absorbed or released during the isothermal change of materials. Latent heat is defined as the amount of heat stored in the material resulting in change of the material's phase with a slight increase or decrease in temperature. It takes place when the phase is changing either from solid to liquid, solid-solid and/or liquid to vapor and vice versa, representing the charging energy required and the discharging energy potential when used in any application. However it is important to mention, that there are many studies pointing out the potential of PCMs, but only few PCM are commercialized and suitable for technical processes (Kandalkar, Deshmukh and Kolhekar). The storage capacity of the LHS system with a solid-liquid process is given by:

$$Q = m\left[\int_{Ti}^{Tm} Cp,s\ dT + \lambda + \int_{Tm}^{Tf} Cp,l\ dT\right] \quad (1.3)$$

The first term of the second member is the sensible heat of the solid phase, λ represents the specific latent heat and, finally, the third term is the sensible heat of the liquid phase. In the Equation (1.3), Cp,s and Cp,l are specific heat of solid and liquid phase respectively and Tm is the melting temperature of the material.

A different mechanism for the storage of energy involves phase transitions with no change in the chemical composition. This is characteristic of phase transitions in elements and compounds that melt congruently, that is, the solid and liquid phases have the same chemical composition. There are also phase transitions in which both phases are solids. As an example, there is a transition between the alpha and beta phases in titanium at 882C. The alpha, lower temperature, phase has a hexagonal crystal structure, whereas the beta phase has a body-centered cubic crystal structure. Because they have different crystal structures they have different values of configurationally entropy, and there is a corresponding change in the enthalpy. In these cases, latent heat is absorbed or supplied at a constant temperature, rather than over a range of temperature, as it is with sensible heat. Isothermal latent heat systems are generally physically much smaller than sensible heat systems of comparable capacity. A further simple example is water. At low temperatures it is solid, at intermediate temperatures it becomes a liquid, and at high temperatures it converts to a gas. Thus, it can undergo two phase transitions, with associated changes in entropy and enthalpy. The Gibbs free energy, or chemical potential, is continuous, for the two phases are in equilibrium with each other at the transition temperature. (Huggins 2010)

1.2.2.1 Phase Change Materials (PCMs)

Phase Change Materials (PCMs) are ideal products for thermal management solutions. This is because they store and release thermal energy during the process of melting & freezing (changing from one phase to another). When such a material freezes, it releases large amounts of energy in the form of latent heat of fusion, or energy of crystallization. Conversely, when the material is melted, an equal amount of energy is absorbed from the immediate environment as it changes from solid to liquid as schematically shown in the Fig 1.2.

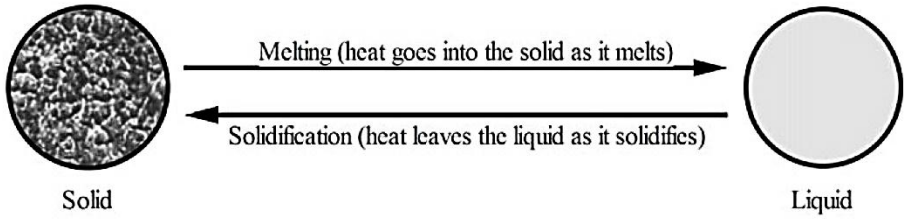

Fig 1.2 *Schematic representation of phase change process (Socaciu 2012)*

This property of PCMs can be used in a number of ways, such as thermal energy storage whereby heat or coolness can be stored from one process or period in time, and used at a later date or different location. PCMs are also very useful in providing thermal barriers or insulation, for example in temperature controlled transport. The simplest, cheapest, and most effective phase change material is water/ice. Unfortunately, the freezing temperature of water is fixed at 0°C (32°F), which makes it unsuitable for the majority of energy storage applications. Therefore a number of different materials have been identified and developed to offer products that freeze and melt like water/ice, but at temperatures from the cryogenic range to several hundred degrees centigrade.

1.2.2.2 Types of PCM

Fig 1.3 illustrates a classification of PCMs, but generally speaking PCMs can be broadly classified into two types: Organic PCMs e.g. Paraffin Wax and Inorganic PCMs e.g. Salt Hydrates (Ravikumar and Srinivasan 2008), (Socaciu 2012), (Zalba et al. 2003)

Early efforts in the development of latent TES materials used inorganic PCMs. These materials are salt hydrates, including Glauber's salt (sodium sulphate decahydrate), which was studied extensively in the early stages of research into PCMs (Patil et al. 2012),(Farid et al. 2004).

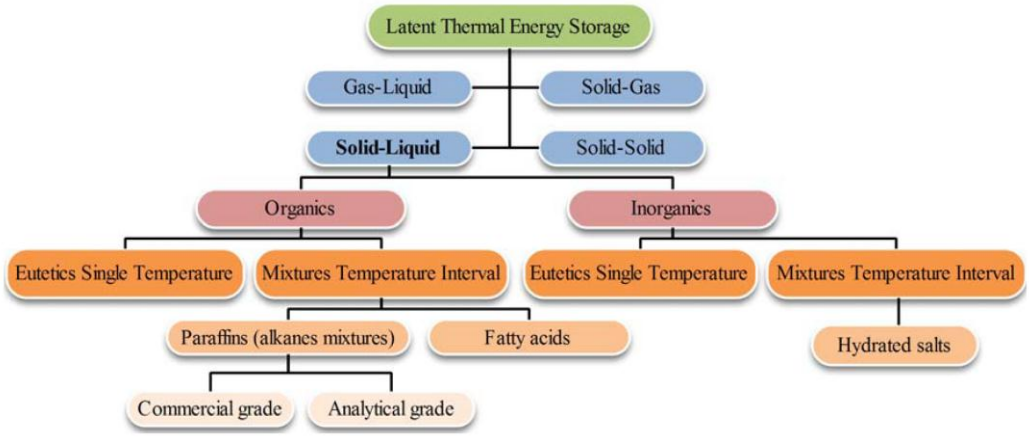

Fig 1.3 *PCMs classifications (Ravikumar and Srinivasan 2008)*

The materials which are to used for thermal energy storage unit must have a high value of latent heat and thermal conductivity. They should have melting temperature lying in the practical range of operation, melt congruently with minimum subcooling and be chemically stable. It should be low in cost, nontoxic and noncorrosive. Materials that have been studied during the last 40 years are hydrated salts, paraffin waxes, fatty acids and eutectics of organic and non-organic compounds. Phase change materials should first be selected on the basis of their melting temperature and their applications. For air conditioning purposes, materials of melting temperature below 15^{o}C is to be selected, while materials that melts above 90^{o}C are used for absorption refrigeration system. All other materials that melt between these two temperatures can be applied in solar heating and for heat load leveling applications. These materials represent the class of materials that has been studied most (Kumar and Shukla 2015)

1.2.2.2.1 Organic phase change materials

Organic PCMs are further described as paraffins and non paraffins. The main interest with organic materials is that they involve long term cyclic chemical and thermal stability without phase segregation and consequent crystallize with little or even no supercooling. Finally, they are non corrosive which is an important feature as listed previously. Sub groups of organic materials include paraffin and non-paraffin organics. Paraffin consists of a mixture of n-alkanes CH_3-(CH_2)-CH_3 into which the crystallization of the (CH_3) - chain is responsible for a large amount of energy absorption. The latent heat of fusion of paraffin varies from nearly 170 kJ/kg to 270 kJ/kg between 5^{o}C to 80^{o}C which makes them suitable for building and solar applications. Non-paraffin organic materials are the most common of the PCMs and they involved varying properties. Although fatty acids are somewhat better than other non paraffin organics, they are even more expensive than paraffins (Abhat 1983). The development of a latent heat thermal energy storage system involves the understanding of three essential subjects: phase change materials, containers materials and heat exchangers (Kumar and Shukla 2015).

1.2.2.2.2 Inorganic phase change materials

Inorganic PCMs are (mostly) used in high-temperature solar applications and one of the most reported challenges is their maintenance. At lower temperatures, they freeze; at high temperatures, they are difficult to handle (Sarbu and Sebarchievici 2018). These PCMs do not super-cool appreciably and their melting enthalpies do not degrade with cycling. The two main types are as follows:

(1) Salt hydrate. This is classified as a congruent, incongruent, and semi-congruent melting method (Sharma et al. 2009) They are alloys of inorganic salts (AB) and n (kmol) of water, forming a typical crystalline solid of general formula $AB{\cdot}nH_2O$, whose solid–liquid transition is actually a dehydration and hydration of the salt. A salt hydrate usually melts either to a salt hydrate with fewer moles of water, i.e.,

$$AB \cdot n\,H_2O \rightarrow AB \cdot m\,H_2O + (n - m)\,H_2O \qquad (1.4)$$

Or to its anhydrous form,

$$AB \cdot n\ H_2O \rightarrow AB + n\ H_2O \quad (1.5)$$

At the melting point, the hydrate crystals break-up into anhydrous salt and water, or into a lower hydrate and water. One problem with most salt hydrates is that of incongruent melting caused by the fact that the released water of crystallization is not sufficient to dissolve all the solid phase present. Due to density difference, the lower hydrate (or anhydrous salt) settles down at the bottom of the container.

(2) Metallic. This category includes the low melting point metals and their alloys. They are scarcely used in heat storage applications because of their low melting enthalpy per unit weight, even if they have high melting enthalpy per unit volume and high thermal conductivity (Ge et al. 2013). Some of the features of these materials are as follows: (i) low heat of fusion per unit weight; (ii) high heat of fusion per unit volume; (iii) high thermal conductivity; (iv) low specific heat; (v) relatively low vapor pressure.

An inorganic mixture based on an industrial by product (bischofite) was developed and characterized for its application as a PCM for low-temperature thermal energy storage (Galazutdinova et al. 2017) The most appropriate composition was established as 40 wt % bischofite and 60 wt % $Mg(NO3)2{\cdot}6H_2O$.

Thermo physical properties, specific heat capacity, cycling, and thermal stability were determined. In addition, it was shown that supercooling may be reduced by increasing the quantity of material. (Sarbu and Sebarchievici 2018)

1.2.2.2.3 Eutectics

A eutectic phase change material is a minimum-melting composition of two or more components, where each component melts and freezes in an orderly and balanced manner. (Sharma et al. 2009) Unlike salt hydrates, eutectic PCMs nearly always melt and freeze without separation.

1.2.2.3 Difficulties with PCMs

Latent heat storage is realized by storing or releasing thermal energy through the phase change process of thermal mediums which is called phase change materials (PCMs). Compared with sensible heat storage materials, PCMs have advantages of high energy storage density and thermal energy storage at a nearly constant temperature. The forms of phase change are solid-solid, solid-liquid, solid-gas and liquid-gas. Solid-gas and liquid-gas have high latent heat compared with others. However, they have great difficulty in practical thermal energy storage application, such as large volume change during solid-gas or liquid-gas phase transition.

The solid-solid phase change has the advantage of small volume change during phase transition, but its latent heat is usually much smaller than the others. Solid-liquid transformation has comparatively larger latent heat than solid-solid and smaller volume change than solid-gas and liquid-gas. Therefore, solid-liquid PCMs are commonly used in the applications of thermal energy storage. The main selection

principles of PCMs are as follows high latent heat, desirable phase change temperature, high thermal conductivity, small volume changes, little or no supercooling, good chemical stability, no chemical decomposition and corrosion resistance to container.

Because of the increasing people's living standard and decreasing energy supply, thermal energy storage can be applied in the fields of solar energy utilization, intelligent building, thermal regulating fabric, waste heat recovery, battery thermal management system, cool storage air-conditioning technology, etc. Consequently, the development of different thermal energy storage technologies will be urgently required. In the context of different applications, thermal energy storage plays different roles. And it can be used as thermal energy storage bodies or auxiliary thermal buffer for heat dissipation. Currently, PCMs are the most widely used thermal energy storage materials, and their state can be stationary or flowing when applied.

In solar energy utilization and industrial waste heat recovery, PCM store solar energy in the form of latent heat and release the stored thermal energy when necessary. This solves the problem of low density, instability and discontinuity of solar radiation with time of the day and the day of the year when utilizing solar energy, or makes a balance between the supply and demand of waste heat in time and space. Different PCMs have different types in solar energy utilization and industrial waste heat recovery. Organic PCMs are mainly used for low temperature utilization of solar energy and industrial waste heat recovery, while inorganic salt, metals and alloys are mainly used for high temperature utilization of solar energy and industrial waste heat recovery.

Application of thermal energy storage technology in solar energy utilization and 89 industrial waste heat recoveries effectively alleviates environment pollution and increases the energy utilization. However, in the field of either solar energy utilization or industrial waste heat recovery, thermal energy storage technology has not yet been put into widespread use. It has many technical problems in practical application, such as high cost, short life of energy storage system, low thermal conductivity of PCMs and energy storage material's high corrosion to equipment. Therefore, the application of thermal energy storage technology in the fields of solar thermal utilization and industrial waste heat recovery can be optimized by improving the thermal conductivity of PCMs, optimizing the energy storage system and reducing the cost in future works.

PCMs have been gradually applied in intelligent building since 1970s. The thermal energy storage technology used for intelligent building is impregnating the PCMs into construction materials, including concrete, plaster, gypsum board or wall surface coating. The PCMs can store surplus cold or heat which is produced by air conditioning, heater and ambient natural environment.

When the indoor temperature of the building is too high or too low, the PCM relieves the stored cold or heat to indoor ambient. Thereby, the indoor comfort is improved by reducing the fluctuation of

indoor temperature. In addition, the PCM can be used to store cold energy converted from electric energy by refrigerating machine in the night and then release cold energy during middle-of-the-day peak period. The application of PCMs in building has good economy for users especially in the areas where peak-valley electricity price exists. But there are three factors that restrict the wide application of PCMs in the field of intelligent building. Firstly, the reversibility and stability of PCM/construction material composites need to be improved.

Secondly, the PCM is liable to leak from construction material after long term thermal cycling. Thirdly, the thermal stress produced during the phase transformation and corrosion of PCMs leads to the destruction of the construction material. Hence the compatibility, stability and durability of PCMs and construction materials need to be further improved by packaging technology of microcapsule and improvement of compound technology of PCM and construction material (Liu and Rao 2017).

1.2.2.4 Applications of PCMs

The intermittent and dynamic nature of solar irradiance contrasts with the necessity to use solar energy in a continuous and static way, which makes the use of energy storage systems essential for solar energy applications. The most common method of thermal energy storage is the sensible heat method, which utilizes the heat capacity and the change in temperature of a given material during the process of charging and discharging. In contrast, solid–liquid PCMs absorb a lot of heat energy during phase changes without any change in temperature. This latent heat of fusion, which is large, compared to the heat capacity, is promising for thermal energy storage and heat transfer because, unlike the sensible heat storage method, the PCM storage method provides much higher storage density, with a smaller temperature difference when storing and releasing heat.

Many different PCMs have been studied in this application, including paraffin waxes, salt hydrates, fatty acids, and eutectic compounds. Depending on the applications, PCMs reselected on the basis of their melting points. For example, PCMs below 158C have been used for air conditioning applications, while PCMs that melt above 908C are available for absorption refrigeration. All other materials that melt between these two temperatures can be applied in solar energy storage applications.

Extensive efforts have been made to apply the latent heat storage method to solar energy systems. For example, a new method for satellite power testing using PCMs has been put forward by Revenger, in which a series of metal PCM cells that are liquid under high temperatures are utilized. The heat released during the relatively cold dark periods can be used to generate electricity through a thermoelectric device. This system can generate at least three times more power than batteries of comparable size, and can therefore be seen as a possible alternative to the conventional satellite solar power system that relies on batteries. Similar to addressing the solar cycle issues, several projects have been devoted to the

development of PCM systems to utilize off-peak electricity, as PCMs can melt or freeze to store electrical energy in the form of latent heat, and the energy is then available when needed. These systems, coupled with conventional active systems, can reduce the peak load. The shift of the peak load to the off-peak load will provide economic benefits, because the electricity tariff is much cheaper at night than during the day in many countries. An active floor system is effective for the off-peak storage of thermal energy. For example, a layer of paraffin wax (map. 40 8C) placed between the heating surface and the floor tiles significantly increased the heat output of the floor from 30Wm_2 to 75 Wm_2. (Hyun et al. 2014)

1.2.2.5 Characterization of PCMs

As the knowledge of the behavior of heat storage materials is very essential to design an application it is important to characterize these materials. The important characteristics of heat storage materials are their heat capacity, the thermal conductivity, the density and viscosity all in dependency on temperature. All these parameters are necessary to size a thermal storage or to develop heat exchanger to charge and discharge such storages. Simulations are also very often used to analyze applications or components of it and their interaction with the storage material. Such simulations will not be valid if the used material data is not describing its behavior in a correct way, so also for this purpose good and reliable results from the characterization are needed.

Talking about PCMs means to have a very strong relationship between temperature and the mentioned characteristics. In principle, it seems to be very easy to characterize materials since there is equipment available to determine all the needed parameter, but unfortunately, the way in which the materials will be measured influences the results.

The working activities of some groups aim to develop measurement procedures for thermal storage materials. The goal is to introduce standard procedures to make it possible to compare measurement results obtained using different measurement equipment at different laboratories.

- To determine the differences in characterization of heat storage materials for heat capacity and melting behavior, viscosity, thermal conductivity, density and cycle stability, water uptake (TCM).
- To develop measurement standards to obtain the “real” materials characteristic.

To develop a standards that lead to the “same” results also when they are determined at different laboratories (Gschwander et al. 2011).

When electronics are operated under transient conditions, increasing the thermal capacitance is a useful technique for limiting temperature increases and/or minimizing the performance requirements of a heat sink. One effective method of increasing thermal capacitance is to include a material that undergoes a change of phase at a desirable temperature. Examples of phase change that have been used in electronics cooling include solid-liquid, liquid-vapor, and solid-solid (e.g., crystalline structure to

amorphous). A solid-liquid phase change is most common for systems that require reuse of the phase change material (PCM). The thermal energy required to melt the PCM is frequently described as the latent heat of fusion. Directing the waste heat from electronics into the PCM can result in a nearly isothermal heat sink while the PCM is melting.

Selecting a PCM for use in electronics cooling requires knowing the range of expected temperatures (the melt temperature of the PCM must be high enough such that melting does not occur until needed). Unfortunately, just knowing the desired melt temperature is not sufficient to select a PCM. There are hundreds of materials that melt in a temperature range useful for electronics cooling.

However, the list of candidates becomes much smaller when issues such as material compatibility, toxicity, availability of thermal property data, and cost are considered.

Desirable characteristics of a solid-liquid PCM include high heat of fusion per volume, congruent melting and freezing characteristics, high thermal conductivity, minimal supercooling, and low thermal expansion. As is the case with most materials, searching for thermal property data will reveal some variability (and in many cases, complete thermal data doesn't exist for some compounds). The organic paraffins represent a reasonable compromise between handling and performance and are available in a wide range of melt temperatures. In general, higher melt temperature paraffins are more expensive, especially for high purity levels. Low thermal conductivity of these materials usually requires the use of an imbedded matrix material to help conduct heat into the PCM. The volume change between solid and liquid states limits their packaging density. (Yu et al. 2012). Table 1.2 presents experimental data on melting temperature, heat of fusion, thermal conductivity and density data for several organic and inorganic compounds, aromatics, and fatty acids, where Table 1.3 shows some advantages and disadvantages of PCMs. Latent TES using PCMs provides an effective way to store thermal energy from a range of sources, high storage capacity, and heat recovery at almost constant temperatures.

Table 1.2 *Measured thermo physical data of some PCMs*

Compound	Melting temperature (°C)	Heat of fusion (kJ/kg)	Thermal conductivity (W/mK)	Density (kg/m^3)
Inorganics				
$MgCl_2 \cdot 6H_2O$	117	168.6	0.570 (liquid, 120 °C) 0.694	1450 (liquid, 120 °C)
$Mg(NO_3)_2 \cdot 6H_2O$	89	162.8	(solid, 90 °C)	1569 (solid, 20 °C)
			0.490 (liquid, 95 °C)	1550 (liquid, 94 °C)
$Ba(OH)_2 \cdot 8H_2O$	78	265.7	0.611 (solid, 37 °C)	1636 (solid, 25 °C)
			0.653 (liquid, 85.7 °C)	1937 (liquid, 84 °C)
$Zn(NO_3)_2 \cdot 6H_2O$	36		1.255 (solid, 23 °C)	2070 (solid, 24 °C)
				1828 (liquid, 36 °C)
$CaBr_2 \cdot 6H_2O$	34	146.9	0.464 (liquid, 39.9 °C)	1937 (liquid, 84 °C)
			–	1956 (liquid, 35 °C)
$CaCl_2 \cdot 6H_2O$	29	115.5	–	2194 (solid, 24 °C)
			–	1562 (liquid, 32 °C)
		190.8	0.540 (liquid, 38.7 °C)	1802 (solid, 24 °C)
Organics				
Paraffin wax	64	173.6	0.167 (liquid, 63.5 ◦C)	790 (liquid, 65 °C)
			0.346 (solid, 33.6 °C)	916 (solid, 24 °C)
Polyglycol E400	8	99.6	0.187 (liquid, 38.6 ◦C)	1125 (liquid, 25 °C)
Polyglycol E600	22	127.2	–	1228 (solid, 3 °C)
			0.187 (liquid, 38.6 °C)	1126 (liquid, 25 °C)
Polyglycol E6000	66	190.0	–	1232 (solid, 4 °C)
			–	1085 (liquid, 70 °C)
Stearic acid	69	202.5	–	848 (liquid, 70 °C)
Palmitic acid	64	185.4	0.162 (liquid, 68.4 °C)	965 (solid, 24 °C)
				850 (liquid, 65 °C)
Capric acid	32	152.7	–	989 (solid, 24 °C)
			0.153 (liquid, 38.5 °C)	878 (liquid, 45 °C)
Caprylic acid	16	148.5	–	1004 (solid, 24 °C)
			0.149 (liquid, 38.6 °C)	901 (liquid, 30 °C)
Biphenyl	71	119.2	–	991 (liquid, 73 °C)
			–	991 (liquid, 73 °C)
Naphthalene	80	147.7	0.132 (liquid, 83.8 °C)	976 (liquid, 84 °C)

Table 1.3 *Advantages and disadvantages of PCMs*

	Organic (Paraffins)	Inorganic (Salt Hydrates)
Advantages	-non-corrosive; -chemically and thermally stable; -no or little sub-cooling.	-high melting enthalpy; -high density.

Disadvantages	-lower melting enthalpy; -lower density; -low thermal conductivity; -flammable.	-sub-cooling; -corrosive; -phase separation; -phase segregation, lack of thermal stability; -cycling stability.

1.2.2.6 Selection of PCMs for Latent TES

Many thermodynamic criteria must be met in order for a PCM to be considered a viable PCM. The material should have a large enthalpy of transition, i.e. latent heat. The purpose of a PCM is to store heat, so the more heat stored the better the material. However, it is important to consider if the specific or volumetric latent heat is more important for the application. Typically, space is the limiting factor, so more often the volumetric latent heat should be considered. Since density changes on phase change and as a function of temperature, the lowest density in the operating temperature range is used to calculate volumetric latent heat; at the lowest density the material takes up the most volume, which sets the size of the PCM. The material should have a high heat capacity in both the liquid and solid phase. As few applications use only the latent heat of a material, having a high heat capacity allows for more thermal storage in the sensible regime.

For the application desired, the PCM should have an appropriate melting point, T_m. If the material does not have a melting point at the application temperature, the PCM is no better than a sensible heat storage material. The material should have a congruent melting point and a small melting range. Impure materials or incongruently melting materials can have wide melting temperature ranges which complicate matters when thermally cycling. For example, stratification may occur with heavier portions settling to the bottom. A high thermal conductivity is also needed. Materials with high thermal conductivity allow quick heating and cooling to occur for good power input and output. PCMs have a few kinetic criteria that must be met as well. They should exhibit a small amount of super-cooling, which occurs when a material fails to crystallize at its melting temperature. Most materials supercool a few degrees but some PCMs can exhibit super-cooling on the order of 80 K. The crystal growth rate of the material must also be high. When the materials begin to solidify, if the rate is too slow, it is difficult to take energy out of the system. Crystal growth rate is a complicated problem that is related to a number of material properties, from viscosity to thermal conductivity. Essentially, the growth rate is dependent on the heat and mass transfer properties of the material. The chemical criteria are mostly related to safety and containment issues.

The PCM must have long term chemical stability, and be able to withstand thousands of repeated freeze-thaw cycles without degrading significantly. To minimize leakage, the material should be non-corrosive, as corrosive materials can eat away at containers. Chemical reactions between the container and PCM should be kept at a minimum. Little or no leakage should occur during the life of the PCM but in the case that there is an accident; the PCM should be non-flammable and non-toxic, neither deadly nor

harmful. Finally, there are a few economic requirements that must be considered. Since most applications require large amounts of PCM, the cost of the PCM must be low. Of course, there is some uncertainty here because of the fluctuation of market prices and the possibility that alternative manufacturing methods might be developed for the material should the demand be increased. At the very least the material should not contain any rare elements since this would unnecessarily increase the cost. The material should also be environmentally friendly. If the goal of using PCMs is to help reduce greenhouse gas emissions and save energy, then the material should not be excessively difficult to produce or cause undue environmental damage in its production. No single material can possibly fulfill all of these stringent requirements, and engineering solutions must be made to accommodate any shortfalls (Mehling and Cabeza 2008)

1.2.3 Thermo-chemical TES unit

The thermo-chemical storage (TCS) uses thermo-chemical materials (TCM), which store and release heat by recersible dothermic/exothermic reaction process (Fig 1.4 c). During the charging process, heat is applied to the material A, resulting in a separation of two parts B + C. The resulting reaction products can be easily separated and stored until the discharge process is required. Then, the two parts B + C are mixed at suitable pressure and temperature conditions, and energy is released. The products B and C can be stored separately, and thermal losses from the storage units are restricted to sensible heat effects, which are usually small compared to those of the heat of reaction. Thermal decomposition of metal oxides for energy storage has been considered (Kerskes et al. 2012). These reactions may have an advantage in that the oxygen evolved can be used for other purposes or discarded and that oxygen from the atmosphere can be used in the reverse reactions. (Sarbu and Sebarchievici 2018)

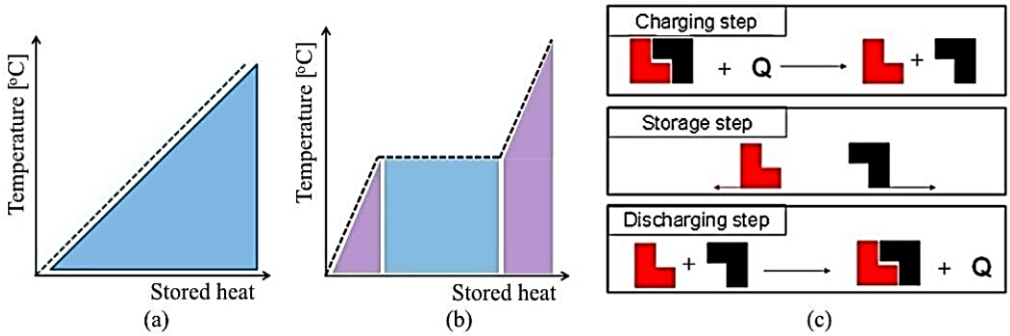

Fig 1.4 *Methods of thermal energy storage: (a) sensible heat; (b) latent heat; (c) thermo-chemical reactions (de Gracia and Cabeza 2015).*

Thermo-chemical reactions, such as adsorption (i.e., adhesion of a substance to the surface of another solid or liquid), can be used to store heat and cold, as well as to control humidity. The high storage

capacity of sorption processes also allows thermal energy transportation. Table 1.4 lists some of the most interesting chemical reactions for TES (Garg, Mullick and Bhargava 2012). While sorption storage can only work at temperatures of up to ~350 ◦C, temperatures of chemical reactions can go much higher. (Sarbu and Sebarchievici 2018)

Table 1.4 *Some chemical reactions for thermal energy storage*

Reaction		Temperature (◦C)	Energy Density (kJ/kg)
Methane steam reforming	$CH_4 + H_2O = CO + 3H_2$	480–1195	6053
Ammonia dissociation	$2NH_3 = N2 + 3H_2$	400–500	3940
Thermal dehydrogenation of metal hydrides	$MgH_2 = Mg + H_2$	200–500	3079 (heat) 9000 (H_2)
Dehydration of metal hydroxides	$CA(OH)_2 = CAO + H_2O$	402–572	1415
Catalytic dissociation	$SO_3 = SO_2 + ½(O_2)$	520–960	1235

1.2.3.1 Thermochemical Energy Storage Components and Processes

C+ heat ↔ A + B, C is the thermochemical material (TCM) for the reaction, while materials A and B are reactants. Substance A can be a hydroxide, hydrate, carbonate, ammoniate, etc. and B can be water, CO, ammonia, hydrogen, etc. There is no restriction on phases, but usually C is a solid or a liquid and A and B can be any phase. In general, a TES cycle includes three main processes: charging, storing and discharging These three processes are illustrated for thermochemical energy storage in Fig 1.5, and are described individually below:

a) Charging: The charging process is endothermic. Thermal energy is absorbed from an energy resource, which could be a renewable energy resource and/or conventional energy sources like fossil fuels. This energy is used for dissociation of the thermochemical material, and is equivalent to the heat of reaction or enthalpy of formation.

After this process, two materials (A and B) with different properties are formed that can be stored. The reaction during charging can be written as:

$$C + \text{heat} \leftrightarrow A + B \tag{1.6}$$

b) Storing: After the charging process, components A and B are separately stored with little or no energy losses. The materials are usually stored at ambient temperatures, leading to no thermal losses (except during the initial cooling of components A and B after charging). Any other energy losses are due to degradation of the materials.

c) Discharging: During this process, A and B are combined in an exothermic reaction. The energy released from this reaction permits the stored energy to be recovered. (H Abedin and A Rosen 2011) After discharging, component C is regenerated and can be used again in the cycle. The discharging reaction can be written as:

$$A + B \leftrightarrow C + \text{heat} \quad (1.7)$$

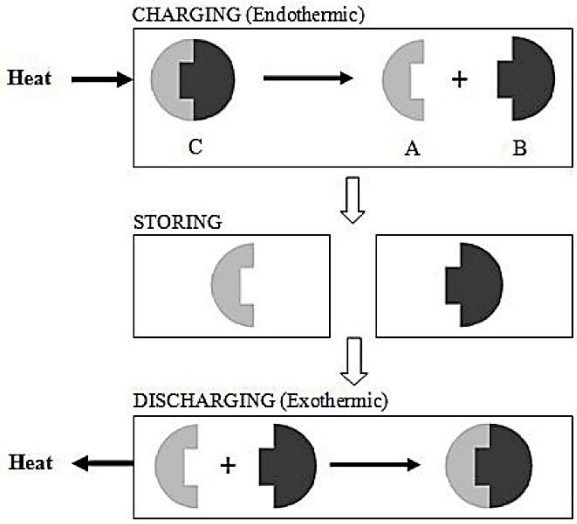

Fig 1.5 *Processes involved in a thermochemical energy storage cycle: charging, storing and discharging. (H Abedin and A Rosen 2011)*

1.3 Conclusion

While there is much work ongoing to develop PCMs with higher thermal conductivities, higher specific heats and higher latent heats, work is still needed on other aspects of PCM performance. As new eutectic blends are developed, the physical and chemical stability of these blends needs to be guaranteed. The safety of PCMs for certain applications is also an issue, as paraffins are flammable, and thus have usage concerns when applied in wallboard and other building materials, and in space based systems. Finally, the cost of most PCMs is currently preventing wider application of these materials. Pure research grade paraffins with well-defined thermal properties are too expensive for sustained usage in systems with short payback periods, and the thermal properties of less expensive blends or eutectic mixtures are not yet well defined. As shown in this part, the potential applications for PCMs for energy storage are vast, and as the development work addresses these current concerns through the creation of next generation PCMs, these materials should find wide acceptance.

Chapter 2

Literature survey

Literature survey

2.1 Introduction

As mentioned in the chapter 1, the phase change processes are encountered in the nature and in various fields of science and engineering. Accordingly, a very large body of literature exists on the variety of phase-change problems. This survey is restricted to the works relevant to the present investigation. It includes a review of the phase-change materials which are or could be used in heat storage applications, theoretical background related to mathematical modeling of phase change processes, and numerical methods used for the problems of solid-liquid phase change. Then, the existing literature on phase change in enclosed spaces is discussed. The presented works concern both transient and periodic melting and solidification. Finally, the recent studies on phase change problems are surveyed.

2.2 Brief literature

The problems of energies consumption have aggravated due to the increase of industrial, commercial and residential activities; parallelly, the current technological development suffers from the depletion of fossil energy. In such case, there is a huge need to use renewable energy sources because they represent a good solution to such problems, and among the known renewable energies, the thermal solar remains the most exploited type. As it is unstable along the time (day and night) and due to its periodic nature, we must use a thermal energy storage device in order to ensure the continuity of this energy during the time. Amongst the types of thermal storage systems, there is the thermal latent heat storage based on the use of phase change materials (PCMs) which have advantages such as high storage density. Many numerical and experimental studies were performed on the latent thermal energy storage systems. From the previous studies of (Yang et al. 2016) and (Trp, Lenic and Frankovic 2006), the thermal storage depends mainly on the HTF inlet velocity (or mass flow rate), HTF inlet temperature, and geometric parameters. Therefore, the choice of the operating conditions and geometric parameters depends on the required heat transfer rate and the time storage in which the energy will be stored or delivered according to (Trp et al. 2006). In order to explore the effect of the adequate choice of the PCM, a great effort has been made for the cases of the low and medium heat storage units especially by (El Qarnia 2009) and (Adine and El Qarnia 2009) whose have investigated the effect of using more than one PCM separated radially as clarify in the Fig 2.1 and have divergent melting temperature in order to ameliorate the system thermal performance. The combination between these materials in the shell space has revealed a high efficiency in the unit thermal behavior during charging or discharging cycle.

Especially for (El Qarnia 2009), the author has studied numerically the thermal performance of a solar latent heat storage unit (LHSU) during charging and discharging cycle by using three kinds of PCMs (n-octadecane, Paraffin wax and Stearic acid) as storage mediums. The results showed that a water production at high temperature depends on the careful selection of PCMs.

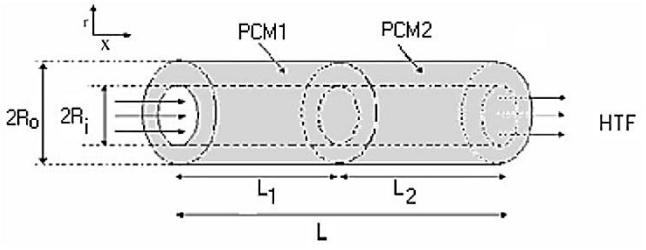

Fig 2.1 *Shell and tube TES unit has two PCMs separated radially (Adine and El Qarnia 2009)*

Recently, (Tao and Carey 2016) have investigated experimentally the effect of PCM thermo-physical characteristics on the performance of shell and tube LHSU in order to improve its performance. The results have showed that the PCM thermo-physical characteristics are the responsible parameters to improve the time and heat transfer of the system. A phase change process dominated by heat conduction in a shell and tube TES unit has been studied experimentally and numerically by solving a developed analytical model by (Kibria et al. 2014) for a medium temperature of melting. In order to evaluate the time of solidification and melting process in terms of HTF outlet temperature, various physical and geometric parameters have been conducted. The results revealed that the inlet temperature of HTF and inner diameter of tube have a strong effect on the heat exchange rate during phase change process compared to the impact of HTF mass flow rate and tube thickness. Newly, an experimental study on the vertical shell and tube latent heat thermal storage (LHTS) unit (see Fig 2.2) has been conducted by (Wang et al. 2016b), the erythritol was considered as PCM and the air has been chosen as HTF, which flows downward during charging and discharging cycle. Their results clarify that the increase of the HTF mass flow rate and inlet temperature reduces the charging process time, while the air inlet pressure has a small effect on the heat transfer inside a PCM.

A numerical study was carried out by (Tao, He and Qu 2012) for phase change thermal energy storage (PCTES) unit used in a dish solar thermal system for high temperature storage. The effect of the enhanced tubes has been studied on the behavior of PCM melting by adopting three enhanced tubes, namely dimpled tube, cone-finned tube and helically-finned tube. The results show that compared with the smooth tube, all of the three enhanced tubes could improve the PCM melting rate. A several studies have been conducted in order to create a heat storage system to ensure the continuity of the energy cycle; amongst them there is a latent heat storage system using phase change materials (PCMs) which features by a high storage density (Alva et al. 2017, Zalba et al. 2003, Sharma et al. 2009, Farid et al. 2004). As

well know that the extension of the heat transfer depends on the expansion of the heat exchange area in terms of kind and shape of the materials that transfer heat.

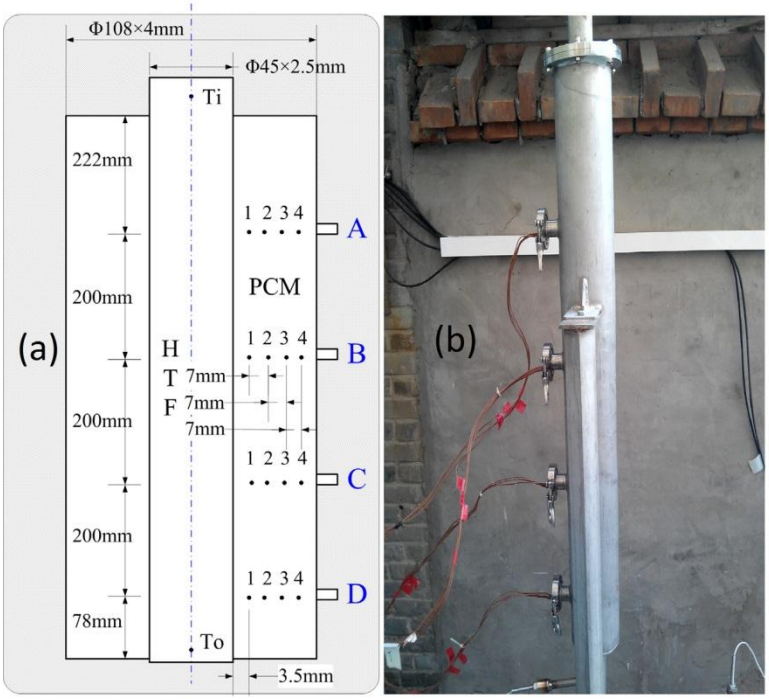

Fig 2.2 *Dimensions (a) and actual photograph (b) of the LHTS unit without insulation*(Wang et al. 2016b)

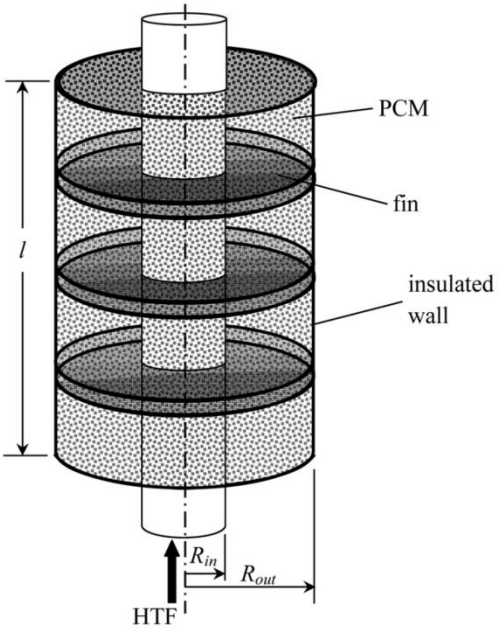

Fig 2.3 *The shell and tube TES unit proposed in the literature* (Mosaffa et al. 2012)

Concerning the geometry of the shell, a comparative study for two-dimensional solidification process was done numerically by (Mosaffa et al. 2012) between cylindrical shell (see Fig 2.3) and rectangular storages LHSU having the same volume and heat transfer area where the air was considered as HTF. On the one hand, it has found that the solidification rate of PCM in cylindrical shell is much

better and rapidly compared to the rectangular shape. On the other hand, the low thermal conductivity of PCM limits the heat transfer rate during both charging and discharging processes In order to enhance the heat transfer exchange during such processes, extended surface (fins) are used. In this sense, (Zhang and Faghri 1996) investigated numerically the effect of internal longitudinal fins. The authors have demonstrated the effectiveness of the fins to improve the heat transfer, while the melting volume fraction (MVF) can be significantly increased by increasing the thickness, height and number of fins. Different forms of latent heat thermal energy storage (LHTES) systems of medium and low melting temperature were studied numerically and experimentally by (Al-Abidi et al. 2013) and (Esapour et al. 2016) to aim enhance their thermal performances during melting process. In the same sense, the Fig 2.4 shows a numerical proposition by (Yang et al. 2016) whose have processed it in order to seek improvement the thermal behavior of vertical LHTES unit, where the effect of two HTF passage configuration by central and annular injection against the single pass configuration are compared numerically. The outcomes of the computations have clarified that both of double HTF passage heat exchanger has a small impact on the PCM melting rate compared to the single pass heat exchanger.

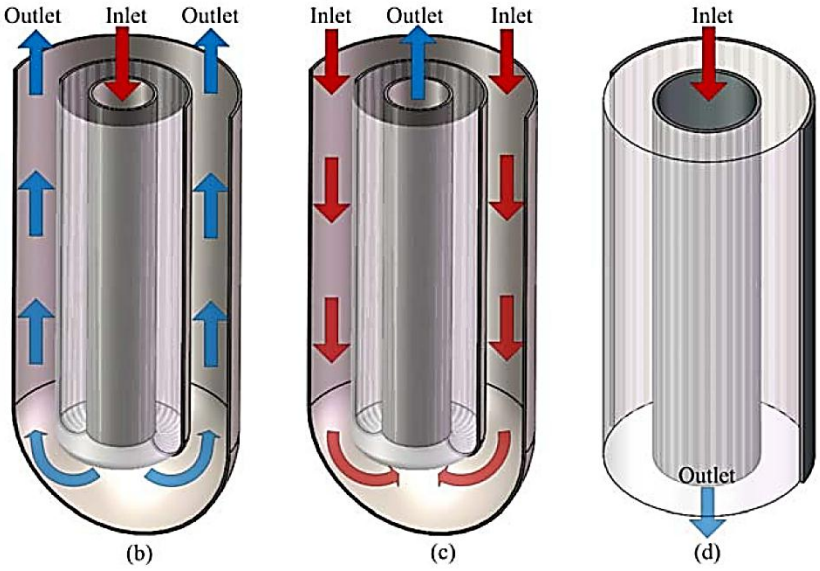

Fig 2.4 *(d) Simple and (b,c) double TES unit HTF passage (Yang et al. 2016)*

To obtain a perfect heat transfer propagation and recirculation inside the PCM, we require either to modify the outer surface of the shell or embed metal sheets by various forms inward the space shell as proposed in several investigations (Li and Wu 2015, Vyshak and Jilani 2007, Zhang and Faghri 1996, Mosaffa et al. 2012). The results of these studies revealed that the geometric parameters must be chosen carefully to obtain a short time of storage system.

As the increase of the heat transfer inside the PCM space could augment the efficiency of the storage unit, the method of including extended surfaces (fins) is used also to ameliorate the heat transfer interchange inside PCMs. This method was experimented in horizontal shell and tube TES unit by (Agyenim, Eames and Smyth 2009) through testing the unit thermal performance in standard configuration (simple unit) then in annular space embedded by circular and longitudinal fins as shown in Fig 2.5. The test outcome elucidated a positive response of the natural convection activity in the longitudinal fins case, which made the melting process be faster compared to the circular fins due to the swiftness of the heat transfer diffusion along the fins.

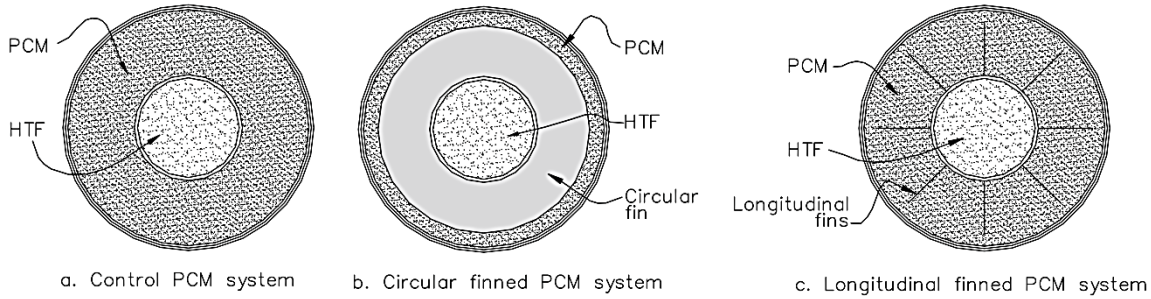

Fig 2.5 *TES unit embedded by circular and longitudinal fins (Agyenim et al. 2009)*

The difference in the melting temperature of the PCMs allows to classifying the storage units into low, medium and high storage temperature. The effects of PCM thermo-physical properties on the thermal storage performance of a shell-and-tube latent heat storage unit at high melting temperature has been inspected experimentally and numerically by various researchers. Conversely, a numerical inquiry has been conducted by (El Meriah, Nehari and Aichouni 2018) in order to assess the heat transfer demeanor between heat storage system has only Paraffin wax and other has Paraffin wax and RT60 that have convergent melting temperature and separated longitudinally inside cylindrical shell and tube TES unit as present in the Fig 2.6. There the numerical results have shown that the thermo-physical characteristics of RT60 as additive substance contribute to speed up the melting process in terms of HTF outlet temperature compared to the first one.

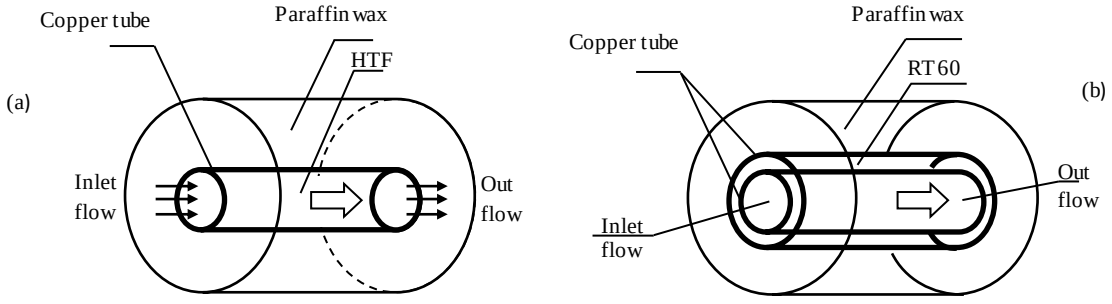

Fig 2.6 *Shell and tube TES unit has two PCMs separated longitudinally (El Meriah et al. 2018)*

Basically, the melting rate is mainly driven by the natural convection, any increase in the intensity of the natural convection currents can leads to considerable improve the PCM melting rate. Presently, numerous studies have addressed the influence of the natural convection on the efficiency of different storage units. Some experimental studies were accomplished to evaluate the natural convection mechanism inside a vertical and horizontal TES container amongst them, the experiment of (Akgün, Aydın and Kaygusuz 2007) which witnessed the use of paraffin in a vertical shell and tube with downward HTF flow while the shell outer surface was designed on cone shape from the bottom. The results analysis of PCM melting process clarified how to the PCM melted zone move under the natural convection effect, where the conical shape of the shell has helped to speed up the PCM melting from the bottom, which has contributed to facilitate the ascent and stretching of the hot PCM liquid layer into the top region. Therefore, the recirculation mechanism from the bottom to the top allows improving the buoyancy force and heat interchange inside the molten PCM as a result of the shell conical shape. Concerning the horizontal shell and tube TES unit, an experimental investigation was done by (Avci and Yazici 2013) in order to analyze the storage behavior of melting and solidification process of paraffin, which depicted that the natural convection become radially affects in the horizontal case, where the natural convection mechanism was fully different in the vertical state of the unit according to the numerical inquiry of (Seddegh, Wang and Henderson 2015) which indicates that the recirculation is more axially in the vertical shell and tube container. As a result of temperature differences within the PCM, the PCM liquid layer has begun to appear around the tube; consequently the buoyancy forces have been formed through the density gradients variation due to the gravity forces effect which contributes to drive the heat transfer recirculation from the tube to the shell inner wall, we can notice the difference in the recirculation cycle between the vertical and horizontal case, where the natural convection mechanism has a greater freedom in the vertical container compared to the horizontal status.

(Hosseini et al. 2012) have tried to clarify experimentally and numerically the effect of the buoyancy force during a melting process inside a horizontal shell and tube TES unit that use RT50 as PCM, where the water considered as HTF. These authors have noticed that the natural convection effect has been observed during the formation of the recirculation regions in the narrow melting area. In addition to that, the numerical results have showed that the increase of HTF inlet temperature allows to growing the PCM melting rate and the size of recirculation regions, which permit to reduce the total melting time to 37%. (Hosseini, Rahimi and Bahrampoury 2014) have investigated numerically and experimentally the effect of HTF inlet temperature boundary condition, were the commercial paraffin RT50 (Rubitherm GmbH) has been considered as PCM and filled in the horizontal shell annulus. The variation of HTF inlet temperature in constant flow rate 1 l/min allows to accelerate the natural convection which leads to

decrease up the total melting time to 19% and 37% when the HTF inlet temperature increases from 70 °C to 70 °C and 75 °C to 80 °C respectively, consequently the theoretical efficiency has been ameliorate from 81.1% to 88.4% and 79.7% to 81.4% in charging and discharging operation consecutively.

(Wang et al. 2016b) have tested in their study a comparison between a vertical and horizontal unit, furthermore they have injected different inlet temperatures, mass flow rates and pressure values of the HTF. This study have disclosed that the natural convection has a strong effect in the vertical position compared to the horizontal one; Moreover, the HTF inlet temperature has a great impact on the melting time compared to its pressure in constant HTF mass flow rate (HTF-air). Concerning the intermediate positions between the vertical and horizontal cases, until here we are need to explore such field in order to find the best position of the storage unit that able to give us a better thermal efficiency. A numerical and experimental investigation has been realized recently by (Kousha et al. 2017) to sake assessment the effect of a shell and tube heat storage inclination from the horizontal to the vertical case (see Fig 2.7) through the inclination value (0°, 30°, 60°, 90°) at upward HTF flow and different Stefan number of 0.47, 0.53, 0.57. This inclination has attested an influence on the melting rate and PCM temperature distribution during melting and solidification process, whereas the core and summary of the results is that a best heat storage unit position be in the tilt 30°, which gives an effectiveness in the natural convection inside PCM that leads to improve the unit thermal behaviors during phase change processes.

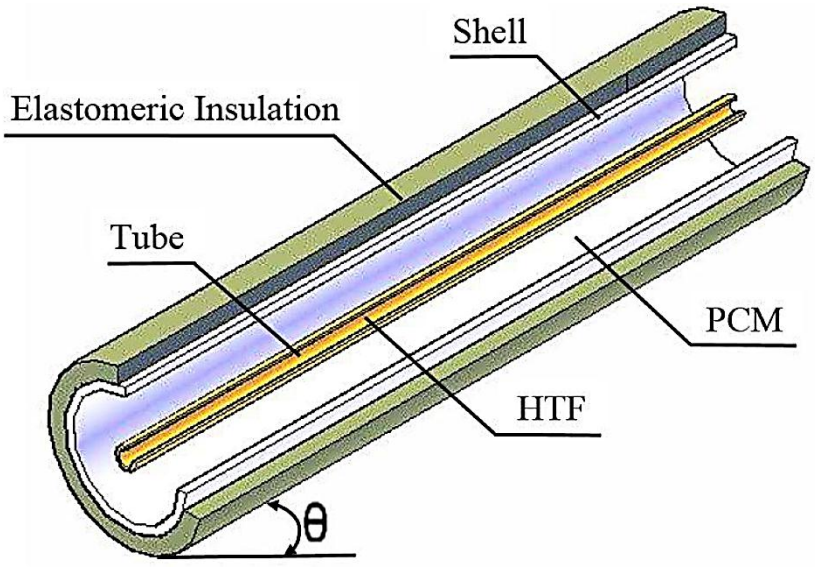

Fig 2.7 *inclined shell and tube TES unit (Kousha et al. 2017)*

The numerical studies results preciseness varies according to the tools utilized and numerical methods applied, and sometimes we have the same technical procedure but we should to diverge in the numerical prediction results. From the above literatures review, the details of the unit inclination effect on

the PCM unsteady thermal efficiency using a downward HTF passage is not clear. Among the previous works, the TES unit of (Kibria et al. 2014) could be useful to be investigated using numerical modeling, in order to improve it by proposing several configurations. In this sense, a two-dimensional and axisymmetric physical model was used to investigate the effect of the physical and geometric parameters not considered by the last authors such as the tube length, shell inner diameter and Reynolds number variation; parameters that were not considered earlier by (Kibria et al. 2014) would contribute to improve the thermal performance of the energy storage unit. Moreover, an improved thermal storage unit is proposed which contains two phase change materials (PCMs), separated longitudinally inward the shell space and have a close melting point and different thermal characteristics. Thermal energy storage based on the use of latent heat is linked inherently to the processes of solid-liquid phase change during which the heat is alternately charged into the system and discharged from it. These phenomena – melting and solidification have unique physical characteristics. They involve a moving boundary that separates two different phases which themselves may have considerably different transport properties.

The exploitation of thermal solar energy has become desired currently from the companies and even members of society as a result of its diversity utilization and application in the hybrid systems such as water heating; sea water desalination and electricity production in the same cycle which makes it the most renewable energy important especially at the researchers. This demand has driven a various experts to find a solution to aim ensure the energy cycle of this source, where their first hypothesis was to create a thermal storage system in order to provide the night cycle by the energy required. Recently, several studies have been guided to use the phase change materials (PCMs) which are considered as a stockist of the heat due to their high storage density. For more knowledge and understanding about this materials (Zalba et al. 2003), (Kenisarin 2010), (Sharma and Sagara 2005) (Cárdenas and León 2013) have been accomplished a literature review concerning the multi kinds of chemical substances that have a high heat interchange in melting and solidifying at certain temperature estimated according to their thermo-physical characteristics, where could employed them in various building and storage systems applications by different heat transfer technical modes. This materials can be stored in several containers forms (Castro, Selvam and Suthan 2016), where phase change physical phenomena of these materials is unified in all tanks shapes, but it differs in terms of numerical and mathematical analyze procedure as mentioned in the literatures(Dutil et al. 2011) (Agyenim et al. 2010).

In the latent heat storage systems, the study objectives vary from researcher to another, some of them focuses to enhance the thermal behaviors of the thermal energy storage (TES) unit by mean of aggrandize the heat transfer area inside phase change material (PCM) as the case of the literature(Al-Abidi et al. 2013), whose have endeavored diligently to examine numerically the effect of embedded longitudinal fins in terms of their lengthiness, thicknesses, numbers and placements inside horizontal

cylindrical triplex tube heat exchangers which shown in the Fig 2.8 to aim appraise the steps of melting process in the presence of the natural convection. Via the combining of gambit and fluent software, the simulations results revealed that all those studied parameters have positive impact on the natural convection vicissitude which contributes to accelerate the PCM melting process except the thicknesses fins has insufficiency to improve the thermal behaviors of the unit.

(Longeon et al. 2013) have estimated experimentally and numerically the thermal performance of a vertical shell and tube TES unit with laminar regime of ascending and descending water flow in both of charging and discharging process. The analysis of 2D typical visualization was extracted from Fluent Computational Fluid Dynamics (CFD) solver where the HTF top injection has shown during the charging process an acceleration in the temperature transition along the tube which leaded to expedite the buoyancy force moves on the radial and axial directions as a result of the molten PCM area stretching near the HTF inlet flow, and this is antithesis with what happened in the HTF bottom injection by reason of the axial temperature distribution loss which hinders the recirculation cycle due to slowing of the extend molten PCM area from the upper PCM region, but on the one hand of discharging cycle both of HTF injection paths have clarified nearly an evenness in the PCM thermal behavior analysis.

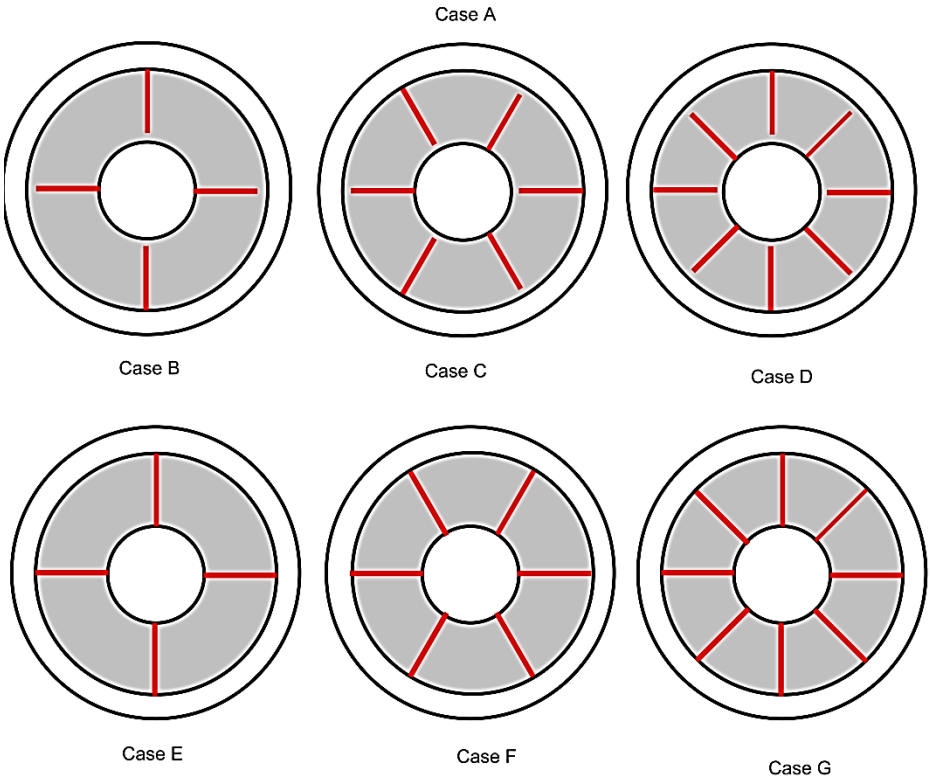

Fig 2.8 *Physical configurations of different fins positions. (Al-Abidi et al. 2013)*

The same idea was adopted numerically by (Li and Wu 2015) in order to assess the charging and discharging time of vertical shell and tube TES unit with and without longitudinal fins, whilst a several

heat transfer fluids (HTFs) and PCMs were experimented. Regardless of change the PCMs and HTFs, the existence of the longitudinal fins within the space annular helps to split up the PCM into a long portions shape which allows to extend the heat exchange area inside it and accelerates the heat transfer by pure conduction along the HTF tube and hence the first PCM liquid layer will be created swiftly and confer it the penetration ability to the top from the middle and sides of the PCM. The result of this design has led to reduce the charging and discharging processes about 14% from the original time of the unit without fins. Based on the shell and tube thermal energy storage configuration, four different heat storage systems have been tested experimentally in order to compare the thermal performance between each one Using RT58 as unified PCM. There (Gasia et al. 2017) have analyzed the heat transfer exchange between PCM and HTF by four heat storage kind as two models with fins and others without it as shown in Fig 2.9. The typical analysis have clarified that the charging process be much faster in the first two heat storage style compared to the last two as a result of the disparity in the heat transfer exchange area extension between them by 9.4 times.

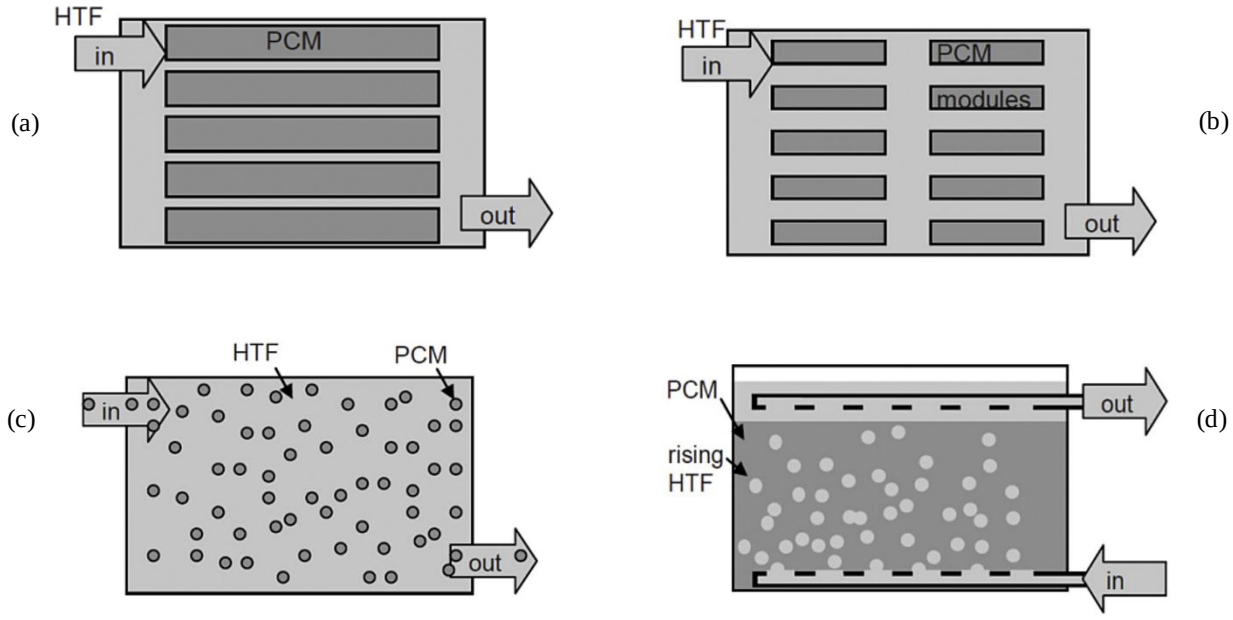

Fig 2.9 *Heat exchangers thermal energy storage units with (fins) direct contact (a), (b) and indirect heat exchange (c), (d) (Gasia et al. 2017)*

Away from the heat transfer area modification to improve a storage system, (Akgün et al. 2007) were someone of the researchers whose have been interested to improve the natural convection mechanism inside a vertical shell and tube phase change thermal energy storage (PCTES) unit. Their experimental investigation has attested a change in the unit outer surface shape from the cylindrical to the conical form which converged into the bottom with angle inclination 5° (see Fig 2.10). A three kinds of

paraffin have uneven melting points were filled inside the annular space as PCM, different HTF inlet temperatures and mass flow rates effect was tested in both of configurations. During charging process, the conical unit has minimized 20% of total melting time which been acquired in cylindrical unit as consequence of coning the lowest outer surface, which helps to facilitate the molten PCM liquid fraction buoyancy. A combined experimental and numerical enquiry has been scrutinized by (Assis et al. 2007) on spherical heat storage system filled by PCM (Rubitherm 27 GmbH) and was treated externally as isothermal as illustrate in the Fig 2.11. The purpose of this inspection was to evaluate the thermo-geometric parameters effect on the PCM melting demeanor in accordance with several shell diameter variation and different dimensionless numbers values. The computational results have been analyzed graphically according to Fluent 6.0 software simulator, which illustrated that smallest shell diameter has a quickest melting time, while Stefan number rise has shown the same outcome with all shell diameter values proposed in terms of PCM liquid fraction advancement.

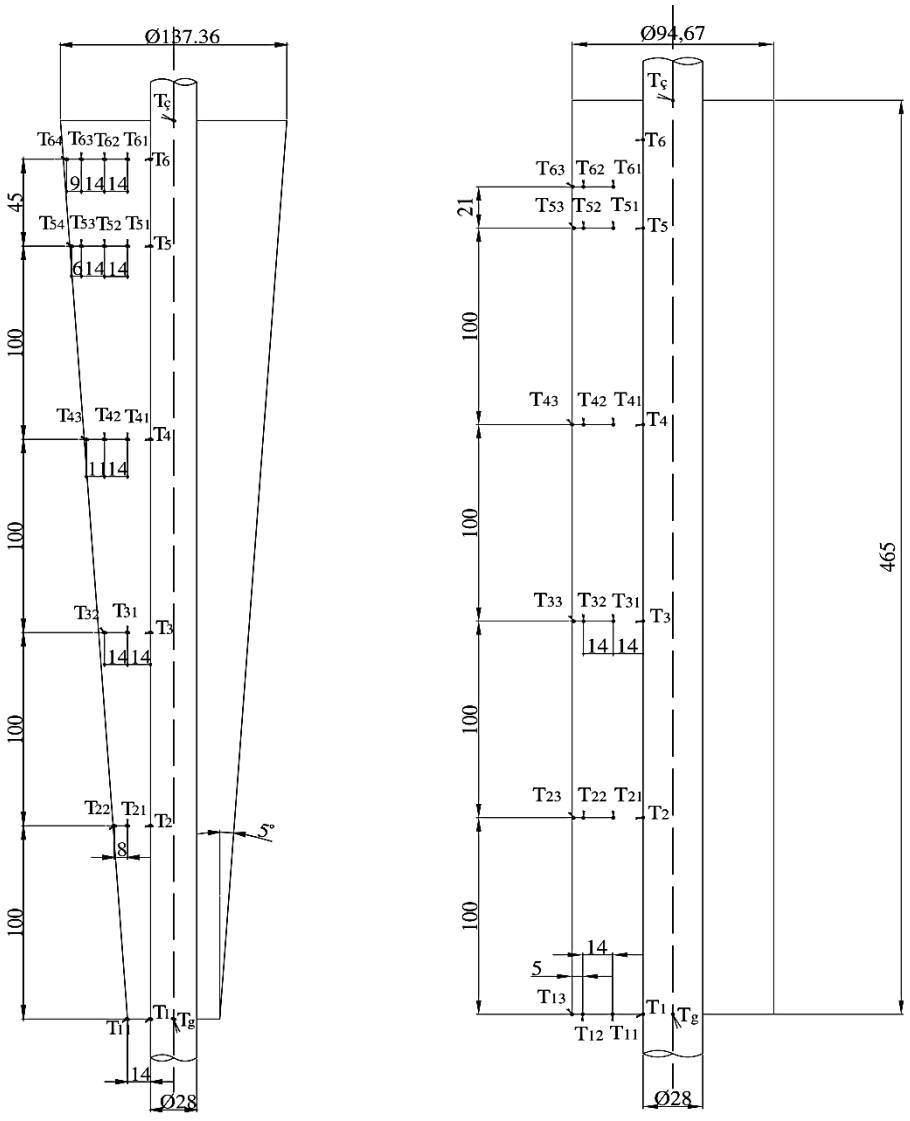

Fig 2.10 *Conical and cylindrical shell of TES unit (Akgün et al. 2007)*

The natural convection became the most physical phenomenon influential on the heat transfer exchange during PCM melting process. In order to enhance the heat transfer rate of vertical shell and tube latent heat storage (LHTS) unit, (Wang, Wang and He 2016a) have examined experimentally the impact of several HTF inlet temperatures and mass flow rates on charging and discharging time with downward HTF flow, where the increment of each parameter was a result to minify the storage system nearly 33.7% and 22.9% respectively, besides that the HTF inlet pressure influence was also performed and has shown a small effectiveness on the heat transfer rate. In addition to that, the recirculation mechanism has been compared between a vertical and horizontal position of the unit, while the optimum case to improve the natural convection effect was present in the vertical place.

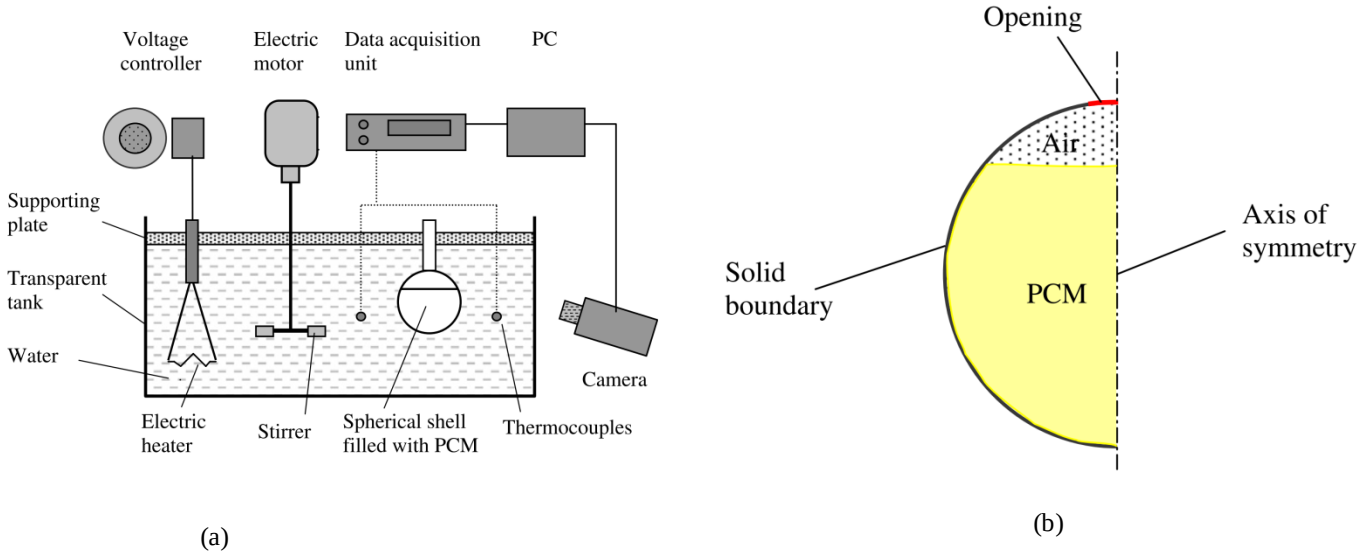

Fig 2.11 *Spherical heat storage system in experimental (a) and numerical (b) study (Assis et al. 2007)*

From the antecedent literature, the heat transfer appraisal was not clear in the confined angles between the vertical and horizontal unit status, consequently there was an experimental study has been carried out by (Kousha et al. 2017) to aim analyze this physical problematic in horizontal shell and tube TES unit which has been assumed that it is in the initial case. The PCM RT35 filled in the annular space which has melted via hot water circulation by laminar regime. The unit inclination effect on the storage system thermal behavior has been resolved numerically during charging and discharging process in the tilt range [0-90°] with various Stefan numbers according to the up warding HTF flow. At several Stefan numbers, the melting process has been clarified a greatest PCM temperature value in the horizontal case compared to the others angles at the first half of melting time, whilst the situation has reversed during the second half time in which the slightest inclination value became possessed an abundant PCM temperature versus the inclination values that comes after, where all inclination positions have shown a greatest PCM temperature compared to the initial case and this transition was a consequence of the natural convection

activity along the PCM volume from the top region to the bottom. Another experimental and numerical inspection has been conducted about the natural convection role to enhance the thermal behavior of the vertical shell and tube latent heat thermal energy storage (LHTES) system used a PCM has a middle storage density. There (Seddegh et al. 2017) have explained a detailed physical depiction of the PCM phase change during charging and discharging cycle, these processes have been realized via downward HTF flow of laminar regime, accordingly to that a contradictory moves in solid-liquid interface have been observed between the melting and solidification process in which a laminar recirculation has been formed inside PCM liquid from the top to the bottom, this cycle allows to accelerate the mushy zone appearance around the HTF tube which helps to decrease the melting time, sequentially the discharging cycle has attested a solid layer creation from the circumference of the shell and tube sides due to the recirculation strength which mediate the PCM liquid volume, consequently both of phase change process have been dominated by conduction and convection heat transfer mode.

(Sokolov and Keizman 1991) developed an attractive PCM application for hot water heating. The system contains a solar pipe consisting of two concentric pipes with the space between them filled with PCM (Fig 2.12). Solar radiation is directly absorbed on the outer surface and then transmitted to the PCM, where it is stored as sensible and latent heat. During energy release, heat is exchanged between a water flow through the inner tube and the PCM storage, and hot water is delivered at the discharge of the solar pipe. In this system, direct solar radiation absorption onto the PCM container and direct heating of water eliminate the need for energy transport media. Some advantages of the system include :

- simple construction; efficient and compact latent heat storage; elimination of expensive components such as a water tank, pump, and control devices; suitability of the system for modular construction and installation; protection against freezing.

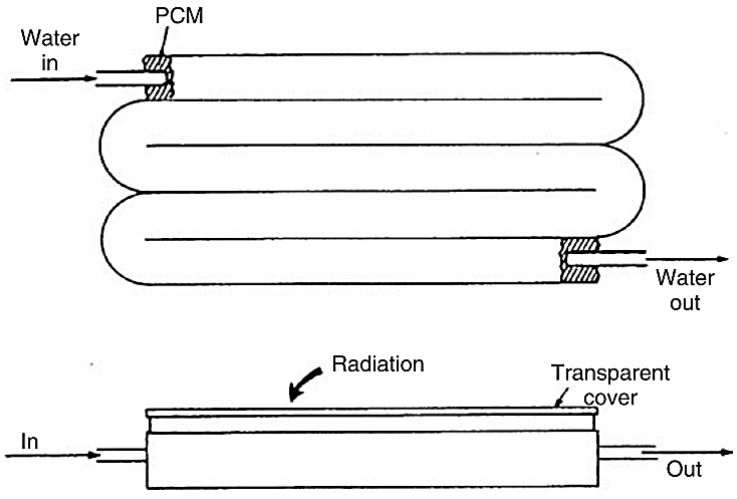

***Fig 2.12** A solar TES pipe using a PCM (Sokolov and Keizman 1991)*

2.3 Conclusion

The behavior of the moving interface is such that its instantaneous position is unknown a priori and must be determined as a part of the solution. The other common features include convection in the melt, volume change due to phase change, melting/solidification extending over a temperature range, and sub-cooling at solidification. This chapter aims to provide an overview of the modern approaches to phase change material (PCM) modeling. Specifically, we focus on the shell and tube model. In which there exist distinct solid and liquid phases separated by a region defined as the solid–liquid interface, or melting/solidification front. And we have mentioned different previous literatures that has a relation with hot thermal energy storage system, where a several numerical and experimental investigation have been conducted in order to ameliorate the thermal behavior of the phase change phenomena.

Chapter 3

Mathematical and Numerical modeling

Mathematical and Numerical modeling

3.1 Introduction

The transition from a partial derivative problem to a discrete problem is based on the classical methods of numerical analysis. There are three main methods to formulate a continuous problem in discrete form, finite difference method, finite element and finite volume. The method used by the code "FLUENT" is that of the finished volumes. The workstation used for these simulations is a computer HP Z840. The discretization of the equations presented in this chapter, reflecting the phenomenon of conduction-convection heat transfer, makes it possible to transform these differential equations into a system of algebraic equations. Several discretization methods are currently used such as: finite volume, finite difference and finite element method, etc... According to that, we can say that the progress of any simulation has been driven following the steps shown in the Fig 3.1

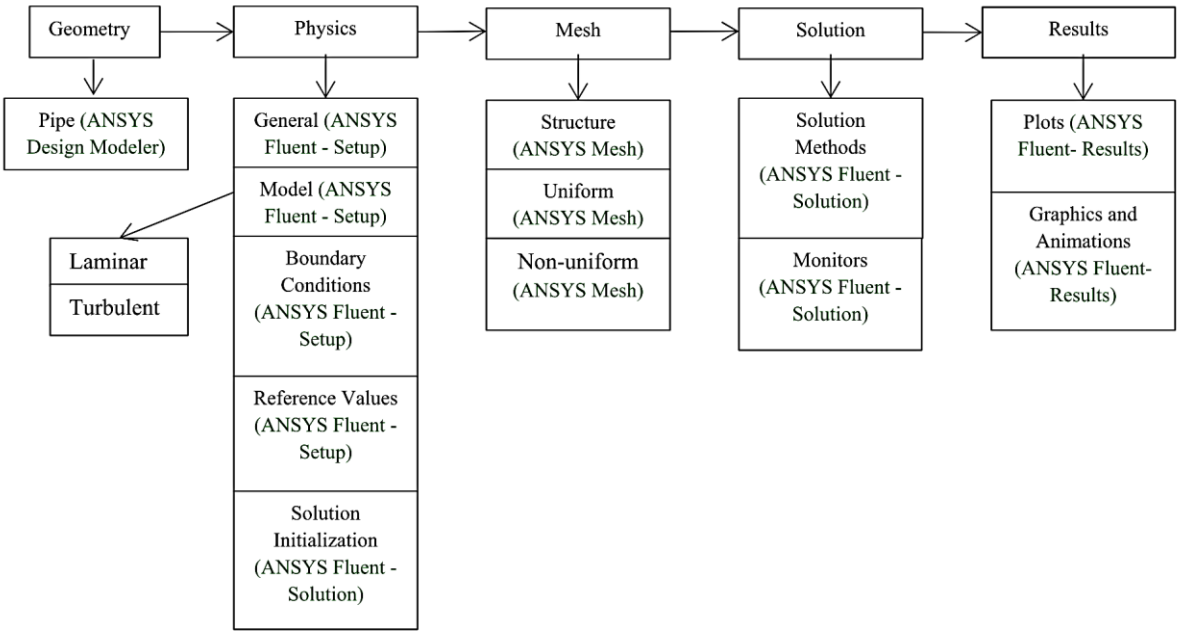

Fig 3.1 *Ansys Fluent steps simulation*

3.2 Finite difference methods

This is the oldest method; the fundamental principle of this method is the field of study mesh knots whose finesse can give an approximation of the contours of the field. Then, by applying the development in each node of the mesh, which makes it possible to obtain a number of algebraic equation equal to the

number of the values of unknowns of the studied magnitudes.

3.3 Finite element methods

The method consists of meshing the space into elementary regions in which the desired quantity is represented by a polynomial approximation. The mesh may consist of triangles or rectangles whose vertices are searched for volumes of the unknown assuming that, in this area, the unknown varies linearly depending on the coordinates. Such a method therefore requires meshing all the studied space. It leads to large computer memory sizes and long computing times that often require workstations for solving industrial problems.

3.4 Finite volume methods

The finite volume method is characterized by its advantage in satisfying the conservation of mass, momentum and energy in all finished volumes as well as in the whole field of computation. It facilitates the linearization of nonlinear terms in conservation equations such as the source term for example. The method involves sharing the compute domain into multiple volumes, where each volume surrounds a node.

3.5 Mathematical model

3.5.1 Governing equations

The phase change physical phenomena is expressed and governed by unsteady continuity, momentum and energy equations as follows:

The continuity:

$$\frac{\partial}{\partial x_i}(\rho u_i) = 0 \tag{3.1}$$

The momentum:

$$\frac{\partial}{\partial t}(\rho u_i) + \frac{\partial}{\partial x_i}(\rho u_j u_i) = \mu \frac{\partial^2 u_i}{\partial x_i \partial x_j} - \frac{\partial p}{\partial x_i} + \rho g_i + S_i \tag{3.2}$$

The energy:

$$\frac{\partial}{\partial t}(\rho h) + \frac{\partial}{\partial x_i}(\rho u_i h) = \frac{\partial}{\partial x_i}\left(k \frac{\partial T}{\partial x_i}\right) + S_h \tag{3.3}$$

Where ρ is the density, g represents the gravitational acceleration, k denotes the thermal conductivity, μ is the dynamic viscosity, S_i and S_h are the source terms, u_i is the velocity component in the i-direction, x_i is a Cartesian coordinate and h is the specific enthalpy.

The sensible enthalpy h_S is given by:

$$h_s = h_{ref} + \int_{T_{ref}}^{T} C_p \, dT \tag{3.4}$$

And the total enthalpy, H is defined as

$$H = h_s + \Delta H \tag{3.5}$$

Where $\Delta H = \gamma L$ is the enthalpy change due to the PCM phase change, h_{ref} is a reference enthalpy at the reference temperature T_{ref}, C_p is the specific heat, L is the specific enthalpy of melting (liquid state) and γ is the liquid fraction during the phase change which occur over a range of temperatures $T_{solidus} < T < T_{Liquidus}$ defined by the following relation 3.6. (a, b, c):

If:

$$\begin{cases} T < T_{solidus} \text{(solid state)}: \gamma = \dfrac{\Delta H}{L} = 0 & \text{(a)} \\ T_{solidus} < T < T_{liquidus} \text{(Mushy state)}: \ 0 < \gamma = \dfrac{\Delta H}{L} < 1 & \text{(b)} \\ T > T_{liquidus} \text{(liquid state)}: \gamma = \dfrac{\Delta H}{L} = 1 & \text{(c)} \end{cases}$$

The source terms S_i and S_h are given by

$$S_i = -A(\gamma) u_i \frac{C(1-\gamma)^2}{\gamma^3 + \varepsilon} \tag{3.7a}$$

$$S_h = \rho L \frac{\partial \gamma}{\partial t} \tag{3.7b}$$

Where $A(\gamma)$ is defined as the "porosity function" which governs the momentum equation based on Carman-Kozeny relationship for flow in porous media. The function reduces the velocities gradually from a finite value of 1 in fully liquid to 0 in fully solid state within the computational cells involving phase change. The epsilon $\varepsilon = 0.001$ infinity avoidance constant due to division by zero and C is a constant reflecting the morphology of the melting front where $C = 10^5$.

3.6 Boundary conditions

The full set of boundary conditions of the first and second study which imposed on the flow field and the thermal boundary conditions imposed on the temperature field are shown in the Fig 3.2 and 3.3. These two shell and tube physical models are shown as general cases of the heat storage system boundary conditions modelization, where usually the PCM is filled inside the annular space of the unit that considerate insulate (Adiabatic wall) with the external environment. Further the HTF has entered inward the inner tube by mass flow rate or generally is conditioned by inlet velocity (gas, liquid) , where the second side of the tube (outlet) is chosen as outflow. The contact between PCM and HTF generally be

with interface line in order to ensure the coupling heat transfer from the HTF to the PCM. The best method to simulate this physical model is by axisymmetric mode, in order to simplify the simulation of the phase change problem, where this way allows us to minimize the maximum total time of the convergence also eliminate the simulator energy losing.

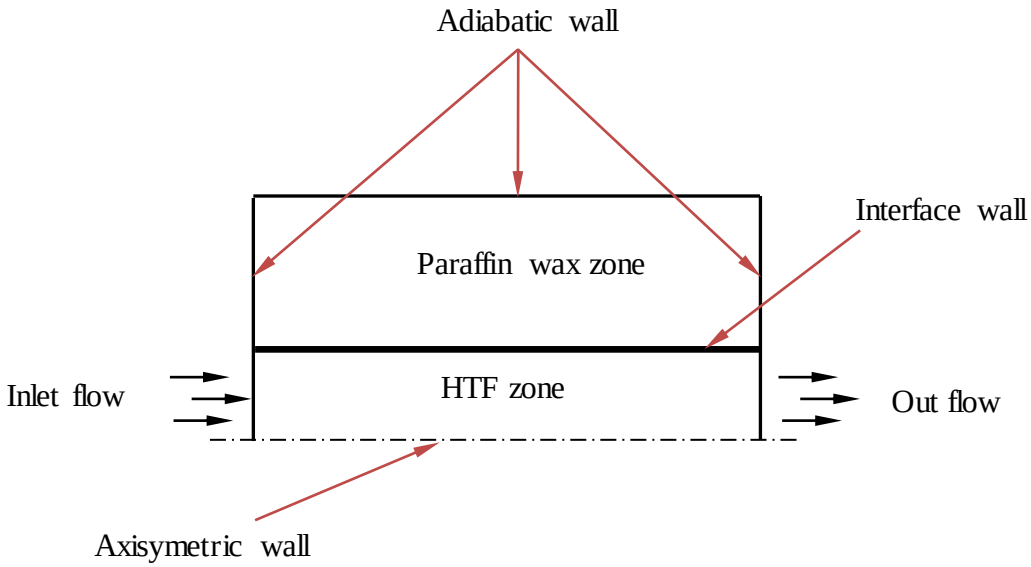

Fig 3.2 *Boundary condition of the first study*

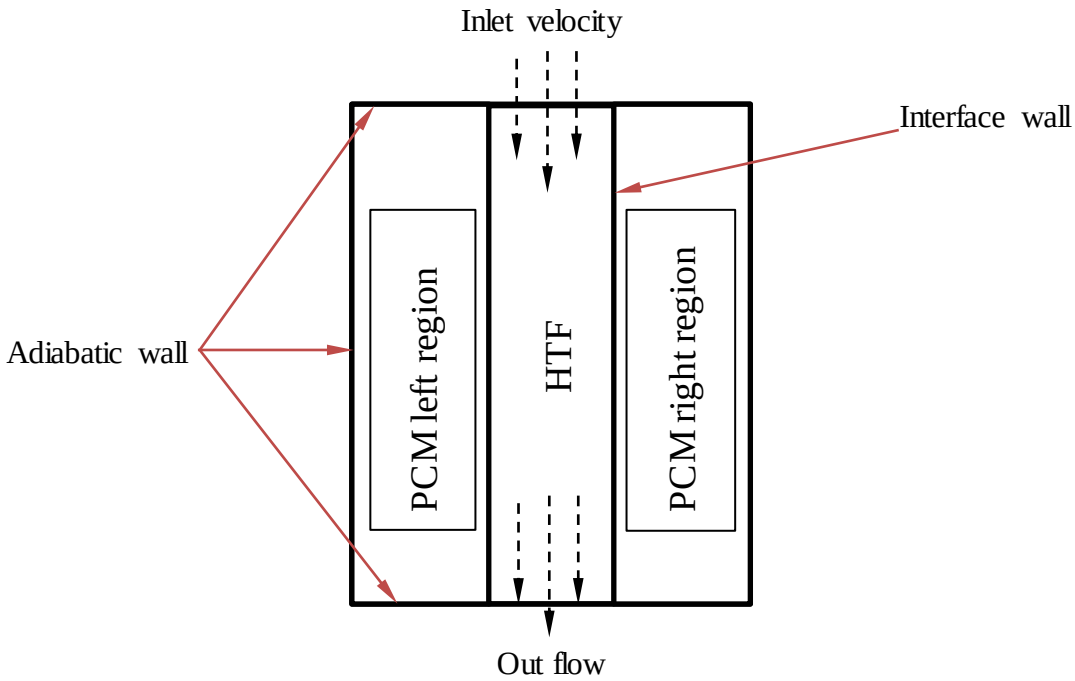

Fig 3.3 *Boundary condition of the second study*

3.7 Grid mesh

The calculation code Ansys Fluent in version 17 processes several types of structured, unstructured

or hybrid meshes. A structured mesh is generally composed of quadrilateral meshes in two dimensions (2D or surface mesh) and hexahedral in three dimensions (3D or voluminal mesh), while an unstructured mesh will be composed of quadrilateral or triangular meshes in 2D and hexahedral or tetrahedral in 3D. In a hybrid mesh the meshes close to the walls are quadrilaterals in 2D and hexahedrons in 3D and the meshes of the remainder of the domain are triangles in 2D and tetrahedrons in 3D. In close wall, it is necessary to have the smallest mesh possible to model well the flows at this place, this particularity is all the more important in turbulent regime, it is called (inflation). In 3D, the links between hexahedra and tetrahedra are prisms or pyramids. Fig 3.4 shows the different types of mesh used by our code.

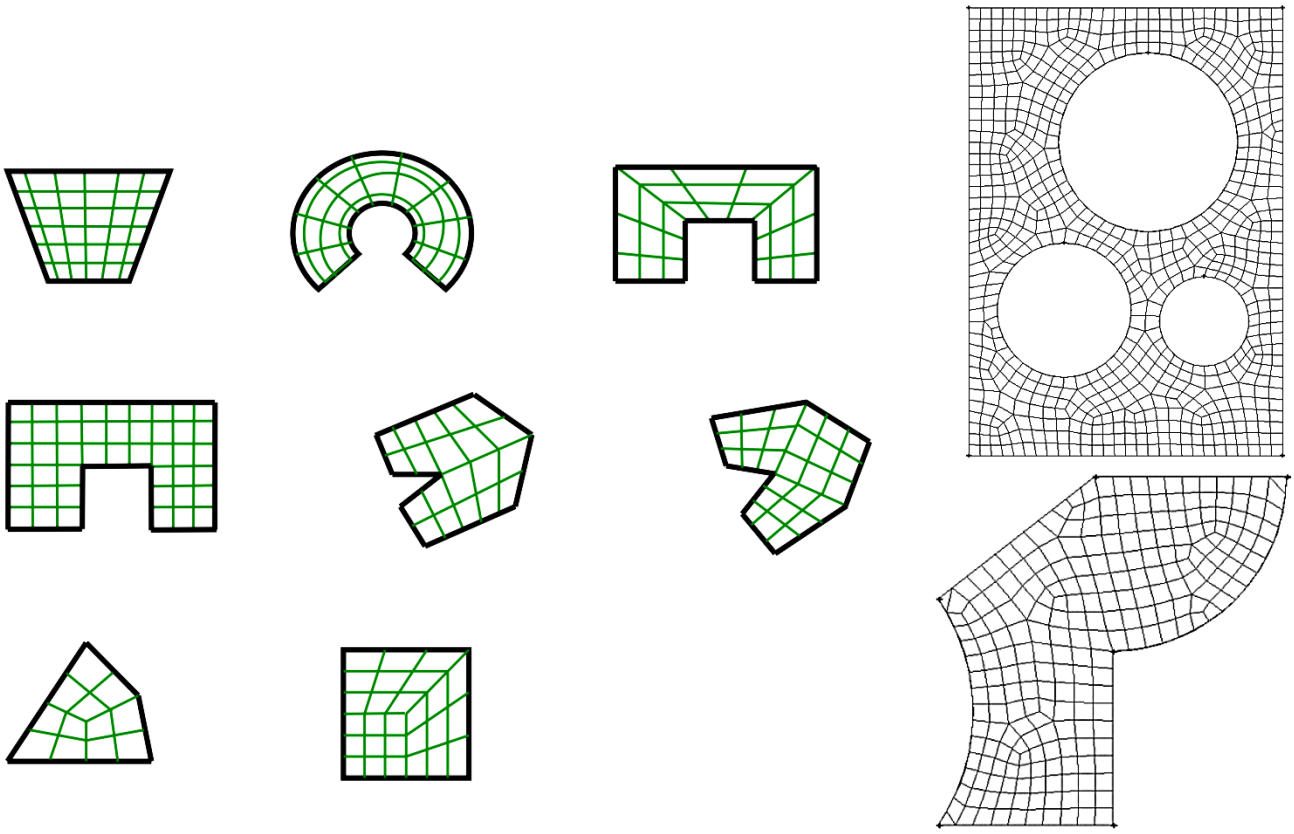

***Fig 3.4** Different typical grid*

The Ansys Fluent manual indicates that when geometries are complex or the range of length scales of the flow is large, a triangular/tetrahedral mesh can be created with far fewer cells than the equivalent mesh consisting of quadrilateral/hexahedral elements. This is because a triangular/tetrahedral mesh allows clustering of cells in selected regions of the flow domain. Structured quadrilateral/hexahedral meshes will generally force cells to be placed in regions where they are not needed. Unstructured quadrilateral/hexahedral meshes offer many of the advantages of triangular/tetrahedral meshes for moderately-complex geometries. A characteristic of quadrilateral/hexahedral elements that might make them more economical in some situations is that they permit a much larger aspect ratio than

triangular/tetrahedral cells. A large aspect ratio in a triangular/tetrahedral cell will invariably affect the skewness of the cell, which is undesirable as it may impede accuracy and convergence. Therefore, if you have a relatively simple geometry in which the flow conforms well to the shape of the geometry, such as a long thin duct, use a mesh of high-aspect-ratio quadrilateral/hexahedral cells. The mesh is likely to have far fewer cells than if you use triangular/tetrahedral cells. Converting the entire domain of your (tetrahedral) mesh to a polyhedral mesh will result in a lower cell count than your original mesh. Although the result is a coarser mesh, convergence will generally be faster, possibly saving you some computational expense. In summary, the following practices are generally recommended:

- For simple geometries, use quadrilateral/hexahedral meshes.
- For moderately complex geometries, use unstructured quadrilateral/hexahedral meshes.
- For relatively complex geometries, use triangular/tetrahedral meshes with prism layers.
- For extremely complex geometries, use pure triangular/tetrahedral meshes.

3.8 Numerical Solving

In order to solve the governing equations during melting process, a commercial code FLUENT 17 has been used based on: SIMPLE algorithm, second order implicit scheme for the time and second order upwind for the space. The local criterion for numerical convergence, i.e. the maximum relative difference between two consecutive iterations is imposed less than 10^{-6}. The numerical calculations were performed for the transient temperature and velocity fields inside the unit, including both the PCM and HTF. The basic conservation equations of continuity, momentum, and energy were solved numerically, using the FLUENT 17 software. Laminar flow inside HTF and liquid PCM has been considered. In order to describe the behavior of the PCM, a so-called "volume-of fluid" model has been activated. The model made it possible to calculate the processes that occur inside the partitions PCM (solid/liquid). In addition, density changes in the PCM and the effect of gravity were taken into account in the second study in order to evaluate the inclination effect of the unit on the PCM molten fraction. The model makes it possible to account for the moving boundary due to the variation of the PCM volume. As a result, the numerical model was rather close to reality. For the mushy region, FLUENT applies the enthalpy-porosity approach, by which the porosity in each cell is set equal to the liquid fraction in that cell. Accordingly, the porosity is zero inside fully solid regions. The following solver settings were used in all the 2-D cases studied in this thesis as :

- Double Precision, Segregated Steady Solver
- Standard Method for Pressure
- Second Order Upwind Discretization for Momentum, Laminar and Energy Equations
- SIMPLE! Algorithm with Pressure-Velocity Coupling

- Convergence criteria of 0.000001

3.8.1 The presentation of the computational code

There are a number of industrial codes, with efficient mesh, allowing the prediction of flows of fluids (FLUENT, CFX, PHOENICS, STAR-CD, TRIO, FEMLAB, CFD-ACE, FLOTRAN, N3S, CFDS-FLOW3D ...). The calculation code "FLUENT" is marketed by the ANSYS group. This group is currently one of the most important centers of competence in the mechanics of digital fluids. It develops and markets a complete solution in the form of general purpose CFD (Computational Fluid Dynamics) software that simulates all fluid, compressible or incompressible flows involving complex physical phenomena such as turbulence, heat transfer, chemical reactions, flows multiphasic for the entire industry. The products and services offered by the "FLUENT" group help engineers develop their products, optimize their design and reduce their risks. Fluent is the world's largest provider of commercial computational fluid dynamics (CFD) software and services. fluent offers general-purpose CFD software for a wide range of industrial applications, along with highly automated, specifically focused packages. Fluent also offers CFD consulting services to customers worldwide. The staff at Fluent consists mostly of individuals with highly technical backgrounds as applied CFD engineers. In addition, fluent employs experts in computational methods, mesh generation, and software development.

This code is widely used in the aerospace and automotive industry and offers a sophisticated interface that facilitates its use. The software "FLUENT" models by the method of the finite volumes of the very varied flows in more or less complex configurations. It is composed, like all CFD type software, of three key elements which are: the pre-processor, the solver and the post-processor. We detail below these three elements in the Fig 3.5.

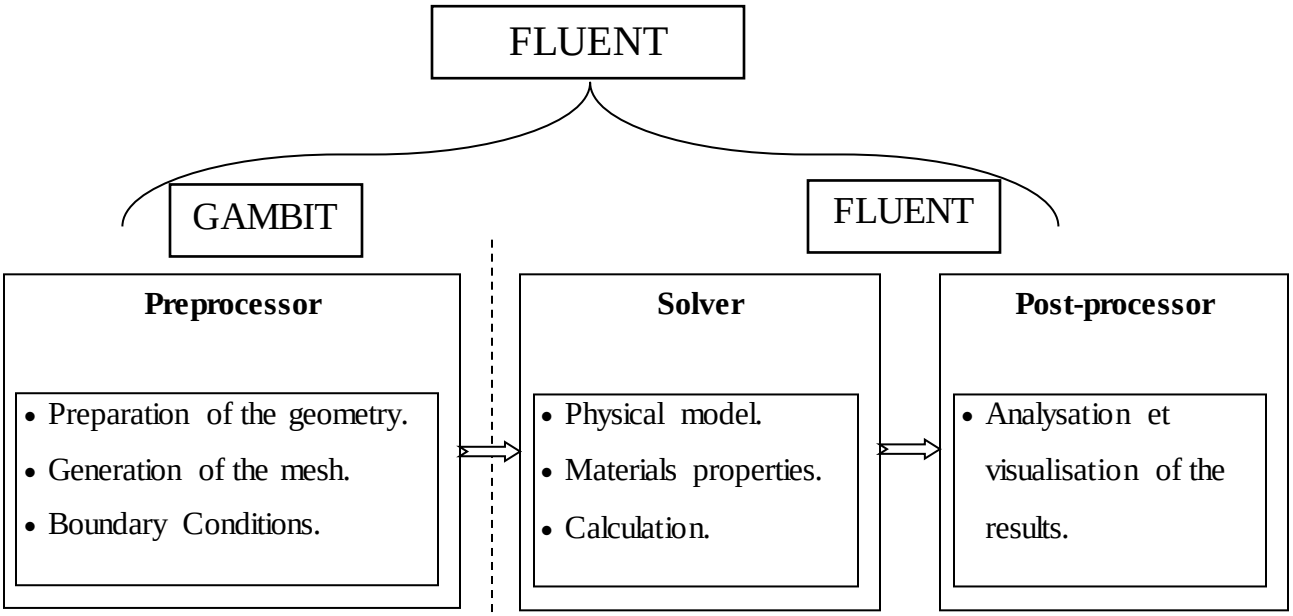

Fig 3.5 *Basic interface of the code "FLUENT"*

3.8.2 Preprocessor "GAMBIT"

It allows the user to build the geometry of the compute domain and subdivide it into small control volumes or compute cells. All these elementary volumes constitute the mesh. The definition of the appropriate boundary conditions, at the level of cells that coincide or touch the boundary of the computational domain, is also done at this level.

3.8.3 Solver "FLUENT"

For incompressible fluids, the calculations are made in relative pressure. The method used is the finite volume method. This method has the advantage of being conservative, that is to say that all the flow coming out of a control volume enters the neighboring volumes. The calculation steps in the solver are as follows:

- Integration of continuous equations on each control volume. Ostrogradski's theorem is used to transform some volume integrals into surface integrals,
- Discretization in space and time (for non-permanent flows) of equations: substitution of partial derivatives by finite difference approximations; transformation of the system of equations into an algebraic system,
- Algebraic system resolution through an iterative process; use of an algorithm to correct pressure and velocity components to ensure conservation of the mass.

3.8.4 Post-processor "FLUENT"

The Post Processor allows you to view the different results on the screen (speed fields, temperature fields, current lines, etc.).

3.8.5 Method of solving transport equations

3.8.5.1 Discretization scheme

Our code uses the finite volume method for solving the systems of equations used to model the movements of fluids. In fact, with the finite volume method, a given physical problem is solved according to three main steps:

- Division of the calculation domain into control volumes via a mesh (see Fig 3.6),
- Integration of the equations on each control volume in order to transform them into algebraic equations,
- Solving the equations thus discretized.

These equations are put in the following general form:

$$\frac{\partial}{\partial t}(\rho\varphi)+\frac{\partial}{\partial x_i}(\rho U_i\varphi)=\frac{\partial}{\partial x_i}\left(\Gamma_\varphi\frac{\partial\varphi}{\partial x_i}\right)+S_\varphi \qquad (3.8)$$

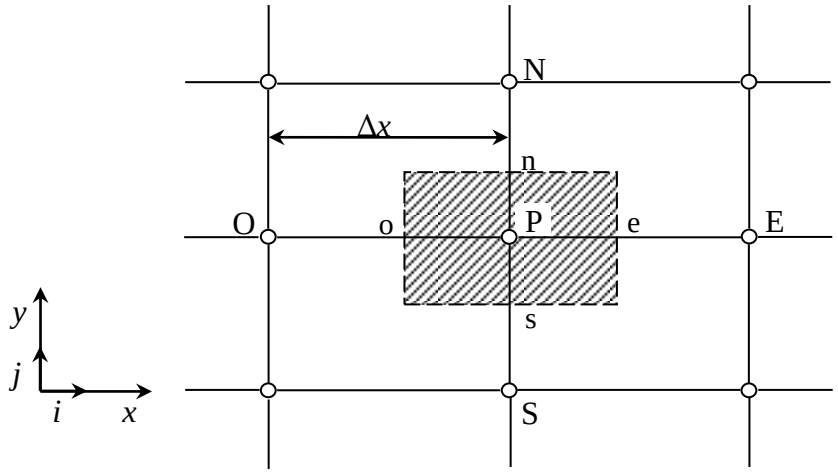

Fig 3.6 *Control volume for the finite volume resolution*

Where represents an intensive magnitude such as Ui, Hm or according to the laminar model used. is a diffusion coefficient and a source term whose respective expressions depend on the chosen turbulence model. In this general form, all non-convective or non-diffusive terms are included in the source term

Fig 3.6 shows the finite volume discretization of the transport equations. The different quantities of the flow are calculated at the center of each control volume, at points P, E, O, N and S. the integration of equation (3.8) into a control volume involves the values, as well as as the diffusion and conservation and

convection flows of these quantities at the borders of the control volume. Thus, for the computation of the magnitudes at the point P, their values at the interfaces e, o, n and s are also necessary.

Several interpolation methods can then be used knowing their values at the center of the adjacent control volumes. The interpolation schemes used in CFD codes are generally based on the finite difference method. This method applied to control volumes is described by many authors such as Patankar (1980) and Roache (1982). Doctoral studies such as those of Buchmann (1995), and Theodosiu (2001). also show the details of the different interpolation schemes used in the CFD codes. In this paragraph, the focus is rather on the criteria to be taken into account to ensure both the stability and accuracy of CFD results. It is thus noted that although a centered finite difference approximation of the second-order diffusion terms is adapted to the majority of the problems, this technique does not give satisfactory results with respect to the convective terms. Indeed, the centered difference method does not correctly take into account the direction of the flow. Fig 3.7 illustrates this major defect.

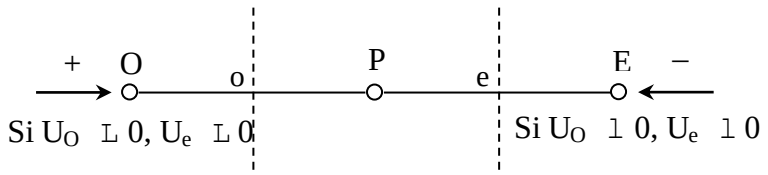

Fig 3.7 *One-dimensional scheme illustrating an elementary volume surrounding a node P*

The values of an entity at interfaces e and o are determined by a linear approximation using the following expressions

$$\varphi_e = \frac{1}{2}\left(\varphi_P + \varphi_E\right) \tag{3.9}$$

$$\varphi_O = \frac{1}{2}\left(\varphi_O + \varphi_P\right) \tag{3.10}$$

On the basis of these two last expressions, it may be noted that the points situated upstream and downstream have the same weight for the calculation of the values at the interface whatever the speed of the flow. But there can be a strong transport from the left to the right (or vice versa) of the interface. In such a case, this formulation is no longer valid because it can generate numerical instabilities when the transport through one side of a control volume is preponderant compared to the diffusion. The number of mesh Peclet allows for this purpose to quantify the relative importance of the convective and diffusive phenomena:

$$Pe_{maille} = \frac{\rho U \Delta x}{\Gamma_\varphi} \tag{3.11}$$

Where ρU and are considered constant along .We have thus been able to observe that when the number of mesh Peclet built on the dimension of the mesh and the speed at the interface is greater than 2,

the centered discretization of the convective terms, in steady state leads to numerical instabilities (Launder & Jones, 1972). To avoid these numerical instabilities, off-center approximations are proposed. The diffusive exchanges are modeled in the same way as in the scheme with centered differences. On the other hand, the convective exchanges take place only from upstream to downstream of the flow. This upwind scheme is first-order accurate based on a Taylor development. It is unconditionally stable from the numerical point of view but likely to introduce an "artificial" numerical diffusion which can affect the precision of the calculation Launder & Spalding (1974). To avoid that the accuracy of the calculation is affected by the effects of digital diffusion, we can refine the mesh and / or align the mesh on the flow.

Unfortunately, the refinement of the mesh is limited by the computing power of computers. In addition, the alignment of the mesh on the flow is only possible with a simple flow whose main direction can be aligned with the mesh. Indeed, when the flows are complex, it is difficult to align the mesh on the movement. Therefore, higher order spatial discretization methods are needed to reduce digital diffusion. Thus, schemes of order 3 and more have been proposed but the implementation of the boundary conditions has proved difficult to achieve. These latter schemes are also unstable. A satisfactory compromise between the stability and accuracy of the predominant convective computation was found with second-order upwind approximations (Versteeg & Malalasekra, 1995). We can also mention the higher-order scheme, QUICK, proposed by Leonard (1974) and used in the doctoral study of Lepers (2000). The latter was able to note that compared to a second-order upwind, the Quick scheme does not greatly improve the accuracy of the numerical results. For our study, the QUICK (Quadratic Upwind Interpolation (Leonard, 1979) interpolation scheme is used, which calculates the value at the interface of a quantity, based on its values at the center of the adjacent control volumes and more distant volumes upstream of the interface considered.

3.8.6 Segregated Algorithms

3.8.6.1 Choice of Pressure-Speed Coupling Method

Three algorithms are available in the calculation software:

- SIMPLE: the most robust.
- SIMPLEC: it gives faster convergence for simple problems.
- PISO: it is useful for problems of unstable flows.

The chosen algorithm in our study is the SIMPLE algorithm (Patankar S. V 1980). At the initialization of the calculation, a pressure field fixed a priori is introduced into the balance equation of the momentum, for calculating a first velocity field. The combination of the mass balance and momentum equations then makes it possible to correct these first pressure and velocity fields. The other transport equations are then resolved and the corrected pressure field is used to initialize the calculation at the next iteration. This

succession of operations is repeated until the convergence criteria are reached. All these process are described schematically in Fig 3.8

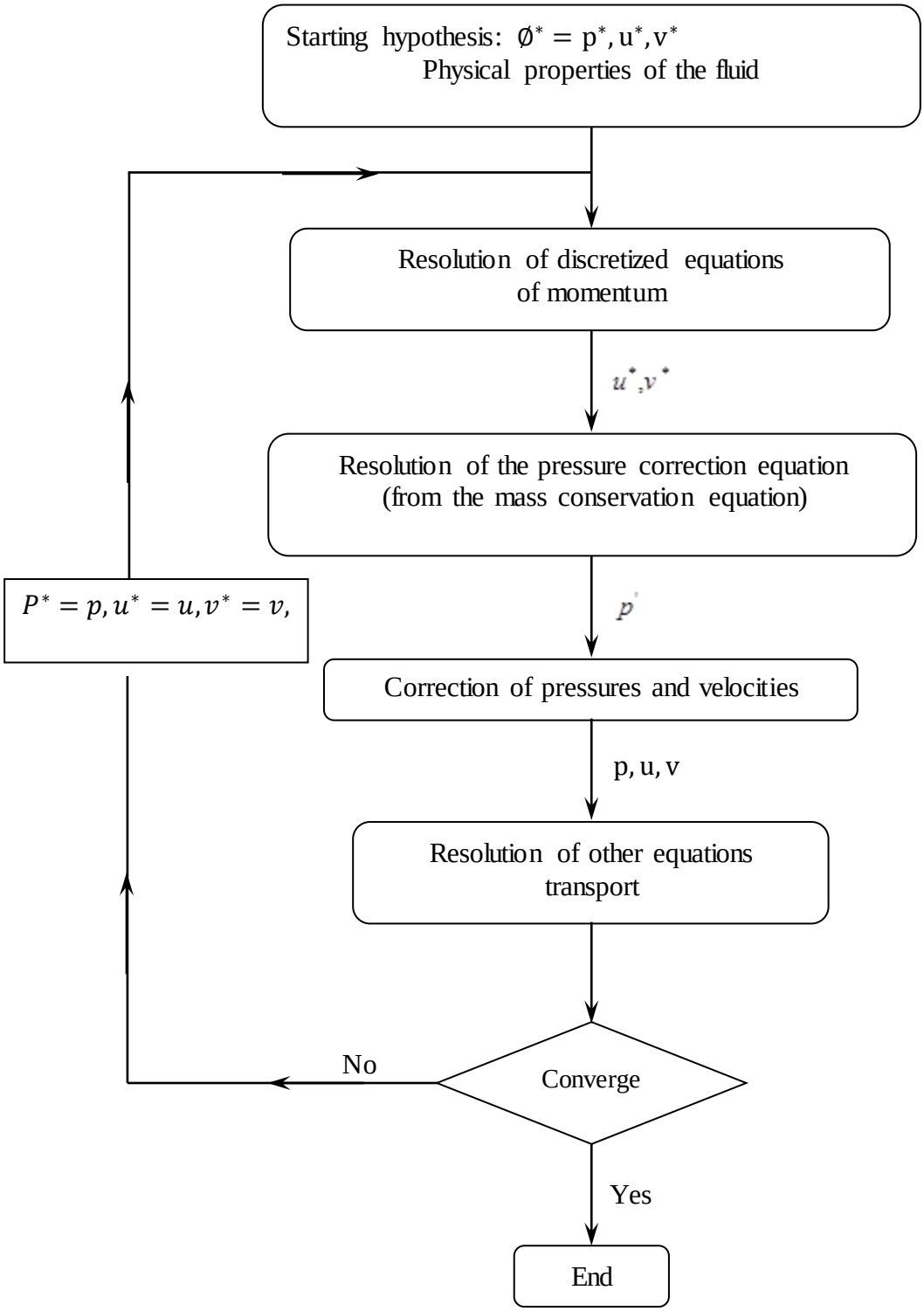

Fig 3.8 *Schema of the algorithm SIMPLE*

3.8.6.2 SIMPLE Algorithm

The discretization of a diffusion transport equation on a control volume by the finite volume method involves the values of the velocities at the interfaces of the volumes (Ue, Uw, Un, Us). It is therefore interesting to calculate these speeds directly on the interfaces (without having to make interpolations). On the other hand, the discretization of the continuity equation and the pressure gradient with the use of a linear interpolation can induce significant errors because a "checkerboard" pressure or speed distribution is seen as a uniform field. To circumvent these difficulties it is preferred to use staggered grids. A main grid is constructed on which pressure, temperature and concentration are calculated. Two grids shifted right and up respectively are used for calculating the horizontal and vertical velocities. The SIMPLE algorithm, acronym for "Semi-Implicit Method for Pressure Linked-Equations" solves the system of discretized equations. This algorithm states the existence of a relationship between the corrected velocities and the corrected pressures, in order to verify the conservation equation of the mass.

3.8.7 Numerical Resolution

3.8.7.1 Convergence control parameter

How to obtain a converged solution is one of the essential elements of flow prediction using CFD codes. The code "FLUENT" proposes different techniques to speed up the process of convergence is increased if a good estimate of the solution is given as initial condition. We use several techniques described below:

3.8.7.2 *Convergence criterion*

The numerical resolution of CFD-type problems requires an iterative process. To appreciate the convergence of the iterative process, convergence criteria must be taken into account. Thus, the convergence of the iterative process is determined by the concept of residue.

After the discretization step, the conservation equation of a given variable on a cell of center P can be expressed as follows:

$$a_p \cdot \phi_p = \sum_{nb} a_{nb} \phi_{nb} + b \tag{3.12}$$

Where: a_p and a_{nb} represent the convective and diffusive contribution, the index nb is related to the centers of adjacent cells. b is the constant part contribution of the source term Φ_ϕ.

The normalized residue then has for expression:

$$R^{\phi} = \frac{\sum_{Domaine} \left| \sum_{nb} a_{nb} \cdot \phi_{nb} + b - a_p \cdot \phi_p \right|}{\sum_{Domaine} \left| a_p \cdot \phi_p \right|} \tag{3.13}$$

These expressions of the residues are valid for all the quantities except the pressure, in the case of this quantity, the residue is determined from the continuity equation:

$$R^{C} = \sum_{Domaine} \left| taux\ de\ création\ de\ matière\ dans\ le\ domaine \right| \tag{3.14}$$

3.8.7.3 *Under-relaxation*

Because of the non-linearity of the solved equations, it is possible, to attenuate the fluctuations of the solution, to reduce the variations of the variables from one iteration to another by introducing a sub-relaxation. There are no general rules for better under-relaxation coefficient values, but there are recommendations for each of the magnitudes, usually based on empirical knowledge.

3.9 Steps to solve the problem

The main steps used in our simulation are:

1. Determination of the domain of computation (construction of the geometry).
2. Discretization of the domain of computation (mesh).
3. Identification of boundary conditions.
4. Choice of the mathematical model.
5. Choice of the solution algorithm.
6. Solution of the mathematical model.
7. Visualization and interpretation.

Chapter 4

Results and Discussions

Results and Discussions

4.1 Introduction

Two studies have been realized here according to the same numerical solving used and subdivided to two sections, where the different between them was in the abolishment of the gravity forces inside the first one in order to evaluate the effect of different physical and geometrical parameters on the heat transfer inside the unit filled by the paraffin wax and RT60, while the second study has focused on the effect of the inclination effect on the melting process of TR35.

4.2 Section I: Effect of the physical and geometrical parameters

4.2.1 Physical model

The PCTES unit under investigation in the first study is shown in Fig 4.1. The first study has clarified two different configurations: (I) shell-and-tube system with paraffin wax; and (II) shell-and-tube system with paraffin wax and RT60. The first configuration consists of a shell-and-tube configuration (see Fig 4.1.a) that has been used previously by (Kibria et al. 2014). The inner tube is made of copper. Distilled water flows through the inner tube as HTF. The phase change material (paraffin wax) fills the annular space. The outer surface of the storage unit is well insulated. The second system shown in Fig 4.1.c is similar to the first configuration concerning the inner tube, HTF used and the outer surface of the storage, but two different phase change materials namely the paraffin wax and RT60 separated by a second tube of copper are used. As the problem under examination is axisymmetric, a schematic 2-D computational domain for all investigated cases is presented for both configuration in the plots Fig 4.1.b and Fig 4.1.d. The thermo-physical properties of the HTF and PCMs used in this section are shown in the Table 4.1

(a) Configuration I

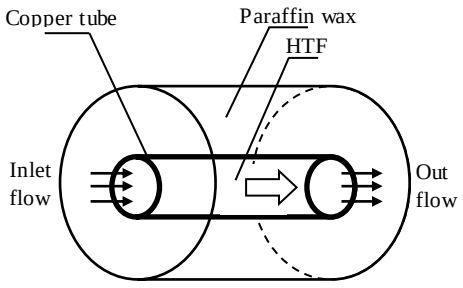

(b) 2D representation of Configuration I

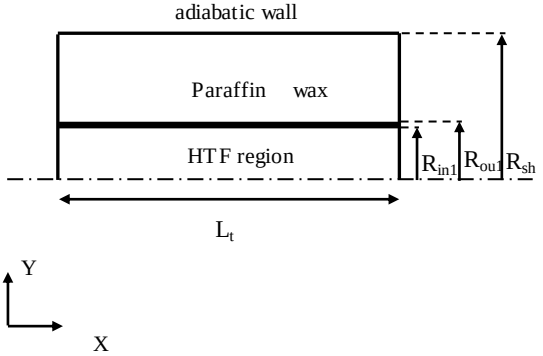

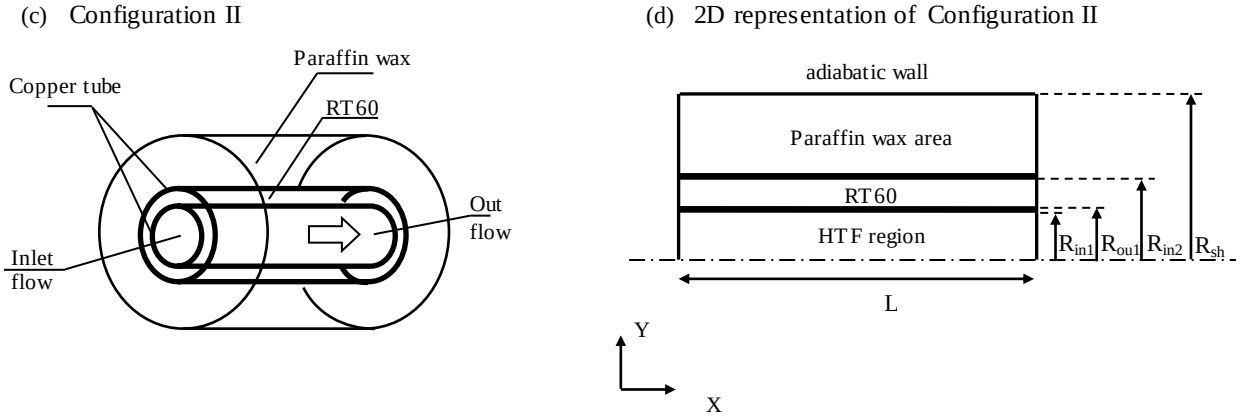

Fig 4.1 *Horizontal latent heat storage unit*

Table 4.1 *Thermo-physical properties of PCMs and HTF [*(Regin, Solanki and Saini 2006), (Campos-Celador et al. 2014), (Da Veiga 2002)*]*

PCM	**Density [kg/m^3]**		**Specific heat [J/kg K]**		**Latent heat [J/kg]**	**Thermal conductivity [W/ m · K]**		**Dynamic viscosity [N s/m^2] or [kg/m s]**		**Melting Temperature [°C]**
	Solid	Liquid	Solid	Liquid		Solid	Liquid	Solid	Liquid	
Paraffin wax	910	790	2000	2150	190000	0.24	0.22	——	0.004108	61
RT60	880	770	2660	2340	123506	0.2	0.2	——	0.00003705	53~61
Heat transfer fluid (HTF)										
Water at 25°C	997		4179			0.613		0.000855		0
Water at 88°C	967.1		4203			0.674		0.000324		

4.2.2 Boundary conditions

The full set of boundary conditions of the first study which imposed on the flow field and the thermal boundary conditions imposed on the temperature field. Since the same geometry of (Kibria et al. 2014) was considered here, the same hypothesis, boundary and initial conditions are adopted in the present study:

(i) The thickness of the inner tube wall is considered;

(ii) The thermo-physical properties of HTF and PCM are constant with respect to the temperature;

(iii) The initial temperature of the latent thermal storage unit is uniform;

(iv) HTF flow is laminar;

(v) Natural convection inside the Paraffin wax was not considered, as the considered shell and tube thermal energy storage unit used is horizontal.

During the charging cycle, the HTF flows by inlet temperature of 88°C and a mass flow rate of 0.072 kg/min. On the other hand, during the discharging, we took the heat stored using cold HTF passage by a temperature of 25°C and a mass flow rate of 0.07 kg/min as used in the literature of (Kibria et al. 2014).

4.2.3 Grid mesh independency

A dense grid distribution is employed near the wall while a uniform grid distribution is used in the streamwise direction. The plots of Fig 4.2.a and 4.2.b show the typical grid distribution over the computational domain of the configurations I and II of the first study. The accuracy of the solution depends on the number and the size of the cells. The grid size used in the computations is chosen by performing a grid independence study (see Fig 4.3). For the first configuration, several meshes were tested to ensure that the solution was independent of the mesh (35x300; 50x300; 65x300). This test indicated that 35×300 cells are adequate. On the other hand, concerning the second configuration (Case A and B) the analysis of the grid independency made for the grid tests (50x300; 65x300; 85x300) indicate in the Fig 4.4 and 4.5 that 65×300 cells are adequate. From above we can say that the grid (35x300) is suitable for the first configuration and the grid (65x300) is convenient for the second configuration.

(a) A part of the grid for conf I

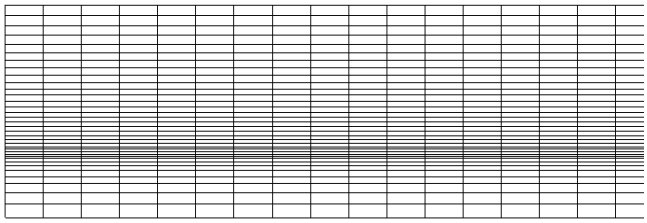

(b) A part of the grid for conf II

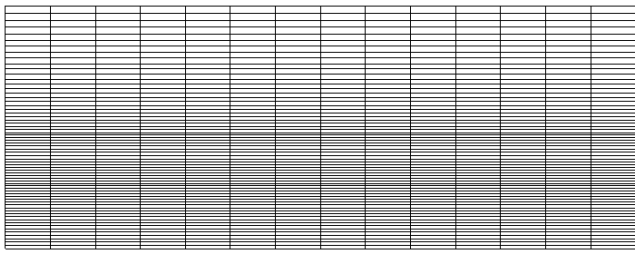

Fig 4.2 *The grid used in first (I) and second (II) configuration*

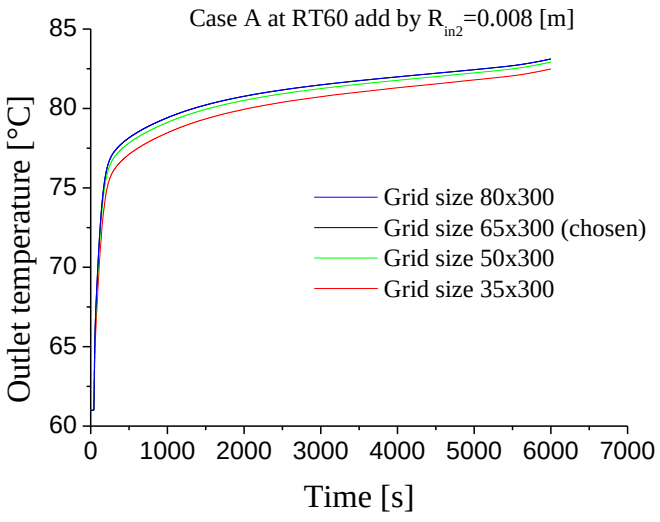

Fig. 4.4 *Grid size independency of the second configuration case A at RT60 add by R_{in2}=0.008[m]*

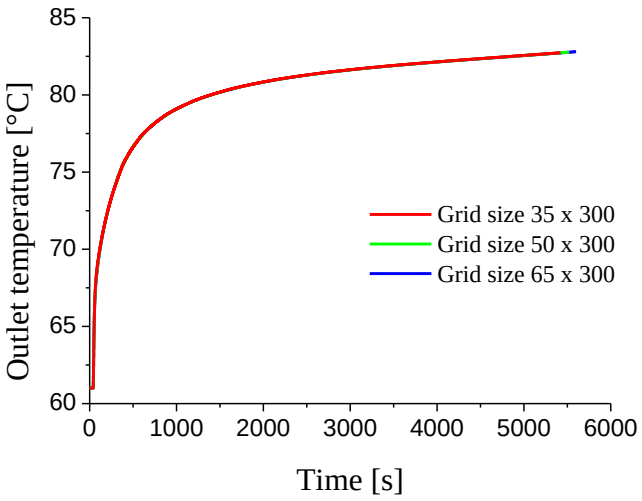

Fig. 4.3 *Outlet temperature in charging cycle in different grid size of configuration I*

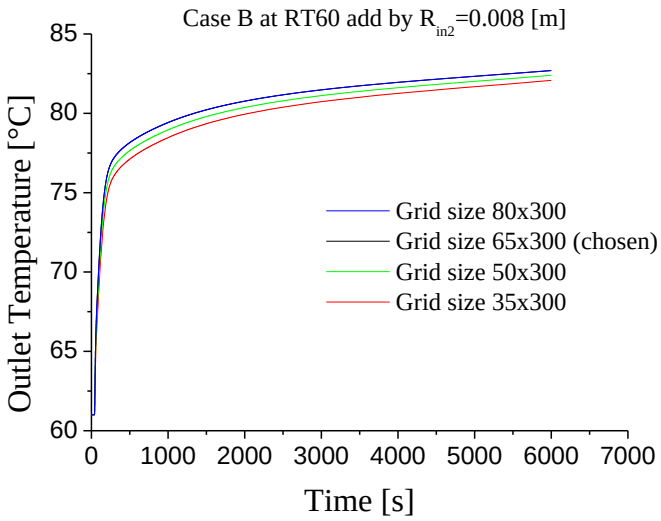

Fig. 4.5 *Grid size independency of the second configuration case B at Rt60 add by R_{in2}=0.008[m]*

4.2.4 Results and discussions

4.2.4.1 Validation

The validation of the numerical results was performed in charging and discharging cycle through a comparison with the experimental and numerical results of (Kibria et al. 2014) according to the measures in the Table 4.2. The validation was performed on the evolution of HTF outlet temperature at the charging and discharging cycle. The comparison between our numerical results in relation to the analytical and experimental results of (Kibria et al. 2014) showed a good agreement in Fig 4.6.

(a) Charging (b) Discharging

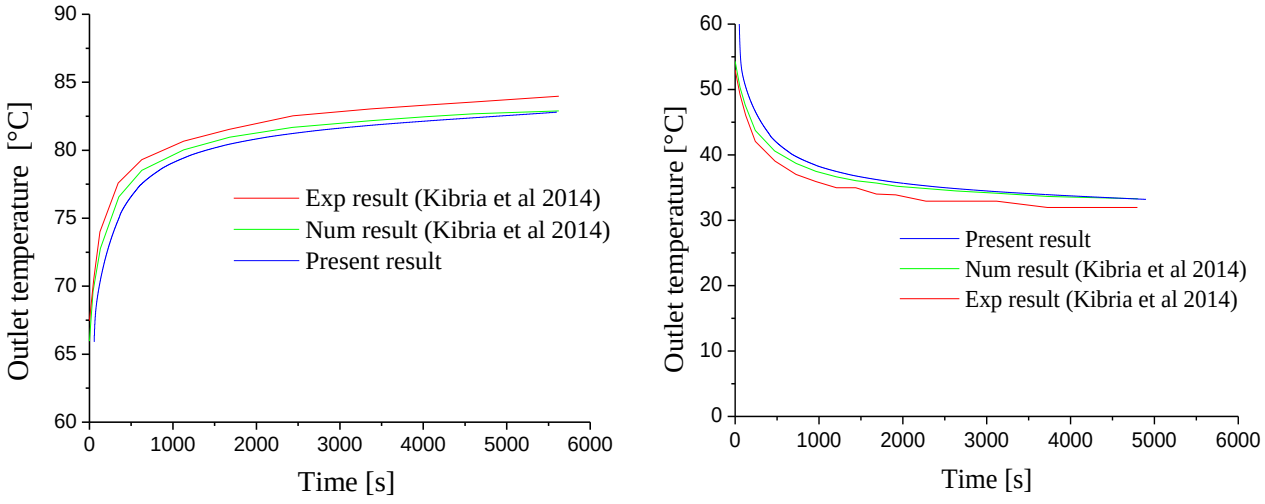

Fig 4.6 *Validation of HTF outlet temperatures in charging and discharging cycle*

Table 4.2 *Geometric parameters of the configuration I (configuration of* (Kibria et al. 2014)*)*

The inner radius of tube 1	**(R_{in1})**	[m]	0.0054
The outer radius of tube 1	**(R_{ou1})**	[m]	0.006
The radius of the shell	**(R_{sh})**	[m]	0.018
The length of tube	**(L_t)**	[m]	1
Thickness of tube 1		[m]	0.0006

At the charging cycle, the PCM is initially at solid state (at the temperature 61°C) and the HTF circulates with inlet temperature equal to 88°C, following the boundary and initial conditions of (Kibria et al. 2014). The HTF outlet temperature increases over time until asymptotic value of 83°C which is lower than the inlet temperature (88°C). This difference is due to the heat absorption by melting Paraffin wax. The results show that the outlet temperature of system is close to those obtained analytically and experimentally by (Kibria et al. 2014), where this process took about 6500s to complete the charging cycle. In discharging process, the HTF absorbs the heat stored in the Paraffin wax whereas the HTF outlet temperature decreases over time until asymptotic value 33°C and the paraffin wax becomes in the solid state. The small discrepancy between the numerical results and those obtained experimentally is due to the simplifications considered in the numerical model. Further validations (not shown here) done for several parameters give a good agreement with the numerical and experimental data of the literature (Kibria et al. 2014).

4.2.4.2 Parametric study

In this investigation, we have made a parametric study following the measures of the standard configuration based to examine the effect of: (i) length of tube; (ii) shell diameter; and (iii) Reynolds number on the time and rate of charging and discharging process. Furthermore, we have tried to propose a new thermal unit composed of a Paraffin wax and RT60. The performances of this new configuration will be compared to the first one. Moreover we have made a numerical inquiry on inclined shell and tube TES unit filled by RT35 as PCM in order to evaluate the melting process behaviors.

4.2.4.2.1 Influence of tube length

Fig 4.7 shows the effect of different tube length L_t on the thermal performance during the charging and the discharging cycles. Considering the first configuration, we have changed the tube length in the range 0.2-1.8m in the scope to quantify this effect for the charging and discharging cycles. From this figure which depicts outlet temperature of HTF versus the tube length variation in the range 0.2-1.8m. We can see that the time of charging and discharging cycles is proportional to the tube length.

An increase of the length leads to an increase of the melting and solidification time. Moreover, the

increase of tube length decreases the asymptotic value of the HTF outlet temperature from 87°C in the case L_t=0.2m to 79°C in the case L_t=1.8m during 5600s. This leads to a gradient of temperature ΔT_{ch} equal to 8°C between HTF outlet temperatures of tube length from 0.2m to 1.8m at charging time. With regard to the discharging process and the effect of increasing the tube length, the asymptotic value of the HTF outlet temperature increases from 25°C to 38.5°C along the 5600s, thus leading to a gradient of temperature ΔT_{dis} equal to 13.5°C. From this figure, it can be seen that the tube length is an important parameter to optimize the melting and solidification time.

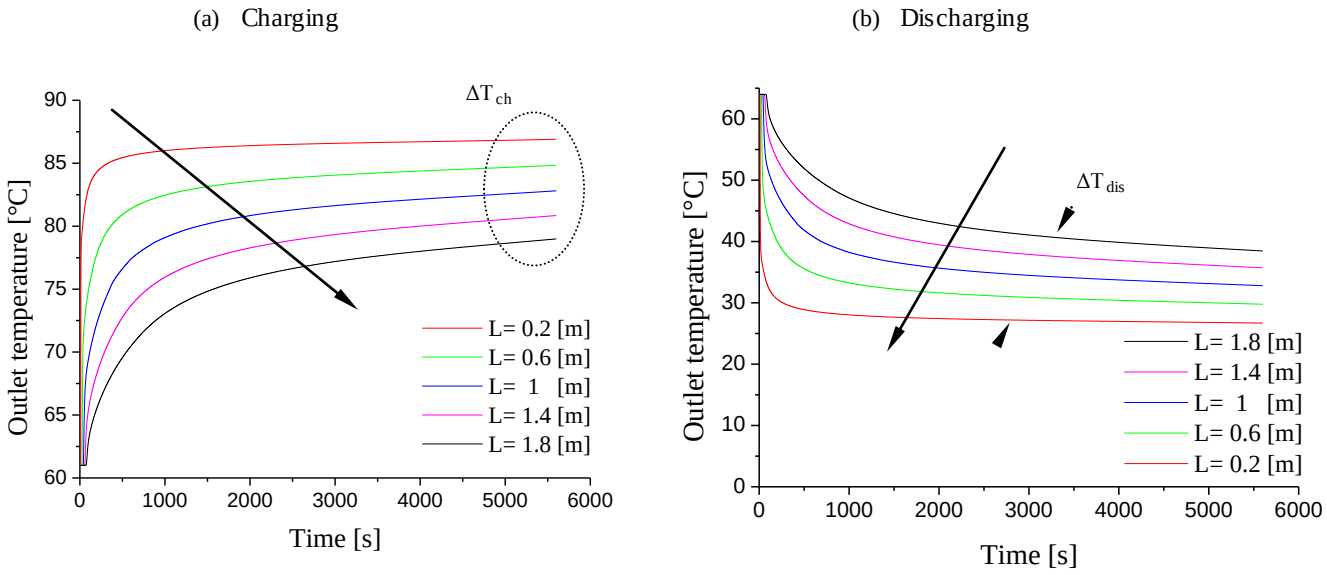

Fig 4.7 *Effect of tube length in charging and discharging cycle*

4.2.4.2.2 Effect of shell diameter

The shell diameter is among the important parameters that have a relation with the progress of solidification and melting. In this case we have changed the shell diameter in the range 24-44 mm. Fig 4.8 shows that the shell diameter reduction allows to complete the discharging and charging rate in a short time. The reduction of shell diameter causes the minimizing of the PCM mass volume. This allows accelerating the heat charging or discharging of the mass through heat transfer process. This contributes to speed up the melting fraction rate of the Paraffin wax during charging process.

It can be seen from the figure, that the shell diameter of 24 mm needs just 3300s to complete almost the charging or the discharging processes, whereas the other cases needed more than 5000s to complete the fully charging or discharging processes. As a result, the gradient in HTF outlet temperature between the shells of minimum and maximum diameter used ΔT_{ch} is equal to 5°C for charging process and ΔT_{dis} is about 8°C for discharging process. Therefore, the quantity of Paraffin wax must be appropriate with the work conditions, in order to optimize the time of storage system.

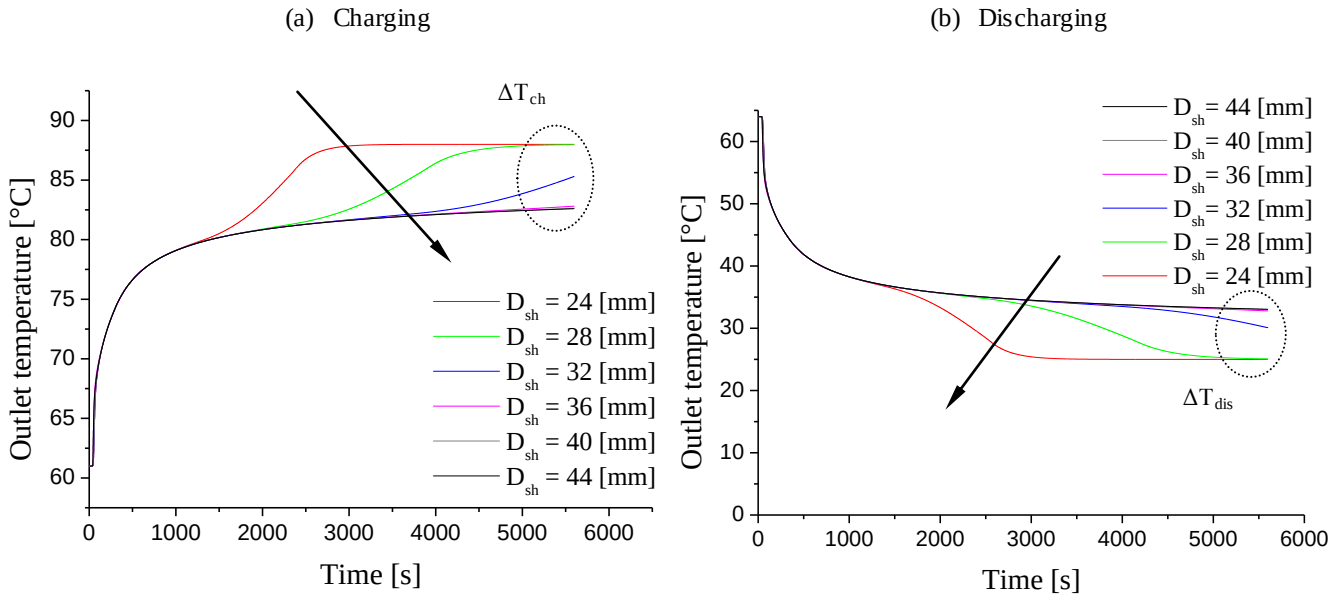

Fig 4.8 *Effect of shell diameter in charging and discharging cycle*

4.2.4.2.3 Effect of Reynolds number

After detailed inquiry of the configuration geometric variation effect in terms of shell and tube sizes on the phase change process of storage system; another important parameter is evaluated here to aim check the storage system in terms of HTF outlet temperature, where the antecedent parameters studied is fixed in order to analyze the outlet temperature of the water when the flow regime varies according to the Reynolds number range Re=100-1500. Physically, this hydraulic parameter is one of the dimensionless numbers which depends on the HTF properties as the viscosity, velocity and tube sizes. Basically in the present investigation, only the laminar regime (no turbulent mode) is considered for the HTF flow. In this contribution, all thermo-geometric parameters of the storage system are constant, except the HTF current nature that is analyzed in the range Re= 100-1500.

The regime of the flow generally is signified by the velocity fluctuations inside the tube, consequently the heat transfer energy has a relative relation with the HTF movement, where a minimal Reynolds number in our case at constant inlet temperature 88°C and PCM volume has insufficient HTF outlet temperature during the melting PCM process, and this elucidates the HTF temperature distribution deceleration along the axial planar of the tube, which results to delay the heat absorption saturation via the PCM, therefore the melting process will take a long duration to complete the total charging time. On the otherwise, increasing of regime flow into Re=1500 shows a strongest effect on the heat transmission inside PCM, where the heat absorption rate increases fleetly from the PCM that leads to minify the total time of storage system, which considered as gain of the thermal energy provided.

The discharging cycle is assumed as important step through driving of the temperature consumed distribution during the time. In this cycle the cold HTF inlet temperature has been estimated about 25°C, in which the heat transfer between HTF and PCM has a similar exchange that performed in the charging step, where the low flow regime leads to slow down the soak up of the heat via the HTF cold by conduction heat transfer exchange mode. A summary of the results clarifies that a swell in the Reynolds number allows diminishing the solidification and melting time as showed in the Fig 4.9. It is clear from this figure, that for high value of Reynolds number (Re=1500), the HTF outlet temperature tends to reach the asymptotic value of 86.5 °C in charging cycle. While for the lower value of Reynolds number (100) the HTF outlet temperature tends to reach the asymptotic value of 69.5°C.

Therefore, the temperature gradient ΔT_{dis} of HTF outlet temperature in discharging cycle is about 9.6°C and in the charging case ΔT_{ch} is estimated by 17°C. Both of phase change processes have a negative and positive advantage, from the side of Reynolds increment we will obtain a shortage melting and solidification time, on the second hand the declining of this parameter reduce the ration of HTF outlet temperature during the time, when we regard at these results, we will find that a preferable heat storage system be should has a shorter charging period and longest discharging time. According to that, the governing of thermal energy cycle in this parameter seems much easier compared to the first two parameters, whereas them too have the same marked in charging and discharging time but the difficulty of the control in suitable geometry is the only obstacle in them.

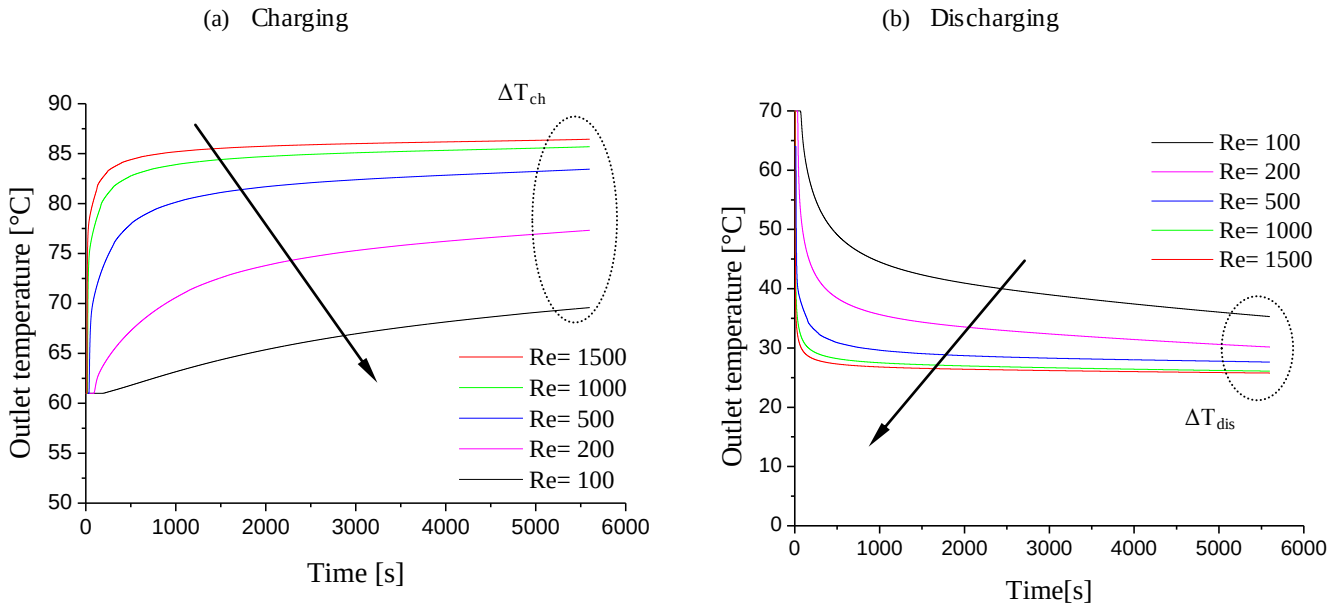

Fig 4.9 *Effect of Reynolds number in charging and discharging cycle*

4.2.4.2.4 Improvement of TES unit

According to the above results, it could be very useful to find an effective way that allows the PCM to absorb the maximum heat provided by the HTF. As a result, we have tried to propose a new configuration, where we inserted a layer of another phase change material namely the RT60, which its melting temperature is equal to 57 °C, which is very close to melting temperature of the paraffin wax (equal to 61 °C). This layer of RT60 makes it possible to distribute the thermal load on the paraffin wax along the axial direction and to ensure it the thermal inertia. In this TES unit, the two PCMs are superposed between the copper tubes. Therefore, the heat exchange in this unit is done by conduction in two steps; (i) heat interchange between HTF and RT60 through the first copper tube, (ii) heat transfer from the RT60 into the paraffin wax through the second copper tube. The same boundary and initial conditions adopted in the first configuration are used here. Different cases according to Table 4.3 and Table 4.4 are numerically predicted. The melting temperature of RT60 is lower than the paraffin wax (61°C), which allows the RT60 to melt before the paraffin wax, which leads to accelerate the melting process of RT60 and its solidification process due to its rapid heat absorption from the HTF.

In this configuration we proposed two cases A and B. The case A (see Table 4.3) has a constant radius of the shell R_{sh} and a variable inner radius of the second tube R_{in2} that consequently reduces the volume of Paraffin wax. This radius is varied in the range 0.008-0.014m. The variation of the inner radius allows us to obtain several proportions in the volume of the two PCMs, from the case the existence of only the Paraffin wax to the case we obtain the Paraffin wax with RT60 (R_{in2}= 0.014m). The results shown in Fig 4.10 indicate a decrease in the time of charging and discharging cycles compared to case of the first thermal storage unit (containing only Paraffin wax), whereas the temperature gradient ΔT_{ch} of the HTF outlet temperature in charging cycle increases in the first time period [0-1500s], then starts to decline. Near the time 4000s, we remark an increase of the outlet temperature and ΔT_{ch}. This is due to the PCMs which have achieved the total phase change from the solid to liquid and we are in sensible phase of heat transfer. In case B (Table 4.4), we have fixed the volume of Paraffin wax (same volume of the first configuration) and we have varied the inner radius of the second tube R_{in2} from 0.008 to 0.014m, which means the shell radius will vary. In this case the time of charging and discharging cycle also decreases compared to the use of a Paraffin wax alone as presented in Fig 4.11. This case is more stable in charging and discharging cycles than case A, as the mass volume of the PCMs of the case B is increased compared to the first case A. However, both cases have a better evolution of the HTF temperature than the paraffin wax alone as shown in Fig 4.10 and Fig 4.11.

Table 4.3 *Geometric parameters of the second configuration II.A*

The inner radius of tube 1	**(R_{in1})**	[m]	0.0054			
The outer radius of tube 1	**(R_{ou1})**	[m]	0.006			
The inner radius of tube 2	**(R_{in2})**	[m]	0.008	0.01	0.012	0.014
The radius of the shell	**(R_{sh})**	[m]	0.018			
The length of tube	**(L_t)**	[m]	1			
The thickness of copper tube 1 and 2		[m]	0.0006			

(a) Charging case

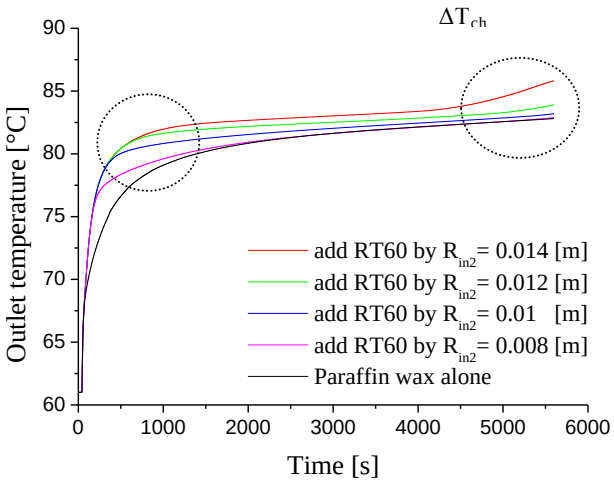

(b) Discharging case

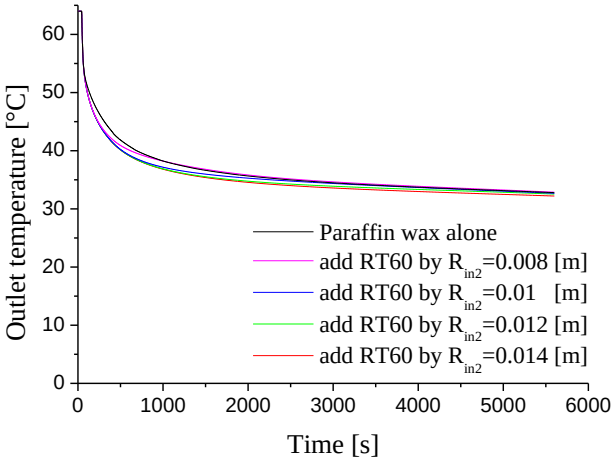

Fig 4.10 *Charging and discharging cycle of the second configuration II.A*

Table 4.4 *Geometric parameters of the second configuration II.B*

The inner radius of tube 1	**(R_{in1})**	[m]	0.0054			
The outer radius of tube 1	**(R_{ou1})**	[m]	0.006			
The inner radius of tube 2	**(R_{in2})**	[m]	0.008	0.01	0.012	0.014
The radius of the shell	**(R_{sh})**	[m]	0.01902	0.02001	0.02114	0.02239
The length of tube	**(L_t)**	[m]	1			

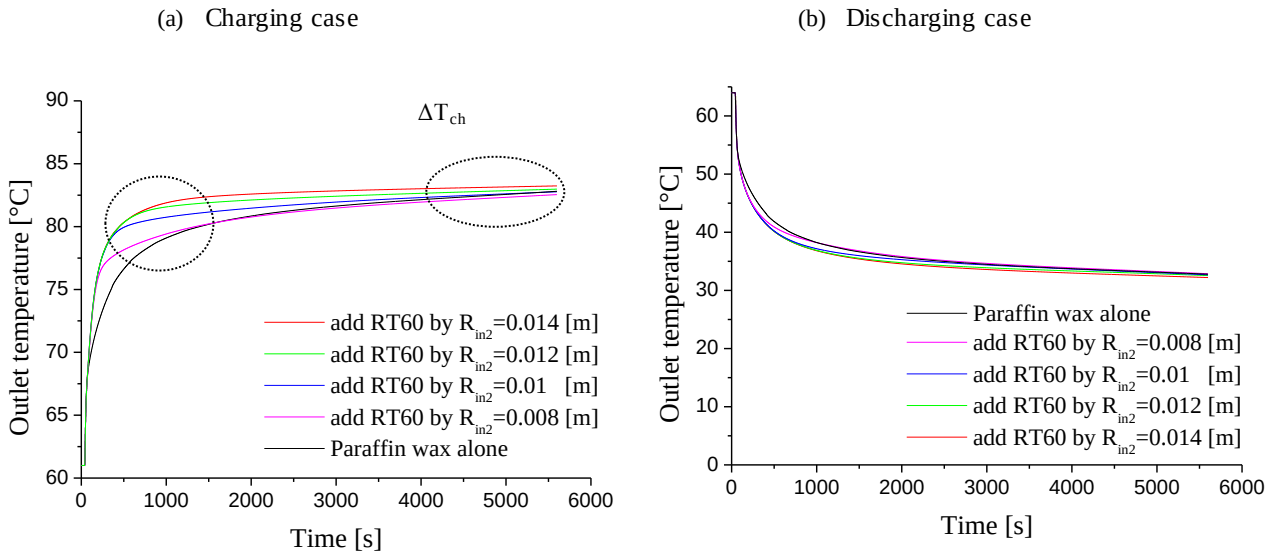

Fig 4.11 *Charging and discharging cycle of the second configuration II.B*

4.3 Section II: Effect of the unit inclination on the PCM thermal behaviors

4.3.1 Physical model

The second study has included a vertical shell and tube TES physical model that has been investigated following the design shown in the Fig 4.12 in order to assess the inclination effect of the unit on the PCM melting process. This unit consists of two vertical and coaxial cylinders as considered in the work of (Longeon et al. 2013). The inner cylinder (tube) is made of stainless steel with inner diameter and thickness of 15 mm and 2.5 mm respectively. Distilled water flows through the inner tube as HTF by laminar regime (Re < 2300) while the PCM (RT35) fills the shell space. The outer cylinder of the storage unit is considered as adiabatic, its inner diameter is equal 44 mm while the unit length is estimated about 400 mm. The thermo-physical properties of phase change materials with water as HTF which are used in this study are shown is Table 4.5

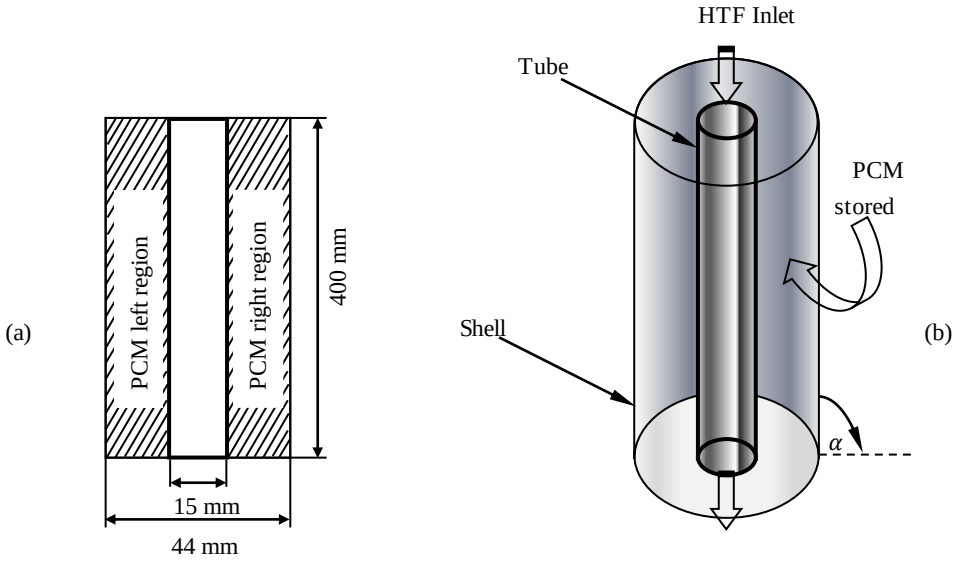

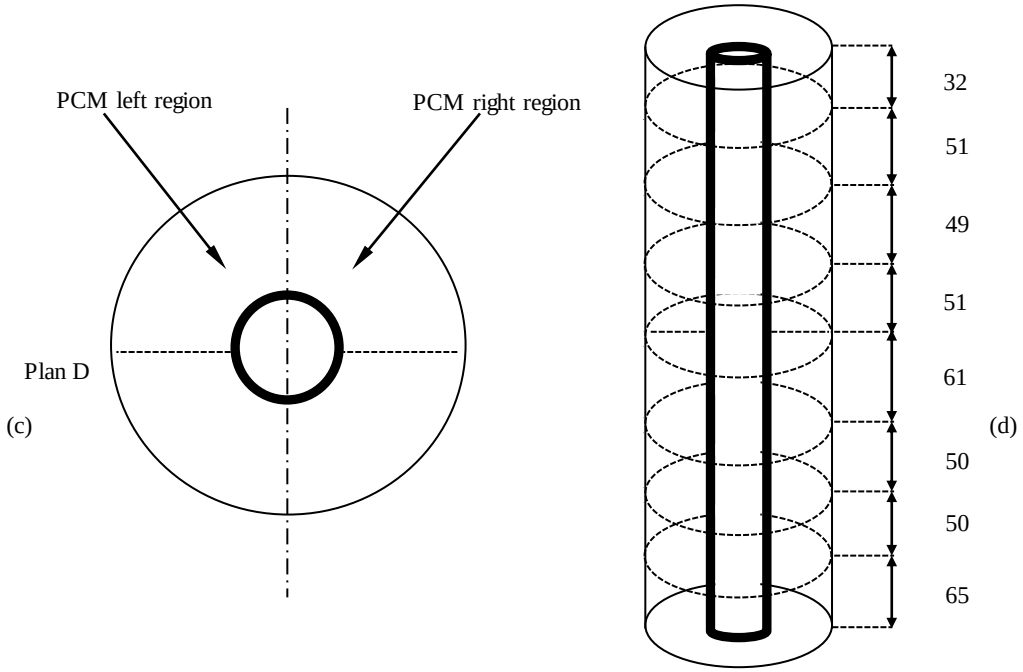

Fig 4.12 *A vertical shell and tube thermal energy storage unit configuration.*

Table 4.5 *Thermo-physical properties of PCM and tube(Longeon et al. 2013)*

Properties	**Rubitherm® RT35**	**Stainless steel**
P [kg/m^3]	880(s) / 760(l)	8010
C_p [J/kg K]	1800(s) / 2400(l)	500
K [W/ m · K]	0.2	7.7
υ [m2/s]	3.3x10^{-6}	
β [1/K]	0.001	
λ [J/kg]	157000	
θ [K]	308	

4.3.2 Boundary condition

Considered the second configuration The hypothesis, initial and boundary conditions of (Longeon et al. 2013) are adopted in the present study as follows:

(i) The tube thickness is considered;

(ii) The thermo-physical properties of HTF and PCM are constant with respect to the temperature except the density in the buoyancy term (Boussinesq approximation)

(iii) The initial temperature of the latent thermal storage unit is uniform;

(iv) HTF flow is laminar, unsteady and incompressible;

(v) Inside the PCM the Boussinesq approximation is assumed to express the density variations and buoyancy force:$\rho = \rho_0[1 - \beta(T - T_m)]$ and $F = -\rho g = \rho_0 g\,[\beta(T - T_m) - 1]$, where ρ_0 is the reference density at melting temperature T_m and β is volumetric expansion coefficient.

From the experimental study of the literature (Longeon et al. 2013), the charging process (melting) starts when the HTF flows downward inside the tube by total inlet temperature 52°C and velocity magnitude of 0.01 m/s, whereas this process initialized at temperature of 22°C which is lower than the melting temperature $T_{ini} < T_m$.

4.3.3 Grid mesh independency

In the second study the plots of Fig 4.13 a and 4.13 b show the typical grid distribution over the computational domain of the configuration. The grid size used in the computations is chosen by performing a grid independency study (see Fig 4.14) of the model in the PCM temperature distribution at the point a (see Fig 4.12 c). Several meshes were tested to ensure that the solution was independent of the grid size 11900, 18000 (chosen) and 25400. A non-uniform Quadratic elements type of mesh has been used to simulate a 2D-planar geometry These structured Quadratic cells are created with fine mesh near the walls using mesh generation software ANSYS GAMBIT 2.4.6. The computational grids in the (xy) plan have been obtained based on the HTF regime in order to obtain a first grid space appropriate for the boundary layer to orderly progress in the energy transfer between the HTF and PCM. Moreover, the time step independency from the melt fraction was checked at 1s, 0.5s (chosen), and 0.1s. The temperature at point a was chosen as test parameter; and after careful examination of the independency, the results has indicated that 18000 cells with time step $\Delta_\tau = 0.5s$ are adequate for the simulations accuracy and time optimization.

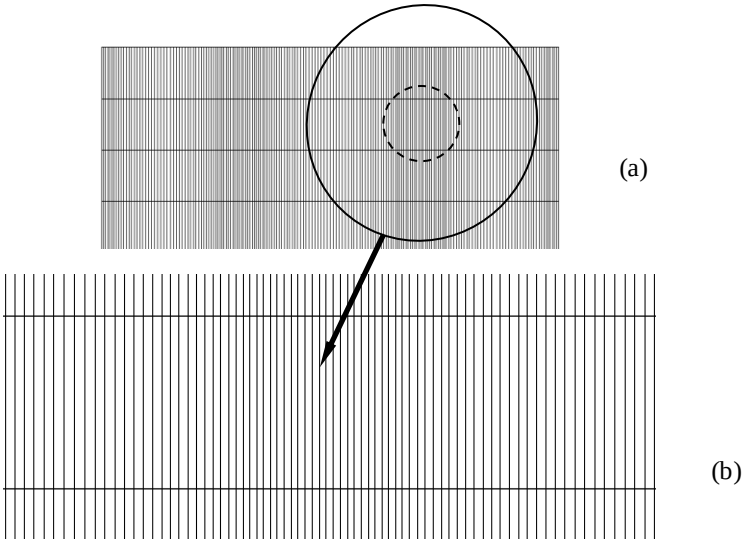

Fig 4.13 *Typical grid distribution (a) and zoom case (b)*

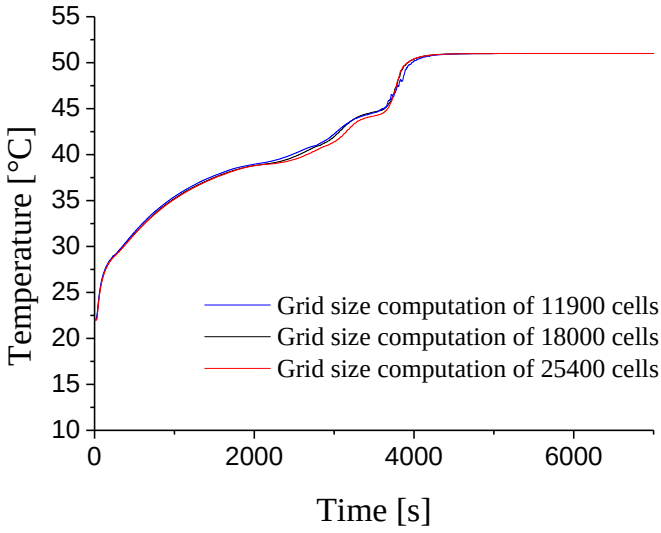

Fig 4.14 *Independency test for different grid size cells during melting process at point a*

4.3.4 Results and discussion

4.3.4.1 Validation

A comparison with the experimental and numerical investigations of the literature (Longeon et al. 2013) has been performed to validate the numerical model. The downward flow (top HTF injection) of the hot HTF (51°C) has been used in this study, this descent circulation has been used experimentally by (Longeon et al. 2013) during the melting process of the organic material (RT35) having a melting point of 35°C. Three points in the radial direction of the section D at the PCM right region have been chosen in order to control the PCM temperature during charging process. A good agreement has been found comparing our results and those obtained by (Longeon et al. 2013) as depicted in the Fig 4.15. The small discrepancy between the numerical result and those obtained experimentally is due to the considered assumptions in the numerical model.

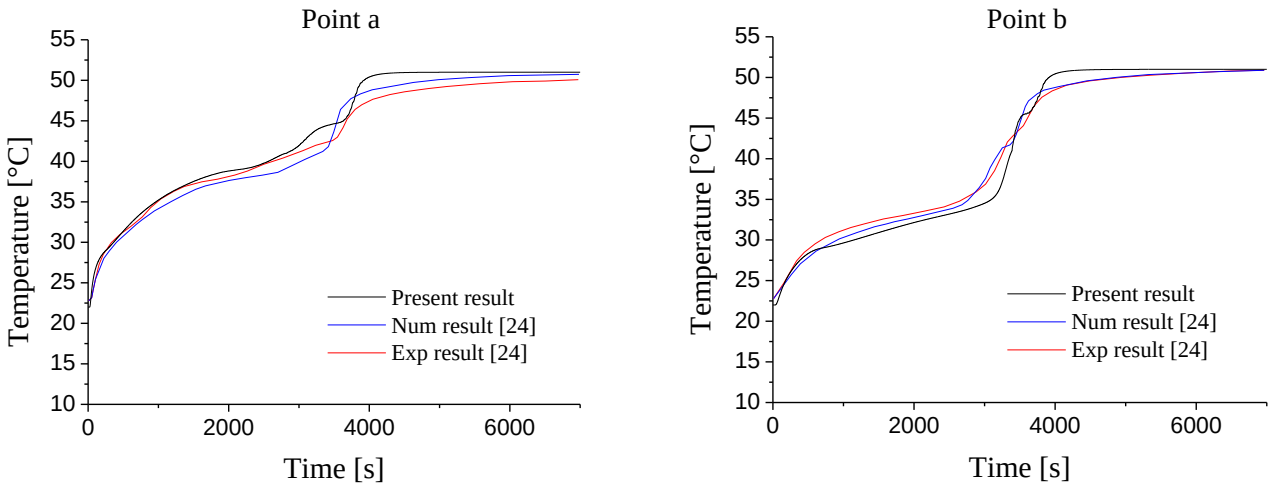

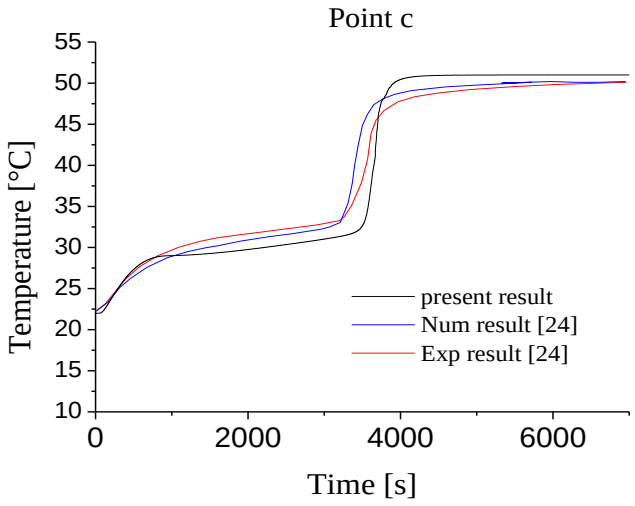

Fig 4.15 *Validation of the numerical model at points a, b, c during melting process.*

4.3.4.2 Parametric study

4.3.4.2.1 Heat transfer modes Evaluation

In such configuration, the heat exchange inside the vertical enclosure space containing the PCM can be explained in two cases (with and without gravity). In the first one the gravity forces are neglected, consequently the heat transfer is activated only via conduction mode. On the other hand, when the gravity forces are considered, the heat exchange employs through the conduction and natural convection (combined mode). In order to estimate the gravity forces effect on the heat exchange, a numerical experiment has been done with and without the gravity forces on the vertical TES unit (see Fig 4.17). The Fig 4.16 displays the PCM temperature that is evaluated radially at the plan D via three points (a,b,c) of both PCM regions as mentioned previously in Fig 4.12 a and 4.12 c; this parameter is controlled by pure conduction and combined mode (conduction and convection) during PCM melting process which has been estimated experimentally about t= 7000s by the author Longeon et al.(Longeon et al. 2013). In the pure conduction, the progress of PCM melting front is presented in four time steps: $\frac{1}{4}$t, $\frac{1}{2}$t, $\frac{3}{4}$t, t. In such case, the HTF starts to transfer the heat into the inner wall of the tube via the laminar forced convection flow, where the tube receives this heat energy and spreads it toward the solid PCM by conduction. The contour of liquid fraction clarifies in the Fig 4.17 case (a) the melting rate progress for the pure conduction heat transfer mode (without gravity) in the vertical unit. From this figure, it can be shown that there is a regularity in the melting rate for both of PCM regions; because all of the axial points of melting front has a similar value while the radial points are gradually different in each time steps of melting process, this would indicate that we have a uniform progress in the vertical lines that express the molten PCM move towards the inner wall of the shell. This observation indicates that there is an axial symmetry

in the PCM liquid fraction inside the shell annulus as displayed in the Fig 4.17 case (a).

As well know that a heat transfer by combined mode in the solid-solid contact is basically performed by conduction heat transfer, the solid PCM initially starts to absorb the heat from the outer surface of the HTF tube, generally this process is faster in the solid surroundings due to its significant thermal conductivity compared to the liquids state, after that a first liquid layer of the PCM is formed around the HTF outer tube wall and becomes larger near the beginning of the hot HTF inlet at a quarter charging time $\frac{1}{4}t$ as shown in the Fig 4.17 case (b) . Here starts the activity of the natural convection on the PCM density variations between cold and hot PCM (solid and liquid respectively) as consequence of the gravity presence $\vec{g}$, the melted zone becomes larger through the buoyancy force move which try to drive the recirculation from the bottom to the up part of the PCM region, this mechanism becomes more agitate as a result of the PCM liquid occupied on the majority of the annular space. A direction of the recirculation cycle from the HTF outer tube wall toward the inner wall of the shell due to the variation in the axial and radial PCM temperatures makes the PCM solid is visualized as a conical shape; as a consequence of the heat flux emitted by downward passage of the hot HTF, which allows to focus and increase the heat transfer in the outer tube wall near the HTF inlet compared to the outer surface tube near the HTF outlet that is leading to tilt the solid-liquid interface from the shell inner wall to the outer sides of the HTF tube. These advances were observed over time $\frac{1}{2}t$, $\frac{3}{4}t$ as displayed in the Fig 4.17 case (b) in which the melting process seemed semi-complete at the total time t=7000s. According to this, the PCM temperatures evaluation has been controlled in both of heat transfer modes via three points placed radially on the one straightness in both of PCM regions at the plan D as clarified in the Fig 4.12.c.

The evaluation has shown a significant difference between two heat transfer modes at the same operation conditions, where the temperature of point a between pure conduction and combined heat transfer mode has made a temperature difference $\Delta_t = 7°C$ at the end of the charging cycle, with regard to the points b and c, their temperature difference Δ_t is estimated about 13°C and 15°C respectively. We can say according to the appraisal of temperature distribution and liquid fraction of PCM between two heat transfer modes that the combined heat transfer is the most dominant mode on the heat interchange during melting process, while the pure conduction has less effectiveness on the heat transfer progress; the reason lies in the buoyancy force of the PCM which is influenced by the gravity forces. Other important reasons have assisted the natural convection function was the use of a vertical shell and tube cylinder that gives a freedom to the heat recirculation drive from the bottom to the up part by means of the difference temperature between the upper and lowest PCM part. Moreover, the down warding flow of the hot water helps to accelerate the buoyancy force in this status, where it has shown a strong effectiveness on the melting rate and charging process time according to the numerical results of (Longeon et al. 2013) which

have examined both of top and bottom HTF injection on melting process. From the Fig 4.17 case (b), the PCM upper part is melted and extended radially near the top (HTF inlet flow), which contributes to facilitate the rise of hot liquid PCM from the lowest part into the upper layer of the PCM solid as a result of the natural convection mechanism, this cycle leads to increase the PCM molten rate during the time.

Thus the sudden elevation of temperature in the points a, b and c was caused of the combined mode influence on the molten PCM rate variation that leads to increase the heat transfer recirculation inside PCM. As a consequence of the heat transfer modes analysis, we have deduced from the previous results that the melting process of the PCM has exceeded two steps: (i) heat transfer by pure conduction mode, where this phase includes the heat absorption by the solid PCM and depends on the nature of PCM thermal conductivity and (ii) heat transfer by combined (conduction and convection) mode which begins effected when the first transition from the solid to the liquid PCM state is occurred, so both of heat transfer modes are complement each other and have an efficient role to improve the heat transfer behavior of PCM melting process as shown in the previous plots.

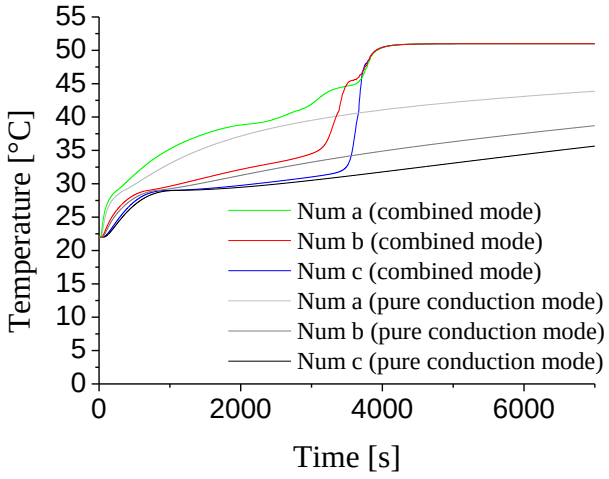

Fig 4.16 *PCM temperature variations in pure conduction model and combined model (conduction and convection) at alpha=0°during melting process.*

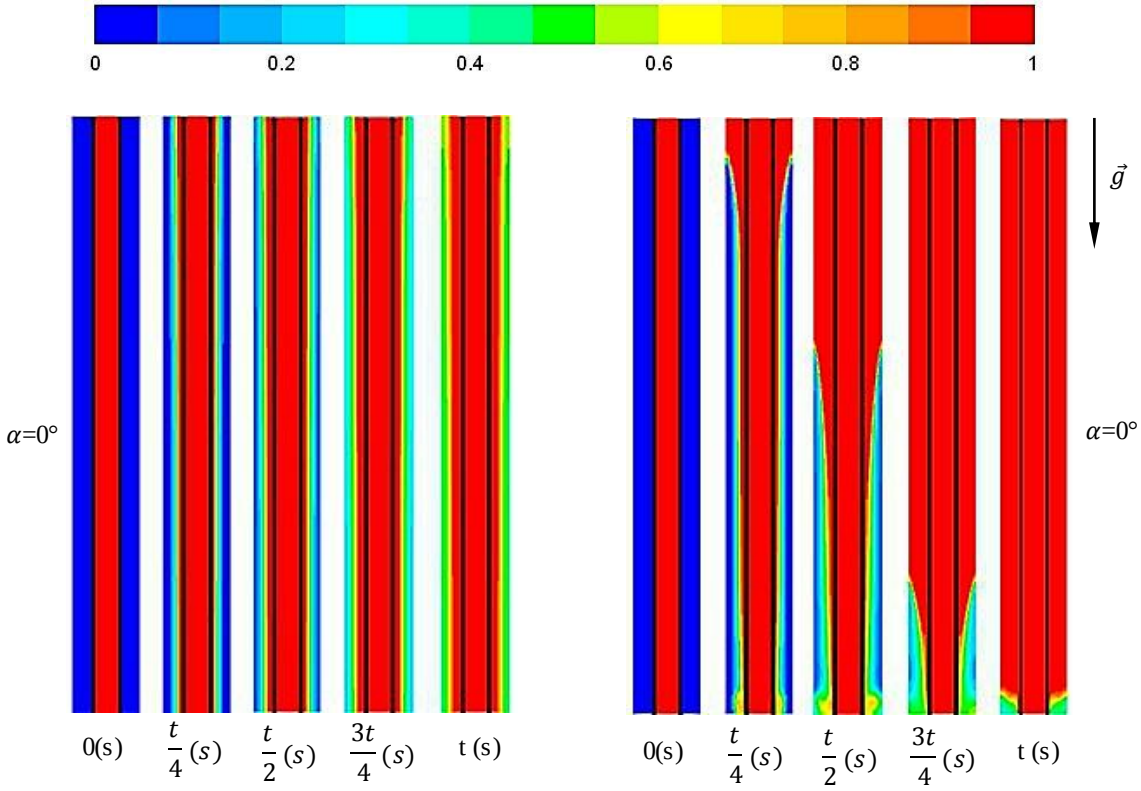

Fig 4.17 *Liquid fraction contour of Pure conduction (a) and combined heat transfer mode (b) at alpha=0°*

4.3.4.2.2 Effect of the unit inclination on the PCM melting front

Numerous studies proved that the configuration geometric kind in terms of shape and position has high influence on the thermal performance of TES systems as mentioned previously in the introduction section. In the present study, the effect of a shell and tube inclination from the vertical to the horizontal position according to the following inclination angles α (15°, 30°, 45°, 60°, 75°, 90°) with downward HTF traffic has been carried out in order to appraise the PCM melting process in terms of its liquid fraction progress. Fig 4.18 clarifies the melting front progress in four time steps $\frac{1}{4}$t,$\frac{1}{2}$t,$\frac{3}{4}$t, and t for different tilt angles from 0° to 90°. The vertical unit (0°) case shows the natural convection effect on the heat transfer interchange between the solid-liquid PCM interface, the rise and fall of the formed liquid layer inside a vertical cylinder made the recirculation aggrandize over time, which has made the hot liquid fraction overcomes to the solid PCM portion, that shows the conical shape formation as a trace of the recirculation mechanization, this is conform with the experimental results of Wang et al.(Wang et al. 2016).The effect of the system inclination on the PCM solid-liquid fraction starts to appear at a quarter time of the process $\frac{1}{4}$t from the range (60°- 90°), in this positions, the left region of the PCM shows a marked change in the molten PCM compared to the right region, where the PCM liquid layer has been created under the PCM solidus, which helps the PCM liquid to rise and extend in the top part of the PCM

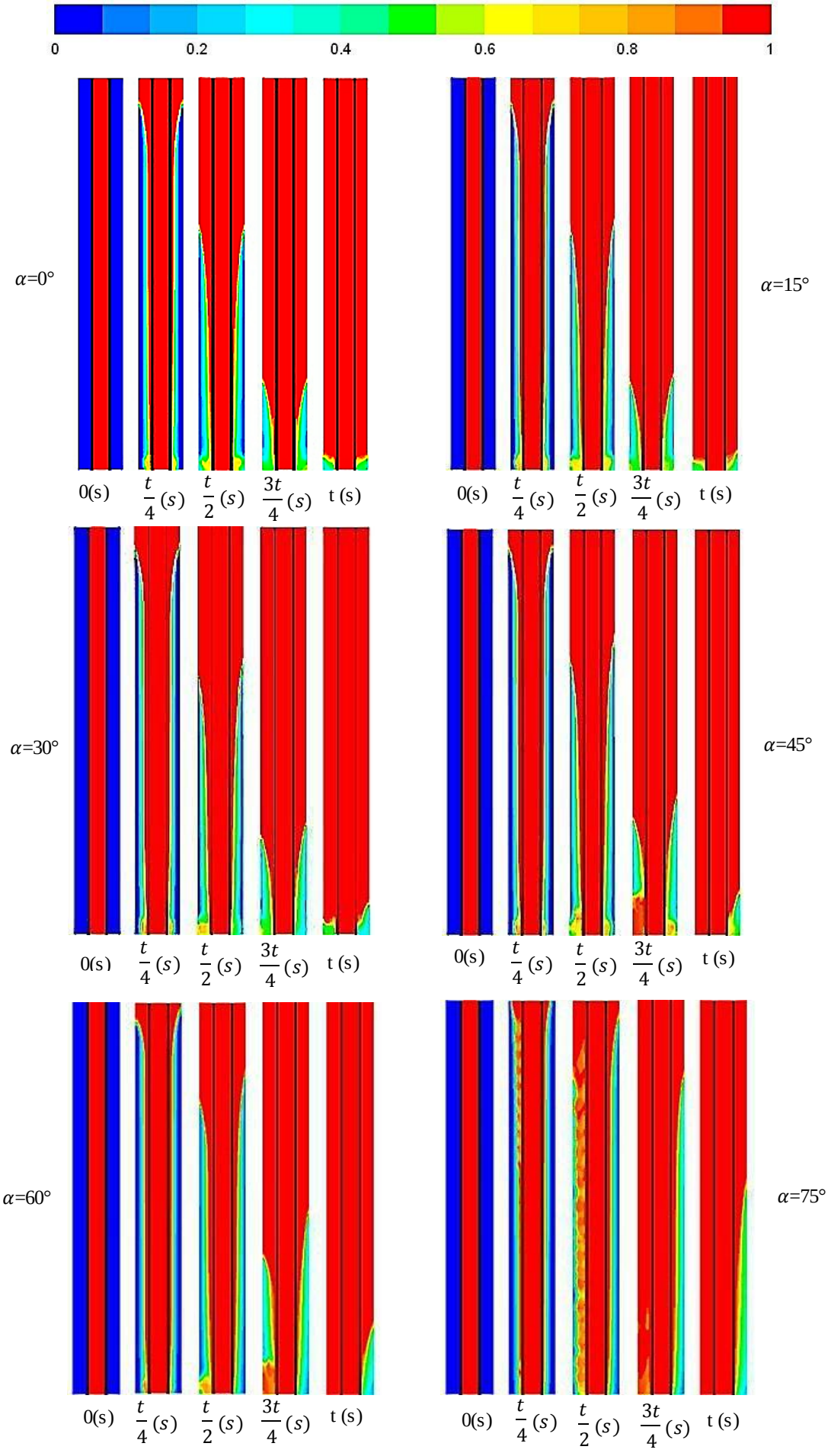
0
0.2
0.4
0.6
0.8
1
α=0°
0(s)
$\frac{t}{4}(s)$
$\frac{t}{2}(s)$
$\frac{3t}{4}(s)$
t (s)
α=15°
0(s)
$\frac{t}{4}(s)$
$\frac{t}{2}(s)$
$\frac{3t}{4}(s)$
t (s)
α=30°
0(s)
$\frac{t}{4}(s)$
$\frac{t}{2}(s)$
$\frac{3t}{4}(s)$
t (s)
α=45°
0(s)
$\frac{t}{4}(s)$
$\frac{t}{2}(s)$
$\frac{3t}{4}(s)$
t (s)
α=60°
0(s)
$\frac{t}{4}(s)$
$\frac{t}{2}(s)$
$\frac{3t}{4}(s)$
t (s)
α=75°
0(s)
$\frac{t}{4}(s)$
$\frac{t}{2}(s)$
$\frac{3t}{4}(s)$
t (s)

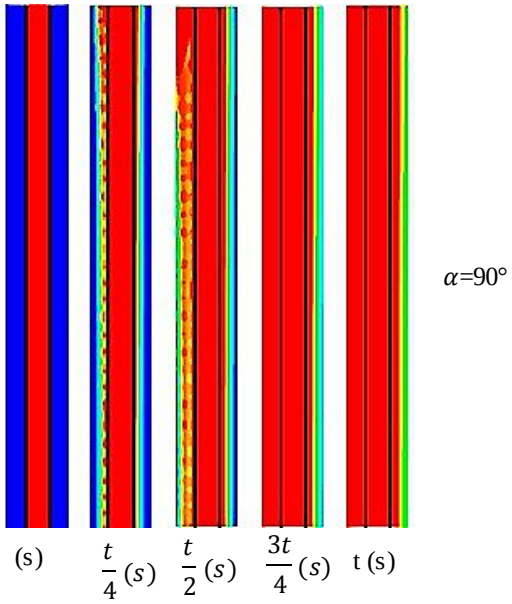

Fig 4.18 *Liquid fraction of combined heat transfer mode at various inclination angles*

In contrast, the PCM liquid layer of the PCM right region seems a low in quantitative terms, resulting from through its emergence above the PCM solid fraction during the inclination, therefore the density weightiness of solid PCM hinders the PCM liquid layer to incursion and expand into the shell inner wall. However, when the melting process reached to the half time$\frac{1}{2}$t, the changes are beginning to appear on the molten PCM shape from the inclination range (30°- 90°), in which the buoyancy force starts to effect on the PCM melting rate extend inside the PCM left region, where the heat recirculation become more freedom through the solid PCM immersion over the PCM liquid due to its solid density weightiness which presses on the middle of hot PCM liquid layer that contributes to drive the recirculation from the upper and lowest sides of the PCM. In the same context, there is no positive change in the PCM right region, where the PCM liquid fraction begins to increase slowly whenever the inclination of the system augment as clarify from the liquid fraction contours. The next transitional phase has shown the unit of storage inclination effect on the buoyancy forces effectiveness in both of PCM region at$\frac{3}{4}$t, during this phase; the buoyancy force drives the recirculation from the sides of the solid PCM left region, which contributes to melt the majority of the solid fraction via besieged the PCM solid from all sides.

The other PCM region experienced a great slowing down in the melting process, so that about half PCM quantity has not melted as a result of the recirculation drive weakness, therefore the unit tilting until 90° at melting process time t=7000 has made the total PCM solid portion can seems as crescent shape under the tube as obtained in the radial plan of the literature (Wang et al. 2016), which not clear here in the (xy) plot. These PCM liquid fraction evolutions were a result of an imbalance in the buoyancy

force inside a left and right PCM region during inclination system at fusion process, while the buoyancy balance was only in the initial case (0° of tilt), so that showed a similarity in the molten PCM shape compared to the other cases. True that there is a natural convection effect on the melting speed of the PCM left region; this does not mean that it is favorable for the storage system of the unit, whilst if we analyze the amount of the PCM solid remaining in each inclination case we will find that the initial case (0° of tilt) has a small quantify of PCM solid portion due to the uniform buoyancy force effect in both of PCM regions. It can be concluded that the PCM unit inclination at downward HTF flow has a negative effect on total PCM melting rate; this is due to the irregular heat transfer area in the PCM surfaces as a result of the natural convection lopsidedness inside the unit, where it has a big scale in the PCM left region compared to the second one.

4.3.4.2.3 Effect of the unit inclination on the PCM temperatures distributions

The change of the molten PCM fraction during the system inclination of the tilt interval (0°-90°) can be explained by the variation and evolution of the axial and radial PCM temperature during melting process, whereas that the axial PCM temperature distribution is the main reason to alteration the PCM radial temperature. In this section, we have evaluated the effect of the system inclination on the temperatures distributions inside PCM, where the Fig 4.19 and 4.20 show the axial temperature distributions in both of PCM regions during melting time of t=7000s, where the axial temperatures fluctuations have been appraised in the point b of each plan A, B, C, D, E, F, G at every time steps according to the tilt position that it is.

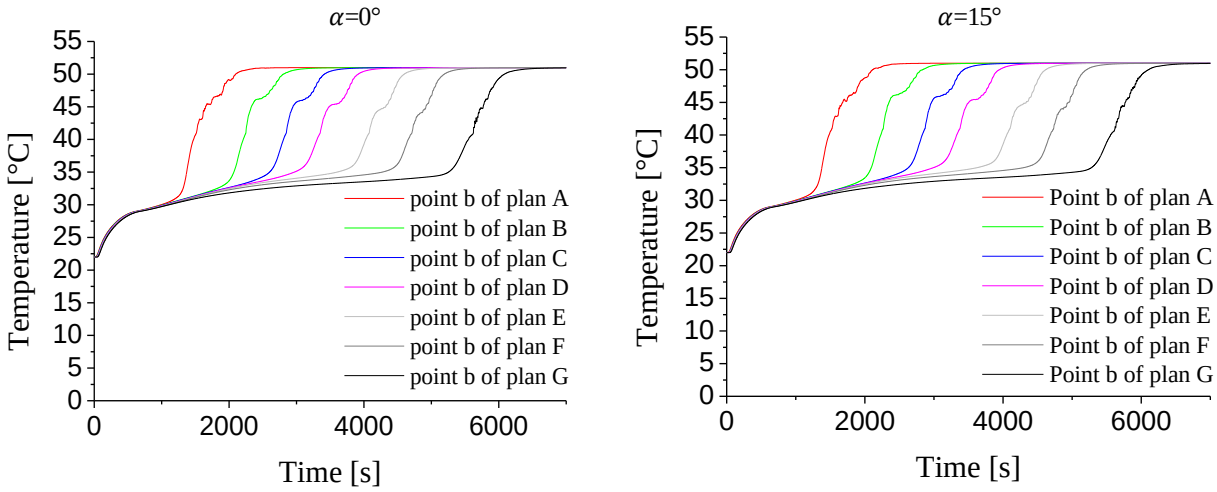

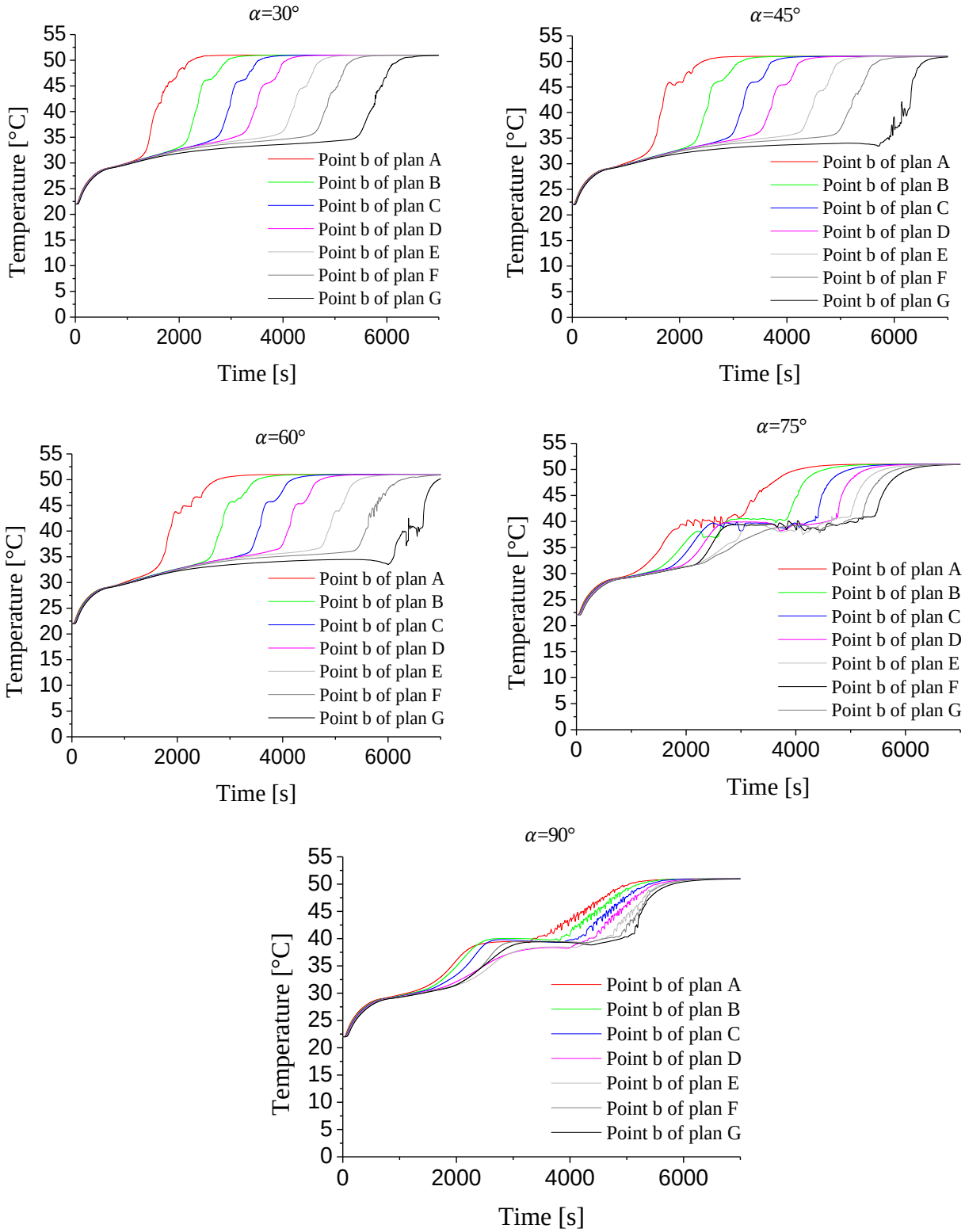

Fig 4.19 *Axial temperature distributions in different plants of the PCM left region*

The vertical case (0° of tilt) have illustrated a similar fluctuation in the axial temperature distributions inside right and left region of the PCM, where it attests a disparity from the plan A to G, this agrees with what is physically occurring within the unit, where the hot HTF flows downward inside the tube, therefore it starts to wastage the heat transfer from the top to the bottom due to the PCM heat

absorption, and this is what did Fig 4.19 and 4.20 explain in the initial case 0°, there the temperature stability is fully different at the point b of each plan, so that the total temperature in the point b of the plan A has taken about 2250s to satiate, while the same point in the plan G has occupied more than 3000s to saturate, there is almost unevenness by 1000s in the temperature saturation between each plan, which explains the formation of PCM liquid fraction in the shape of conical as clarify in the vertical case and indicates a regular distribution of axial and radial temperature in both of PCM regions as displayed in the Fig 4.19 ,4.20 and 4.21 at initial case (0° tilt).

After that, we have observed a dissimilar progress in the axial and radial temperature distributions between left and right PCM region during the inclination of the system from 15° to 90° at charging process as depicted in the Fig 4.19 , 4.20 and 4.21, the reason for that is the natural convection effect which has dominated profusely in the left PCM region compared to the other region, this variation in turn causes to the negative influence on the radial temperature distribution as shown in the Fig 4.20 which at the same time affecting the efficiency of the recirculation. It is true that the axial temperature distribution is gradually changed in both of PCM regions, but the effectiveness lack of the natural convection in the right PCM region as a result of the inclination makes the upper limit value of the axial temperature has diminished in this region from 51°C towards 39°C between the tilt interval (0°-90°) as demonstrated according to the Fig 4.19, a marked decline of temperature distributions as a result of the TES inclination and this has adversely affected on the PCM liquid fraction and unit storage system as a whole.

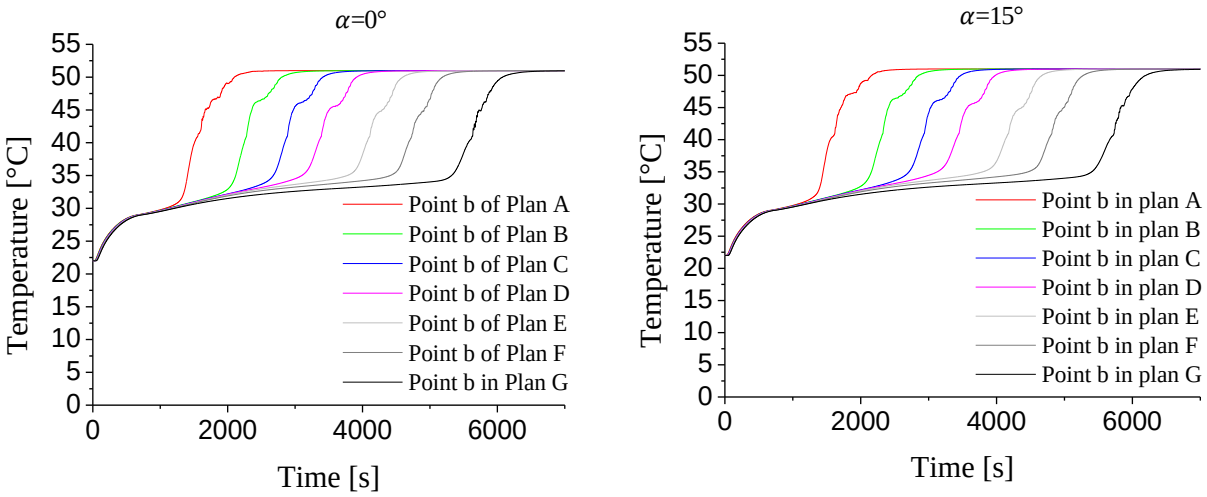

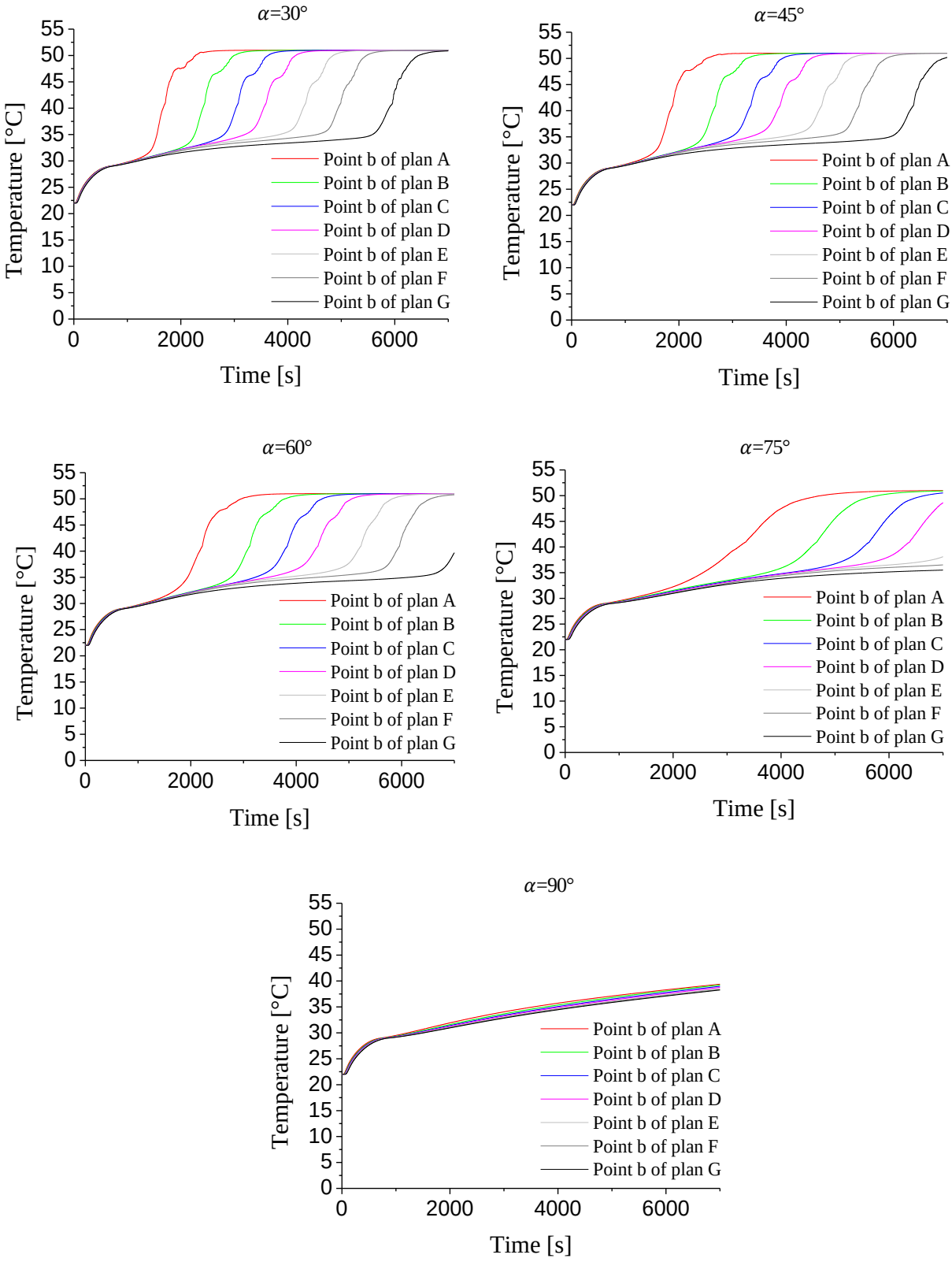

Fig 4.20 *Axial temperature distributions in different plans of the PCM right region*

On the other hand the left region is kept on the maximum temperature ratio in all points b, which is axially located on the level of plans A to G, there was only a troubled and non-uniform advancement in

the axial temperature fluctuations, these fluctuations can be imputed to the unstable flow structures in the liquid PCM. There the axial temperatures in the range of angles (0°-30°) increases uniformly, with no significant fluctuations, against this we observe that the temperatures at the interval tilt (45°-90°) began to fluctuate; these fluctuations can be justified by the presence of irregular convection cells in the PCM solid-liquid interface along the unit, whereas the system tilting leads to scale down the time difference Δ_t between the PCM axial points to reach a same uttermost temperature, as a result of the heighten in the recirculation agitation; where the axial temperature transfer from the plan to the other has been conducted in short interval time when the system tilt has been changed from the angle 0° to 90° as shown in the Fig 4.18. These results are conform to those obtained by Kousha et al. (2017), where the inclination system attested a sudden positive leaping on the axial PCM temperature progress in the vertical state by HTF upward flow against the unit horizontal case at full melting time. Moreover, the plan D witnessed a variation of the radial temperature distributions at the points a, b, c of both PCM regions. The beginning of the change has been appeared at the tilt interval (15°-60°), where the temperatures distributions in both PCM regions have taken a longer time to reach the supreme limit value as clarified in the Fig 4.20.

After that, the radial temperature data has changed completely so that it has exhibited a diminution in the right PCM region and non-stability of the temperatures fluctuations in the other region. Accordingly, we can say that a heat transfer inside a slanted shell and tube makes the temperatures distributions unequal inside a shell annulus; therefore will affect on the creation of the liquid PCM shape which contributes to strengthen the recirculation cycle inside it. Furthermore, we have concluded that the vertical position of the unit have a positive advantage on the PCM liquid recirculation in our condition work as a result of descending HTF flow that extends the upper molten PCM which gives the rising PCM liquid layer a great freedom uniformly in the movement compared to the horizontal status, whereupon we can obtain a perfect storage system in the vertical installation in terms of HTF outlet temperature inasmuch to the similarity of the PCM temperature distribution of both of PCM regions.

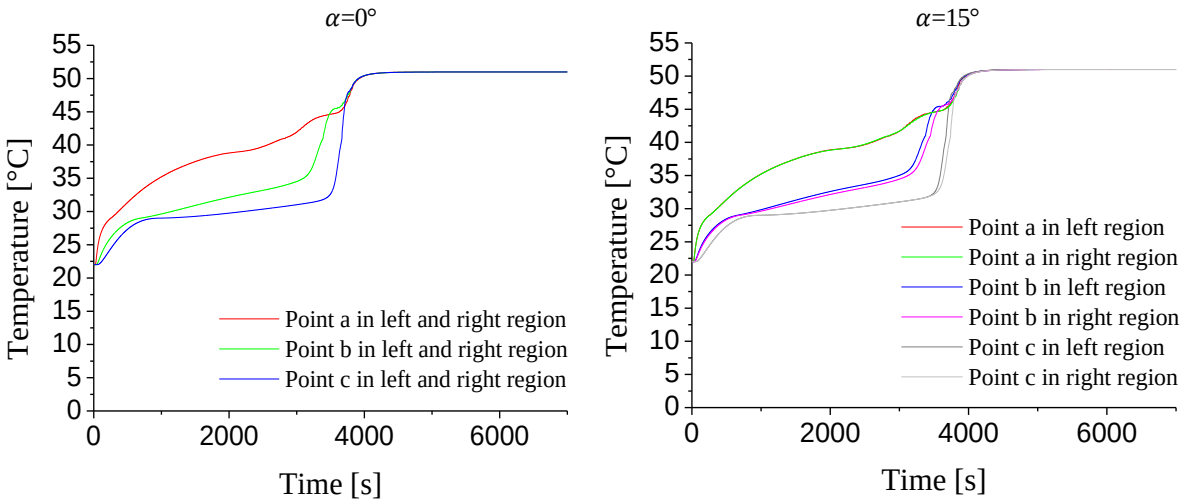

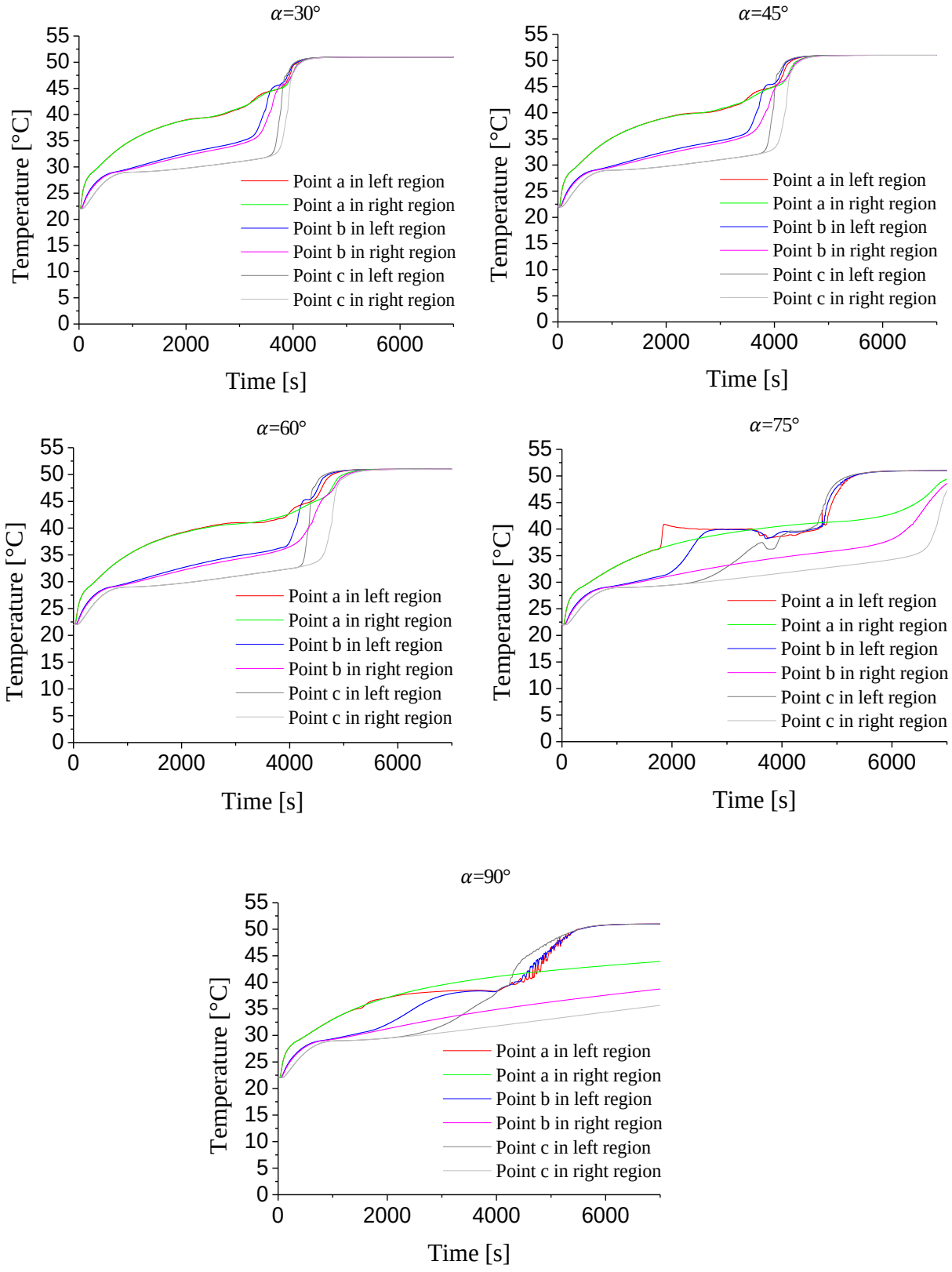

Fig 4.21 *Radial temperature distributions in plant D of the PCM right and left region*

4.4 Conclusion

As the appropriate choice of the physical and geometric parameters allows to optimize the thermal storage unit, the first section of the present study was devoted to examine the effect of these parameters on the shell and tube thermal energy storage unit that investigated previously by (Kibria et al. 2014). Moreover, improvements of this storage unit were investigated through new configurations. A two-dimensional numerical method based on the Enthalpy formulation has been used to predict the heat transfer between HTF and PCM. The laminar forced convection inside the tube during charging and discharging process was considered, whereas the natural convection has been ignored inside the PCM enclosure. A parametric study has been conducted in order to study the effect of the tube length, shell diameter and Reynolds number. Improvement of the thermal performances of this unit was proposed and investigated. The results of the parametric study have shown that the tube length and shell diameter have a great effect on the HTF outlet temperature, moreover the Reynolds number is the most influential parameter which has an impact on the time and rate of solidification and melting process.

From the present results, the design parameters should be selected carefully in order to optimize the performance of the storage unit. In addition to that, the new thermal energy storage unit filled by RT60 and Paraffin wax allowed for better efficiency of the rate storage and HTF outlet temperature compared to the unit containing only the Paraffin wax.

Specially the configuration which has filled by RT 35. We have noticed in the second inquiry that The effect of inclination system from 0° to 90° have shown that the PCM radial temperature distribution in the plan D according to the points a, b, c has been reduced gradually in the PCM right region compared to the left region which attests a sudden diminution during melting process. The same behavior has been observed in the axial temperature distributions, i.e the system tilting has caused a progressive reduction of the temperature from the top plan A to the lowest one G at the same point b; whereas, the PCM right region was the most affected as a result of the tilting operation compared to the left zone. Among the inclinations studied, the initial case (0° of tilt) which represents the vertical position showed a regularity and uniformity in the PCM temperature distribution and the fractionation of the molten PCM. The numerical results revealed that the heat transfer in combined mode for the vertical position is the responsible to improve the heat exchange between the HTF and PCM, where the recirculation has contributed to increase the molten PCM which led to augment the PCM storage density. Concerning the natural convection inside the inclined TES unit, a passive effect on the recirculation inside PCM liquid was noticed, where it has showed irregularity in the molten PCM fraction which in turn led to a non-stability in the radial and axial PCM temperature.

General Conclusion

General Conclusion

An extensive review has been conducted concerning the use of PCMs in thermal storage tanks, focusing on both commercial equipment and experimental studies. PCMs are used inside the tanks, either for heating or cooling applications, by means of different kinds of systems. A common solution is to have PCM in a pipe inside the tank; however PCMs are also widely used and have been studied extensively inside cylindrical shell and tube thermal energy storage unit.

In order to obtain on the perfect heat exchange between the PCM and the fluid, many configuration geometrics have been suggested. Shell-and-tube geometry is the most widely used geometry in different studies. As a result of its simple design, we have used it as the preferable model to study the phase change physical phenomena of PCM.

A common issue of PCM systems is the reduction in the heat transfer rate that occurs due to the formation of a solid film around the heat exchanger surfaces. Many solutions have been proposed in the literature to minimize this problem, such as employing fins of different geometries or introducing high conductivity elements. Heat transfer may also be enhanced increasing the heat exchange surface available in the tanks such as for instance using parallel plates.

A wide range of compounds can be used as PCMs, but they are normally classified into organic compounds, inorganic compounds and eutectic compounds. Each kind of compound has their advantages and disadvantages concerning criteria such as latent heat, thermal conductivity, safety, physical-chemical stability or price.

The main factor for the selection of the correct PCM is the phase change temperature (or temperature range), which depends on the application and on the source that provides the thermal energy. Heat pumps, used for heating or cooling, have a quite limited temperature range, as the working temperatures have a great effect on their behaviors. Consequently, the types of PCMs that can be used with heat pumps are limited.

The advantage of using PCMs is that it is possible to reduce the size of the tank due to the higher thermal energy storage density. This is highly important from a commercial point of view, irrespective of the heat source.

In the present work, we have presented an energy storage system in general terms for different energy kind and especially for the thermal energy in order to evaluate it thermo-hydraulically. We have made two studies; the first one witnessed a numerical investigation on the heat transfer evaluation of the shell and tube TES unit filled by paraffin wax. The physical model used here is assumed as two dimensional, where the PCM phase change phenomena is analyzed by the Enthalpy formulation that drive by the commercial code Ansys Fluent 17 during solidification and melting process. The physical processes validation is conducted successfully by comparison against experimental and numerical results of the

literature. The objective of this study is carry out the effect of the geometric and the physical parameters on the heat storage efficiency of the unit such as; tube length, shell inner diameter and Reynolds number variation. The second part of this study includes the modification of a shell and tube design, where a new configuration is conceived which is longitudinally filled by two PCMs (RT60 and Paraffin wax) that have close melting temperatures. The second contribution has been conducted here about the inclination effect on the melting process of RT35 Organic material. The numerical simulations of the phase change is done along about 7000s during solidification and melting process, where several observations are extracted and summarized as follow:

- Both of shell and tube sizes (consequently the volume of PCM) have a strong effect on the storage time, where a reduction these sizes leads an early charging and discharging.
- The increase of the flow regime in terms of Reynolds number in the range 100-1500 leads to enhance the HTF outlet temperature early.
- Concerning the new geometric design, two superposed PCMs and separated by a second tube filled the longitudinal space of the shell in different quantities. Two cases are conceived and assessed: (i) case A shows the expansion of RT60 volume with reduction the paraffin wax portion as the total volume is maintained constant, (ii) while for the case B, the volume of RT60 is changed in the radial direction with respect a constant volume of the paraffin wax. The outcomes of this conception show a positive advantage in the addition of RT60 on speed up the charging, where the case B more stable.
- The unit inclination effect from the vertical to the horizontal case on melting process of RT35 has been shown a negative point on the solid-liquid interface of molten PCM and temperature distribution inside the PCM volume as whole.

References

References

Abhat, A. (1983) Low temperature latent heat thermal energy storage: heat storage materials. *Solar energy,* 30**,** 313-332.

Arena, S. 2016. Modelling, design and analysis of innovative thermal energy storage systems using PCM for industrial processes, heat and power generation. Universita'degli Studi di Cagliari.

de Gracia, A. & L. F. Cabeza (2015) Phase change materials and thermal energy storage for buildings. *Energy and Buildings,* 103**,** 414-419.

Farid, M. M., A. M. Khudhair, S. A. K. Razack & S. Al-Hallaj (2004) A review on phase change energy storage: materials and applications. *Energy conversion and management,* 45**,** 1597-1615.

Galazutdinova, Y., M. Grágeda, L. F. Cabeza & S. Ushak (2017) Novel inorganic binary mixture for low-temperature heat storage applications. *International Journal of Energy Research,* 41**,** 2356-2364.

Garg, H., S. Mullick & V. K. Bhargava. 2012. *Solar thermal energy storage*. Springer Science & Business Media.

Ge, H., H. Li, S. Mei & J. Liu (2013) Low melting point liquid metal as a new class of phase change material: An emerging frontier in energy area. *Renewable and Sustainable Energy Reviews,* 21**,** 331-346.

Gschwander, S., A. Lazaro, L. F. Cabeza, E. Günther, M. Fois & J. Chui (2011) Development of a Test Standard for PCM and TCM Characterization Part 1: Characterization of Phase Change Materials. *IEA Report A,* 2.

H Abedin, A. & M. A Rosen (2011) A critical review of thermochemical energy storage systems. *The open renewable energy journal,* 4.

Huggins, R. A. 2010. *Energy storage*. Springer.

Hyun, D. C., N. S. Levinson, U. Jeong & Y. Xia (2014) Emerging applications of phase-change materials (PCMs): teaching an old dog new tricks. *Angewandte Chemie International Edition,* 53**,** 3780-3795.

Kandalkar, G., S. J. Deshmukh & R. R. Kolhekar Latent Heat Storage for Cooling Application: A.

Kerskes, H., B. Mette, F. Bertsch, S. Asenbeck & H. Drück (2012) Chemical energy storage using reversible solid/gas-reactions (CWS)–results of the research project. *Energy Procedia,* 30**,** 294-304.

Kumar, A. & S. Shukla (2015) A review on thermal energy storage unit for solar thermal power plant application. *Energy Procedia,* 74**,** 462-469.

Lane, G. A. (1983) Solar heat storage: latent heat materials.

Liu, C. & Z. Rao (2017) Challenges in various thermal energy storage technologies. *Sci. Bull,* 62**,** 231-233.

Mehling, H. & L. F. Cabeza. 2008. Solid-liquid phase change materials. In *Heat and cold storage with PCM,* 11-55. Springer.

Patil, N., P. Das, S. Bhattacharyya & S. Sahu (2012) An experimental assessment of cooling of a 54-rod bundle by in-bundle injection. *Nuclear Engineering and Design,* 250**,** 500-511.

Ravikumar, M. & P. Srinivasan (2008) PHASE CHANGE MATERIAL AS A THERMAL ENERGY STORAGE MATERIAL FOR COOLING OF BUILDING. *Journal of Theoretical & Applied Information Technology,* 4.

Sarbu, I. & C. Sebarchievici (2018) A Comprehensive Review of Thermal Energy Storage. *Sustainability,* 10**,** 191.

Sharma, A., V. V. Tyagi, C. Chen & D. Buddhi (2009) Review on thermal energy storage with phase change materials and applications. *Renewable and Sustainable energy reviews,* 13**,** 318-345.

Socaciu, L. G. (2012) Thermal energy storage with phase change material. *Leonardo Electronic Journal of Practices and Technologies,* 20**,** 75-98.

Yu, B. F., Z. K. Wang, X. Fang & Z. Q. Ye. 2012. Research Progress of Personalized Content Management System. In *Applied Mechanics and Materials*, 862-866. Trans Tech Publ.

Zalba, B., J. M. Marín, L. F. Cabeza & H. Mehling (2003) Review on thermal energy storage with phase change: materials, heat transfer analysis and applications. *Applied Thermal Engineering,* 23**,** 251-283.

Adine, H. A. & H. El Qarnia (2009) Numerical analysis of the thermal behaviour of a shell-and-tube heat storage unit using phase change materials. *Applied Mathematical Modelling,* 33**,** 2132-2144.

Agyenim, F., P. Eames & M. Smyth (2009) A comparison of heat transfer enhancement in a medium temperature thermal energy storage heat exchanger using fins. *Solar Energy,* 83**,** 1509-1520.

Agyenim, F., N. Hewitt, P. Eames & M. Smyth (2010) A review of materials, heat transfer and phase change problem formulation for latent heat thermal energy storage systems (LHTESS). *Renewable and Sustainable Energy Reviews,* 14**,** 615-628.

Akgün, M., O. Aydın & K. Kaygusuz (2007) Experimental study on melting/solidification characteristics of a paraffin as PCM. *Energy Conversion and Management,* 48**,** 669-678.

Al-Abidi, A. A., S. Mat, K. Sopian, M. Y. Sulaiman & A. T. Mohammad (2013) Internal and external fin heat transfer enhancement technique for latent heat thermal energy storage in triplex tube heat exchangers. *Applied Thermal Engineering,* 53**,** 147-156.

Alva, G., L. Liu, X. Huang & G. Fang (2017) Thermal energy storage materials and systems for solar energy applications. *Renewable and Sustainable Energy Reviews,* 68, Part 1**,** 693-706.

Assis, E., L. Katsman, G. Ziskind & R. Letan (2007) Numerical and experimental study of melting in a spherical shell. *International Journal of Heat and Mass Transfer,* 50**,** 1790-1804.

Avci, M. & M. Y. Yazici (2013) Experimental study of thermal energy storage characteristics of a paraffin in a horizontal tube-in-shell storage unit. *Energy Conversion and Management,* 73**,** 271-277.

Cárdenas, B. & N. León (2013) High temperature latent heat thermal energy storage: Phase change materials, design considerations and performance enhancement techniques. *Renewable and Sustainable Energy Reviews,* 27**,** 724-737.

Castro, P. P., P. K. Selvam & C. Suthan (2016) Review On The Design Of Pcm Based Thermal Energy Storage Systems. *Imperial Journal of Interdisciplinary Research,* 2**,** 203-215.

Dutil, Y., D. R. Rousse, N. B. Salah, S. Lassue & L. Zalewski (2011) A review on phase-change materials: Mathematical modeling and simulations. *Renewable and Sustainable Energy Reviews,* 15**,** 112-130.

El Meriah, A., D. Nehari & M. Aichouni (2018) Thermo-convective Study of a Shell and Tube Thermal Energy Storage Unit. *Periodica Polytechnica Mechanical Engineering,* 1587-379.

El Qarnia, H. (2009) Numerical analysis of a coupled solar collector latent heat storage unit using various phase change materials for heating the water. *Energy Conversion and Management,* 50**,** 247-254.

Esapour, M., M. J. Hosseini, A. A. Ranjbar & R. Bahrampoury (2016) Numerical study on geometrical specifications and operational parameters of multi-tube heat storage systems. *Applied Thermal Engineering,* 109, Part A**,** 351-363.

Gasia, J., J. Diriken, M. Bourke, J. Van Bael & L. F. Cabeza (2017) Comparative study of the thermal performance of four different shell-and-tube heat exchangers used as latent heat thermal energy storage systems. *Renewable Energy,* 114**,** 934-944.

Hosseini, M. J., M. Rahimi & R. Bahrampoury (2014) Experimental and computational evolution of a shell and tube heat exchanger as a PCM thermal storage system. *International Communications in Heat and Mass Transfer,* 50**,** 128-136.

Hosseini, M. J., A. A. Ranjbar, K. Sedighi & M. Rahimi (2012) A combined experimental and computational study on the melting behavior of a medium temperature phase change storage material inside shell and tube heat exchanger. *International Communications in Heat and Mass Transfer,* 39**,** 1416-1424.

Kenisarin, M. M. (2010) High-temperature phase change materials for thermal energy storage. *Renewable and Sustainable Energy Reviews,* 14**,** 955-970.

Kibria, M. A., M. R. Anisur, M. H. Mahfuz, R. Saidur & I. H. S. C. Metselaar (2014) Numerical and experimental investigation of heat transfer in a shell and tube thermal energy storage system. *International Communications in Heat and Mass Transfer,* 53**,** 71-78.

Kousha, N., M. Hosseini, M. Aligoodarz, R. Pakrouh & R. Bahrampoury (2017) Effect of inclination angle on the performance of a shell and tube heat storage unit–An experimental study. *Applied Thermal Engineering,* 112**,** 1497-1509.

Li, Z. & Z.-G. Wu (2015) Analysis of HTFs, PCMs and fins effects on the thermal performance of shell–tube thermal energy storage units. *Solar Energy,* 122**,** 382-395.

Longeon, M., A. Soupart, J.-F. Fourmigué, A. Bruch & P. Marty (2013) Experimental and numerical study of annular PCM storage in the presence of natural convection. *Applied energy,* 112**,** 175-184.

Mosaffa, A. H., F. Talati, H. Basirat Tabrizi & M. A. Rosen (2012) Analytical modeling of PCM solidification in a shell and tube finned thermal storage for air conditioning systems. *Energy and Buildings,* 49**,** 356-361.

Seddegh, S., M. M. Joybari, X. Wang & F. Haghighat (2017) Experimental and numerical characterization of natural convection in a vertical shell-and-tube latent thermal energy storage system. *Sustainable Cities and Society*.

Seddegh, S., X. Wang & A. D. Henderson (2015) Numerical investigation of heat transfer mechanism in a vertical shell and tube latent heat energy storage system. *Applied Thermal Engineering,* 87**,** 698-706.

Sharma, S. D. & K. Sagara (2005) Latent heat storage materials and systems: a review. *International Journal of Green Energy,* 2**,** 1-56.

Sokolov, M. & Y. Keizman (1991) Performance indicators for solar pipes with phase change storage. *Solar Energy,* 47**,** 339-346.

Tao, Y. B. & V. P. Carey (2016) Effects of PCM thermophysical properties on thermal storage performance of a shell-and-tube latent heat storage unit. *Applied Energy,* 179**,** 203-210.

Tao, Y. B., Y. L. He & Z. G. Qu (2012) Numerical study on performance of molten salt phase change thermal energy storage system with enhanced tubes. *Solar Energy,* 86**,** 1155-1163.

Trp, A., K. Lenic & B. Frankovic (2006) Analysis of the influence of operating conditions and geometric parameters on heat transfer in water-paraffin shell-and-tube latent thermal energy storage unit. *Applied Thermal Engineering,* 26**,** 1830-1839.

Vyshak, N. R. & G. Jilani (2007) Numerical analysis of latent heat thermal energy storage system. *Energy Conversion and Management,* 48**,** 2161-2168.

Wang, W.-W., L.-B. Wang & Y.-L. He (2016a) Parameter effect of a phase change thermal energy storage unit with one shell and one finned tube on its energy efficiency ratio and heat storage rate. *Applied Thermal Engineering,* 93**,** 50-60.

Wang, Y., L. Wang, N. Xie, X. Lin & H. Chen (2016b) Experimental study on the melting and solidification behavior of erythritol in a vertical shell-and-tube latent heat thermal storage unit. *International Journal of Heat and Mass Transfer,* 99**,** 770-781.

Yang, X., Y. Li, Z. Lu, L. Zhang, Q. Zhang & L. Jin (2016) Thermal and Fluid Characteristics of a Latent Heat Thermal Energy Storage Unit. *Energy Procedia,* 104**,** 425-430.

Zhang, Y. & A. Faghri (1996) Heat transfer enhancement in latent heat thermal energy storage system by using the internally finned tube. *International Journal of Heat and Mass Transfer,* 39**,** 3165-3173.

Buchmann P.(1995) Modélisation numérique de la convection naturelle en cavité et d'écoulements libres de jets : Application à la climatisation d'un local de grand volume.Thèse Doctorat, conservatoire des arts et métiers, Pagination multiple**.**

Launder B. E and Jones.W. P. (1972) The Prediction of Laminarization with a Two-Equation Model of Turbulence». *International Journal of Heat and Mass Transfer,*15, 301-314**.**

Launder B. E. and Spalding D. B. (1974) The numerical computation of turbulent flows. *Computer Methods in Applied Mechanics and Engineering,* 3, 269-289.

Leonard A. (1974) Energy cascade in large-eddy simulations of turbulent fluid flows. *Adv.In Geophysics*, 18, 237-248**.**

Lepers S. (2000) Modélisation des écoulements de l'air dans les bâtiments à l'aide des codes CFD : contribution à l'élaboration d'un protocole de validation .Thèse de doctorat de l'INSA de Lyon**.**

Leonard B. P. (1979) A stable and accurate convective modeling procedure based on quadratic upstream interpolation. *Computer Methods Applied in Mechanical Engineering,* 19, 1, 59-98**.**

Patankar, S. V. (1980). NumericalHeat Transfer and Fluid Flow . *Taylor & Francis,* 978-0-89116-522-4.

RoacheP. J (1982) Computational fluid dynamics. *Albuquerque: Hermosa Publishers,* 446 , (ISBN 0-913478-05-9)**.**

Theodosiu C. (2001) Modélisation des Systèmes Techniques dans le Domaine des Equipements des Bâtiments à l'aide des Codes de type CFD .Thèse Doctorat, l'INSA de Lyon**.**

Versteeg H. K. and Malalasekra W. (1995) *An introduction to computational fluid dynamics. Essex: Longman Scientific & Technical***.**

Campos-Celador, Á., G. Diarce, J. T. Zubiaga, T. V. Bandos, A. M. García-Romero, L. M. López & J. M. Sala (2014) Design of a Finned Plate Latent Heat Thermal Energy Storage System for Domestic Applications. *Energy Procedia,* 48**,** 300-308.

Da Veiga, W. R. 2002. Characteristics of a semicircular heat exchanger used in a water heated condenser pump. Rand Afrikaans University.

Regin, A. F., S. C. Solanki & J. S. Saini (2006) Latent heat thermal energy storage using cylindrical capsule: Numerical and experimental investigations. *Renewable Energy,* 31**,** 2025-2041.

Wang, Y., L. Wang, N. Xie, X. Lin & H. Chen (2016) Experimental study on the melting and solidification behavior of erythritol in a vertical shell-and-tube latent heat thermal storage unit. *International Journal of Heat and Mass Transfer,* 99**,** 770-781.

Abstract

First, the effect of geometrical parameters (tube length and shell diameter) and Reynolds number on the charging and discharging time in terms of HTF outlet temperature are investigated here in a heat storage unit by latent heat. The obtained results reveal that the tube length and the shell diameter are among the most influential geometrical parameters on the melting and solidification time, similarly the Reynolds number has too much effect to speed up the charging cycle. Moreover, an improved thermal storage unit is proposed which contains two phase change materials (PCMs), separated longitudinally inward the shell space and have a close melting point and different thermal characteristics. This configuration is more stable and speeds up the charging and discharging processes compared to the first unit. In addition to that, several unit positions were examined to interpret physically the thermal demeanor of the fusion process in terms of; heat transfer modes estimation, PCM melting rate, axial and radial temperatures distribution. The obtained results clarify that the TES unit inclination according to the range angles [0-90°] makes an imbalance of the natural convection in the PCM liquid fraction which contributes to create an instability and diminution of the heat transfer during the melting process.

Resumé

Tout d'abord, l'effet des paramètres géométriques (longueur du tube et diamètre de la calandre) et le nombre de Reynolds sur le temps de charge et de décharge en termes de température de sortie HTF sont étudiés ici dans une unité de stockage thermique par la chaleur latente. Les résultats obtenus révèlent que la longueur du tube et le diamètre de la calandre comptent parmi les paramètres géométriques les plus influents sur le temps de fusion et de solidification. De même, le nombre de Reynolds a trop d'effet pour accélérer le cycle de charge. En outre, il est proposé une unité de stockage thermique améliorée contenant deux matériaux à changement de phase (MCP), séparés longitudinalement vers l'intérieur de la calandre et présentant un point de fusion proche et des caractéristiques thermiques différentes. Cette configuration est plus stable et accélère les processus de charge et de décharge par rapport à la première unité. En plus de cela, plusieurs positions unitaires ont été examinées pour interpréter physiquement le comportement thermique du processus de fusion en termes de: estimation des modes de transfert de chaleur, taux de fusion PCM, répartition des températures axiales et radiales. Les résultats obtenus expliquent que l'inclinaison de l'unité TES en fonction des angles de portée [0-90 °] crée un déséquilibre de la convection naturelle dans la fraction liquide PCM, ce qui contribue à créer une instabilité et une diminution du transfert thermique pendant le processus de fusion.

ملخّص

أولاً ، قد تم هنا دراسة تأثير المعلمات الهندسية (طول الأنبوب وقطر الغلاف) ورقم (Reynolds) رينولدز على زمن الشحن والتفريغ الطاقة الحرارية بدلالة درجة حرارة خروج HTF في وحدة التخزين الحراري بالحرارة الكامنة. تظهر النتائج أن طول الأنبوب وقطر الغلاف هما من بين أكثر المعلمات الهندسية تأثيرًا على وقت الذوبان والتصلب. وبالمثل ، فإن رقم رينولدز له تأثير كبير على تسريع دورة الشحن. بالإضافة إلى ذلك ، يتم اقتراح وحدة تخزين حرارية محسنة تحتوي على مادتين متغيرتي الطور (PCMs) مفصولان طوليًا بداخل الغلاف ولهما نقطة انصهار قريبة وخصائص حرارية مختلفة. هذا النموذج هو أظهر استقرارًا أكثر وتسريع في عمليات الشحن والتفريغ مقارنةً بالوحدة الأولى(التي تمتلك PCM وحيد). بالإضافة إلى ذلك ، تم فحص عدة مواضع للوحدة لتفسير السلوك الحراري لعملية انصهار الPCM من حيث: تقدير أنماط نقل الحرارة ، معدل انصهار PCM ، توزيع درجة الحرارة المحورية والنصف قطرية. توضح النتائج التي تم الحصول عليها أن ميل وحدة TES لزوايا النطاق [0-90 °] يؤدي إلى خلل في الحمل الحراري الطبيعي في جزء السائل PCM ، مما يساهم في خلق عدم الاستقرار والانخفاض في النقل الحراري أثناء عملية الانصهار.

Periodica Polytechnica
Mechanical Engineering

62(2), pp. 101-109, 2018
https://doi.org/10.3311/PPme.10873

Thermo-convective Study of a Shell and Tube Thermal Energy Storage Unit

Abderrahmane Elmeriah[1*], Driss Nehari[1], Mohamed Aichouni[2]

RESEARCH ARTICLE

Received 19 April 2017; accepted after revision 03 January 2018

Abstract

In this paper, we have studied numerically thermo-convective characteristics between a heat transfer fluid (HTF) and phase change material (PCM) in shell and tube thermal energy storage (TES) unit. The paraffin wax is considered as a PCM, filled in a shell which is thermally isolated with the external environment, while the water plays a role of a HTF and flows inside the tube at the moment of charging and discharging cycle. The heat transfer between HTF and PCM is performed by conduction and forced convection, this transfer allows to change the physical state of PCM solid-liquid to obtain a quantity of storable heat in order to create a thermal battery. Enthalpy formulation is used to analyze the heat transfer during melting and solidification process. A good agreement was found between our numerical predictions and the results of the literature. On the other hand, we have investigated the effect of geometrical parameters (tube length and shell diameter) and Reynolds number on the charging and discharging cycles. The obtained results reveal that the tube length and the shell diameter are the most influential parameters on the time of storage system. Similarly, the Reynolds number has much impact on the HTF outlet temperature and the time of solidification and melting process. Furthermore, we have proposed a new thermal storage unit containing the Paraffin wax and RT60 that it gives us a good rate and time of storage compared to the first unit that has only the paraffin wax.

Keywords

heat transfer fluid, phase change material, latent heat storage, shell and tube

[1] Smart Structure Laboratory, University Center of Ain-Temouchent, 46000 Ain-Temouchent, Algeria

[2] The Engineering College, University of Hail, P.O. Box 2440, Hail, Saudi Arabia

[*] Corresponding author, e-mail: elmeriahabderrahmane@gmail.com

1 Introduction

The problems of energies consumption have aggravated due to the increase of industrial, commercial and residential activities; parallelly, the current technological development suffers from the depletion of fossil energy. In such case, there is a huge need to use renewable energy sources because they represent a good solution to such problems, and among the known renewable energies, the thermal solar remains the most exploited type. As it is unstable along the time (day and night) and due to its periodic nature, we must use a thermal energy storage device in order to ensure the continuity of this energy during the time. Amongst the types of thermal storage systems, there is the thermal latent heat storage based on the use of phase change materials (PCMs) which have advantages such as high storage density. Many numerical and experimental studies were performed on the latent thermal energy storage systems.

From the previous studies of Yang et al. [1] and Trp et al. [2], the thermal storage depends mainly on the HTF inlet velocity (or mass flow rate), HTF inlet temperature, and geometric parameters. Therefore, the choice of the operating conditions and geometric parameters depends on the required heat transfer rate and the time storage in which the energy will be stored or delivered according to Trp et al. [2]. In order to explore the effect of the adequate choice of the PCM, El Qarnia [3] has studied numerically the thermal performance of a solar latent heat storage unit (LHSU) during charging and discharging cycle by using three kinds of PCMs (n-octadecane, Paraffin wax and Stearic acid) as storage mediums. The results showed that a water production at high temperature depends on the careful selection of PCMs. Recently, Tao and Carey [4] have investigated experimentally the effect of PCM thermo-physical characteristics on the performance of shell and tube LHSU in order to improve its performance. The results have showed that the PCM thermo-physical characteristics are the responsible parameters to improve the time and heat transfer of the system. A phase change process dominated by heat conduction in a shell and tube TES unit has been studied experimentally and numerically by solving a developed analytical model by Kibria et al. [5] for a medium temperature of melting. In order to evaluate the time

of solidification and melting process in terms of HTF outlet temperature, various physical and geometric parameters have been conducted. The results revealed that the inlet temperature of HTF and inner diameter of tube have a strong effect on the heat exchange rate during phase change process compared to the impact of HTF mass flow rate and tube thickness.

A numerical and experimental investigation has been carried out by Hosseini et al [6] using the commercial paraffin RT50 (Rubitherm GmbH) as PCM. Their results revealed that a rising of HTF inlet temperature from 70°C to 75 and 80°C at a constant flow rate of 1 L/min allows to increase the theoretical efficiency in charging and discharging process from 81.1% to 88.4% and 79.7% to 81.4% respectively. Recently, an experimental study on the vertical shell and tube latent heat thermal storage (LHTS) unit has been conducted by Wang et al. [7], the erythritol was considered as PCM and the air has been chosen as HTF, which flows downward during charging and discharging cycle. Their results clarify that the increase of the HTF mass flow rate and inlet temperature reduces the charging process time, while the air inlet pressure has a small effect on the heat transfer inside a PCM.

Concerning the geometry of the shell, a comparative study for two-dimensional solidification process was done numerically by Mosaffa et al. [8] between cylindrical shell and rectangular storages LHSU having the same volume and heat transfer area where the air was considered as HTF. On the one hand, it has found that the solidification rate of PCM in cylindrical shell is much better and rapidly compared to the rectangular shape. On the other hand, the low thermal conductivity of PCM limits the heat transfer rate during both charging and discharging processes. In order to enhance the heat transfer exchange during such processes, extended surface (fins) are used. In this sense, Zhang and Faghri [9] investigated numerically the effect of internal longitudinal fins. The authors have demonstrated the effectiveness of the fins to improve the heat transfer, while the melting volume fraction (MVF) can be significantly increased by increasing the thickness, height and number of fins.

On the other hand, Al-Abidi et al. [10] have investigated numerically using the commercial code Fluent 6.3.26 the triplex tube heat exchanger (TTHX). A different effect of geometric parameters were considered, such as the internal and external fins, the fin length, number of fins, and fin thickness, in order to accelerate the melting rate of RT82 as a PCM. The results have shown that these parameters have a significant influence on the thermal behavior of melting process, whereas the effect of fin thickness is small compared to the fin length and number of fins, which have a strong effect on the melting rate time. A numerical study was carried out by Tao et al. [11] for phase change thermal energy storage (PCTES) unit used in a dish solar thermal system for high temperature storage.

The effect of the enhanced tubes has been studied on the behavior of PCM melting by adopting three enhanced tubes, namely dimpled tube, cone-finned tube and helically-finned tube. The results show that compared with the smooth tube, all of the three enhanced tubes could improve the PCM melting rate. Among the previous works, the TES unit of Kibria et al. [5] could be useful to be investigated using numerical modeling, in order to improve it by proposing several configurations. In this sense, a two-dimensional and axisymmetric physical model was used to investigate the effect of the physical and geometric parameters not considered by the last authors such as the tube length, shell inner diameter and Reynolds number variation; parameters that were not considered earlier by Kibria et al. [5] would contribute to improve the thermal performance of the energy storage unit. Moreover, an improved thermal storage unit is proposed which contains two phase change materials (PCMs), separated longitudinally inward the shell space and have a close melting point and different thermal characteristics.

2 Mathematical model

The PCTES unit under investigation is shown in Fig. 1. Two different configurations of this unit were studied: (I) shell-and-tube system with paraffin wax; and (II) shell-and-tube system with paraffin wax and RT60. The first configuration consists of a shell-and-tube configuration (see Fig. 1.a) that has been used previously by Kibria et al. [5]. The inner tube is made of copper. Distilled water flows through the inner tube as HTF. The phase change material (paraffin wax) fills the annular space. The outer surface of the storage unit is well insulated. The second system shown in Fig. 1(c) is similar to the first configuration concerning the inner tube, HTF used and the outer surface of the storage, but two different phase change materials namely the paraffin wax and RT60 separated by a second tube of copper are used. As the problem under examination is axisymmetric, a schematic 2-D computational domain for all investigated cases is presented for both configuration in the plots Fig. 1(b) and Fig. 1(d). Since the same geometry of Kibria et al. [5] was considered here, the same hypothesis, boundary and initial conditions are adopted in the present study:

(i) The thickness of the inner tube wall is considered;
(ii) The thermo-physical properties of HTF and PCM are constant with respect to the temperature;
(iii) The initial temperature of the latent thermal storage unit is uniform;
(iv) HTF flow is laminar;
(v) Natural convection inside the Paraffin wax was not considered, as the considered shell and tube thermal energy storage unit used is horizontal.

During the charging cycle, the HTF flows inside the tube by inlet temperature of 88°C and a mass flow rate of 0.072 kg/min. On the other hand, during the discharging after storage, we took the heat stored using cold HTF passage by a temperature

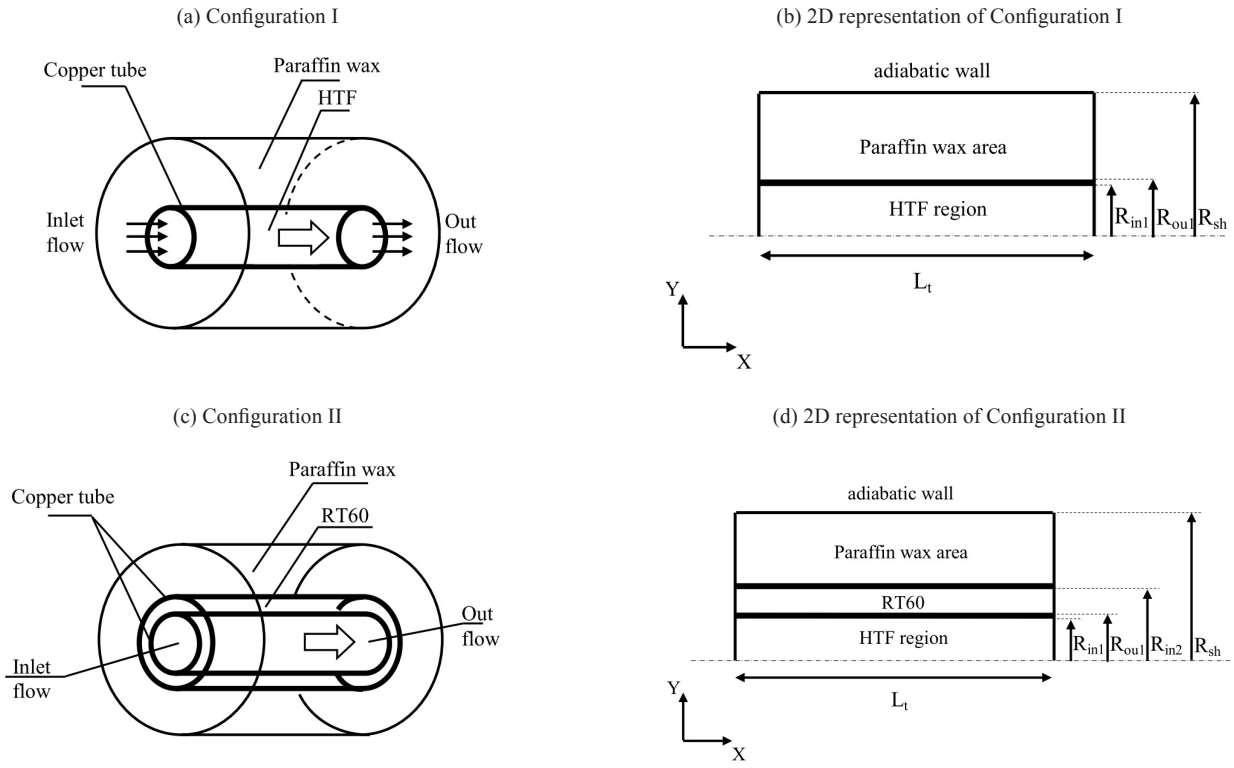

Fig. 1 Latent heat storage unit

of 25°C and a mass flow rate of 0.07 kg/min as used in the experimental work of Kibria et al. [5]. The thermo-physical properties of phase change materials with water as HTF which are used in the present investigation are shown in Table 1. This two-dimensional problem is governed by unsteady energy and Navier-stokes equations:

The continuity:

$$\frac{\partial}{\partial x_i}\left(\rho u_i\right)=0$$

The momentum:

$$\frac{\partial}{\partial t}\left(\rho u_i\right)+\frac{\partial}{\partial x_i}\left(\rho u_j u_i\right)=\mu\frac{\partial^2 u_i}{\partial x_i \partial x_j}-\frac{\partial p}{\partial x_i}+S_i$$

The energy:

$$\frac{\partial}{\partial t}\left(\rho h\right)+\frac{\partial}{\partial x_i}\left(\rho u_i h\right)=\frac{\partial}{\partial x_i}\left(k\frac{\partial T}{\partial x_i}\right)+S_h$$

Where ρ is the density, k denotes the thermal conductivity, μ is the dynamic viscosity, S_i and S_h are the source terms, u_i is the velocity component in the i-direction, x_i is a cartesian coordinate and h is the specific enthalpy.

The sensible enthalpy h_S is given by:

$$h_s=h_{ref}+\int_{T_{ref}}^{T}C_p dT$$

And the total enthalpy, H is defined as

$$H=h_s+\Delta H$$

Where $\Delta H=\gamma L$ is the enthalpy change due to phase change, h_{ref} is the reference enthalpy at the reference temperature T_{ref}, C_p is the specific heat, L is the specific enthalpy of melting (liquid state) and γ is the liquid fraction during the phase change which occur over a range of temperatures $T_{solidus} < T < T_{Liquidus}$ defined by the following relation 6.(a,b,c):

Table 1 Thermo-physical properties of PCMs and HTF [12-14]

PCM	Density [kg/m^3]		Specific heat [J/kg K]		Latent heat [J/kg]	Thermal conductivity [W/ m · K]		Dynamic viscosity [N s/m^2] or [kg/m s]		Melting Temperature [°C]
	Solid	Liquid	Solid	Liquid		Solid	Liquid	Solid	Liquid	
Paraffin wax	910	790	2000	2150	190000	0.24	0.22	—	0.004108	61
RT60	880	770	2660	2340	123506	0.2	0.2	—	0.00003705	53~61
Heat transfer fluid (HTF)										
Water at 25°C	997		4179			0.613		0.000855		0
Water at 88°C	967.1		4203			0.674		0.000324		

If:

$$\begin{cases} T < T_{solidus}\left(solid\ \ state\right): \gamma = \dfrac{\Delta H}{L} = 0 \left(a\right) \\ T_{solidus} < T < T_{liquidus}\left(Mushy\ \ state\right): 0 < \gamma = \dfrac{\Delta H}{L} < 1 \left(b\right) \\ T > T_{liquidus}\left(liquid\ \ state\right): \gamma = \dfrac{\Delta H}{L} = 1 \left(c\right) \end{cases}$$

3 The Numerical method and the grid used

The governing equations are solved by using the commercial code FLUENT 17 with the first order implicit scheme for the time and the second order upwind scheme for the space. Moreover, the SIMPLE algorithm is used.

The local criterion for numerical convergence, i.e. the maximum relative difference between two consecutive iterations is imposed less than 10^{-6}. The computational grids in the (xy) plane have been obtained using the non-uniform Quadratic elements type of mesh to simulate the axisymmetric geometry. These structured quadratic cells are created with fine mesh near the walls using mesh generation software ANSYS GAMBIT 2.4.6.

A dense grid distribution is employed near the wall while a uniform grid distribution is used in the streamwise direction. The plots of Fig. 2.a and Fig. 2.b show the typical grid distribution over the computational domain of the configurations I and II. The accuracy of the solution depends on the number and the size of the cells. The grid size used in the computations is chosen by performing a grid independence study (see Fig. 3).

(a) A part of the grid for conf I

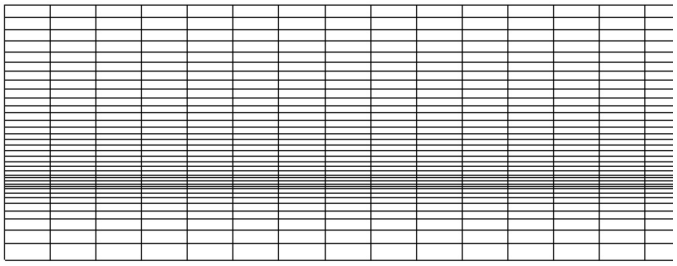

(b) A part of the grid for conf II

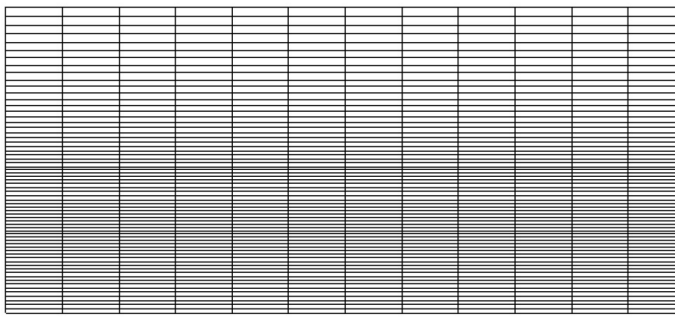

Fig. 2 The grid used in first (I) and second (II) configuration

For the first configuration, several meshes were tested to ensure that the solution was independent of the mesh (35x300; 50x300; 65x300). This test indicated that 35×300 cells are adequate. On the other hand, concerning the second configuration (Case A and B) the analysis of the grid independency made for the grid tests (50x300; 65x300; 85x300) indicate (not shown here) that 65×300 cells are adequate. From above we can say that the grid (35x300) is suitable for the first configuration and the grid (65x300) is convenient for the second configuration.

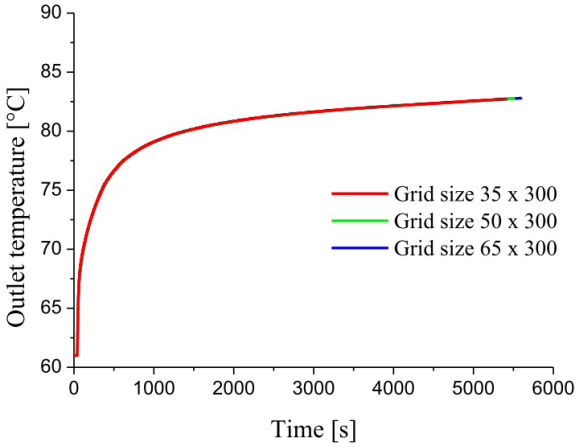

Fig. 3 Outlet temperature in charging cycle in different grid size of configuration I

4 Results and discussion

Before performing the study of parameters effect on the thermal storage, the validation of the numerical results was performed in charging and discharging cycle through a comparison with the experimental and numerical results of Kibria et al. [5] for the parameters presented in Table 2.

Table 2 Geometric parameters of the configuration I (configuration of Kibria et al. [5])

The inner radius of tube 1	(R_{in1})	[m]	0.0054
The outer radius of tube 1	(R_{ou1})	[m]	0.006
The radius of the shell	(R_{sh})	[m]	0.018
The length of tube	(L_t)	[m]	1
Thickness of tube 1		[m]	0.0006

4.1 Validation

The validation was performed on the evolution of HTF outlet temperature at the charging and discharging cycle. The comparison between our numerical results in relation to the analytical and experimental results of Kibria et al. [5] showed a good agreement in Fig. 4.

At the charging cycle, the PCM is initially at solid state (at the temperature 61°C) and the HTF circulates with inlet temperature equal to 88°C, following the boundary and initial conditions of Kibria et al. [5]. The HTF outlet temperature increases over time until asymptotic value of 83°C which is lower than the inlet temperature (88°C). This difference is due to the heat absorption by melting Paraffin wax. The results show

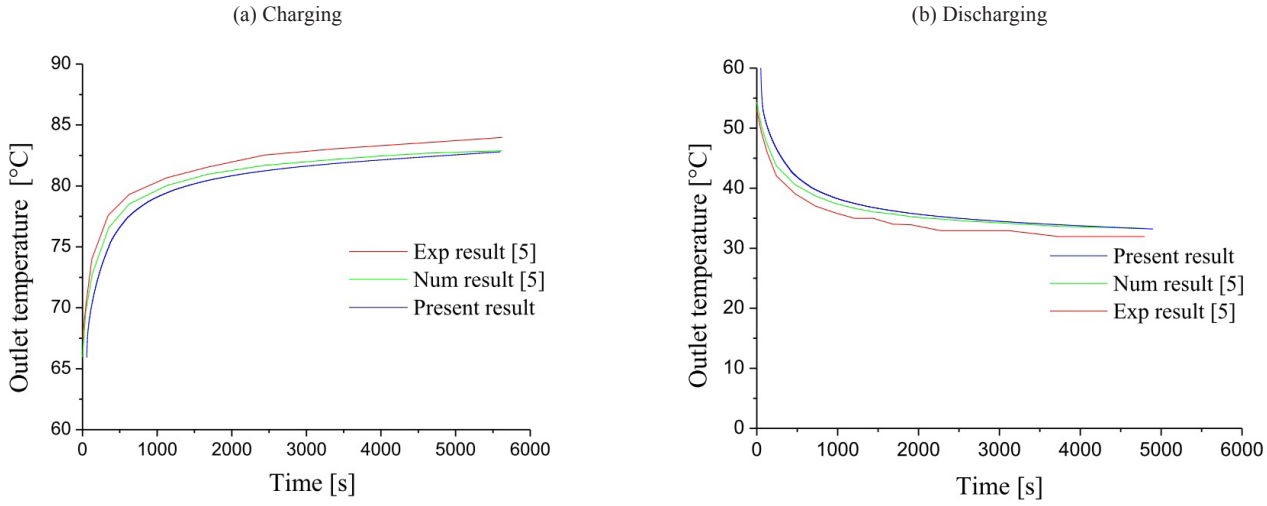

Fig. 4 Validation of HTF outlet temperatures in charging and discharging cycle

that the outlet temperature of system is close to those obtained analytically and experimentally by Kibria et al. [5], where this process took about 6500s to complete the charging cycle. In discharging process, the HTF absorbs the heat stored in the Paraffin wax whereas the HTF outlet temperature decreases over time until asymptotic value 33°C and the paraffin wax becomes in the solid state. The small discrepancy between the numerical results and those obtained experimentally is due to the simplifications considered in the numerical model. Further validations (not shown here) done for several parameters give a good agreement with the numerical and experimental data of the literature [5].

4.2 Parametric study

In this investigation, we have made a parametric study following the measures of the first configuration (Table 2) based to examine the effect of: (i) length of tube; (ii) shell diameter; and (iii) Reynolds number on the time and rate of charging and discharging process. Furthermore, we have tried to propose a new thermal unit composed of a Paraffin wax and RT60. The performances of this new configuration will be compared to the first one.

4.2.1 Influence of tube length

Fig. 5 shows the effect of different tube length L_t on the thermal performance during the charging and the discharging cycles. Considering the first configuration, we have changed the tube length in the range 0.2-1.8m in the scope to quantify this effect for the charging and discharging cycles. From this figure which depicts outlet temperature of HTF versus the tube length variation in the range 0.2-1.8m. We can see that the time of charging and discharging cycles is proportional to the tube length. An increase of the length leads to an increase of the melting and solidification time. Moreover, the increase of tube length decreases the asymptotic value of the HTF outlet temperature from 87°C in the case L_t=0.2m to 79°C in the case L_t=1.8m during 5600s. This leads to a gradient of temperature ΔT_{ch} equal to 8°C between HTF outlet temperatures of tube

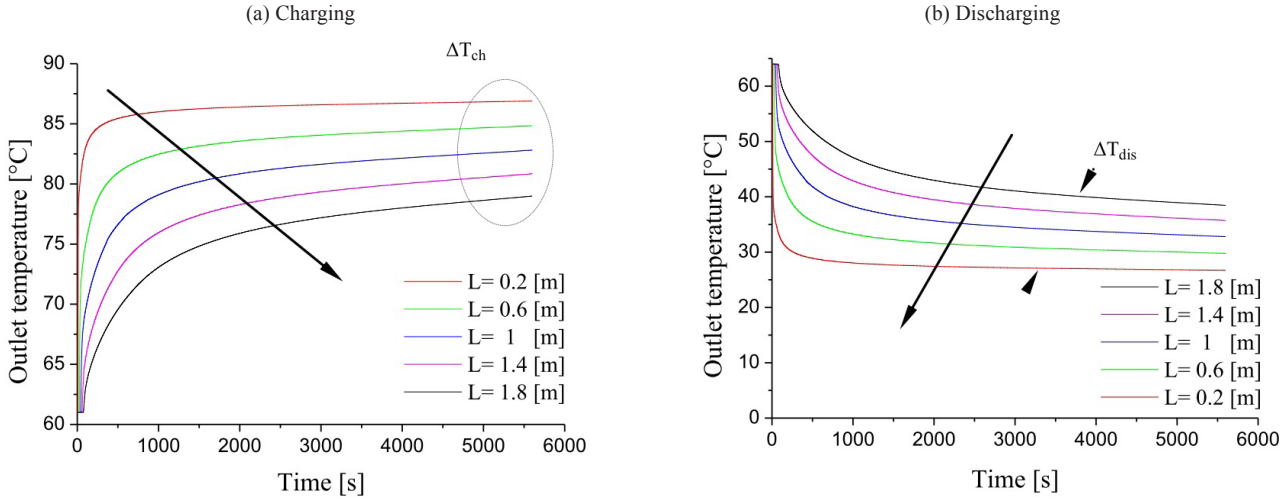

Fig. 5 Effect of tube length in charging and discharging cycle

length from 0.2m to 1.8m at charging time. With regard to the discharging process and the effect of increasing the tube length, the asymptotic value of the HTF outlet temperature increases from 25°C to 38.5°C along the 5600s, thus leading to a gradient of temperature ΔT_{dis} equal to 13.5°C. From this figure, it can be seen that the tube length is an important parameter to optimize the melting and solidification time.

4.2.2 Effect of shell diameter

The shell diameter is among the important parameters that have a relation with the progress of solidification and melting. In this case we have changed the shell diameter in the range 24-44 mm. Fig. 6 shows that the shell diameter reduction allows to complete the discharging and charging rate in a short time. The reduction of shell diameter causes the minimizing of the PCM mass volume. This allows accelerating the heat charging or discharging of the mass through heat transfer process. This contributes to speed up the melting fraction rate of the Paraffin wax during charging process.

It can be seen from the figure, that the shell diameter of 24 mm needs just 3300s to complete almost the charging or the discharging processes, whereas the other cases needed more than 5000s to complete the fully charging or discharging processes. As a result, the gradient in HTF outlet temperature between the shells of minimum and maximum diameter used ΔT_{ch} is equal to 5°C for charging process and ΔT_{dis} is about 8°C for discharging process. Therefore, the quantity of Paraffin wax must be appropriate with the work conditions, in order to optimize the time of storage system.

4.2.3. Effect of Reynolds number

As we know, the Reynolds number depends on the HTF properties as the viscosity, velocity, and the size of the tube. In the present investigation, only the laminar regime is considered for the flow of HTF. In this contribution, the effect of Reynolds number is investigated in the range Re= 100-1500. The increase of Reynolds number allows to decrease the solidification and melting time as shown in the Fig. 7. It is clear from this figure, that for the charging cycle and for the high value of Reynolds number (Re=1500) the HTF outlet temperature tends to reach the asymptotic value of 86.5 °C, while for the lower value of Reynolds number (100), the HTF outlet temperature tends to reach the asymptotic value of 69.5°C. Therefore, the temperature gradient ΔT_{dis} of HTF outlet temperature in discharging cycle is about 9.6°C and in the charging case ΔT_{ch} is 17°C.

4.2.4 Improvement of TES unit

According to the above results, it could be very useful to find an effective way that allows the PCM to absorb the maximum heat provided by the HTF. As a result, we have tried to propose a new configuration (Fig. 1(d)), where we inserted a layer of another phase change material namely the RT60, that its melting temperature is equal to 57 °C, which is very close to melting temperature of the paraffin wax (equal to 61 °C). This layer of RT60 makes it possible to distribute the thermal load on the paraffin wax along the axial direction and to ensure it the thermal inertia. In this TES unit, the two PCMs are superposed between the copper tubes. Therefore, the heat exchange in this unit is done by conduction in two steps; (i) heat interchange between HTF and RT60 through the first copper tube, (ii) heat transfer from the RT60 into the paraffin wax through the second copper tube. The same boundary and initial conditions adopted in the first configuration are used here. Different cases according to Table 3 and Table 4 are numerically predicted. The melting temperature of RT60 is lower than the paraffin wax (61°C), which allows the RT60 to melt before the paraffin wax, which leads to accelerate the melting process of RT60 and its solidification process due to its rapid heat absorption from the HTF.

In this configuration we proposed two cases A and B. The case A (see Table 3) has a constant radius of the shell R_{sh} and a variable inner radius of the second tube R_{in2} that consequently reduces the volume of Paraffin wax. This radius is varied in the

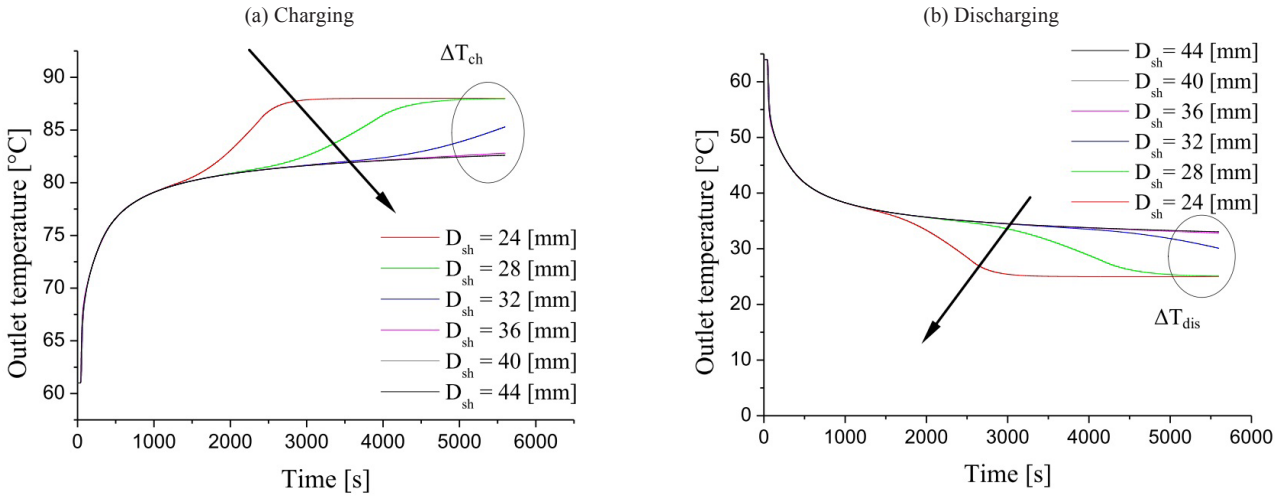

Fig. 6 Effect of shell diameter in charging and discharging cycle

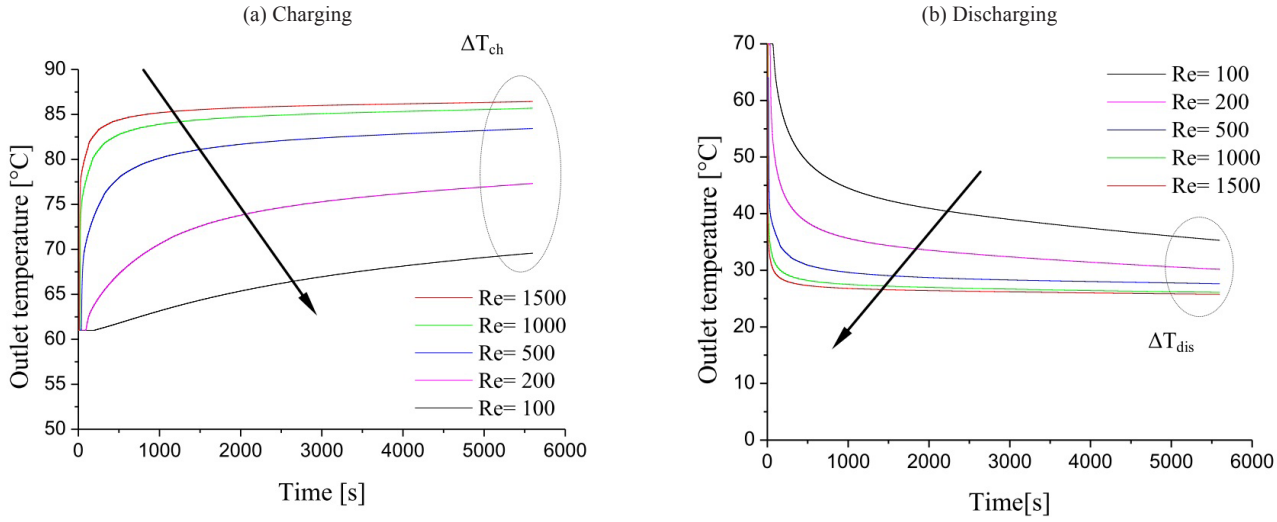

Fig. 7 Effect of Reynolds number in charging and discharging cycle

Table 3 Geometric parameters of the second configuration II.A

The inner radius of tube 1	(R_{in1})	[m]	0.0054			
The outer radius of tube 1	(R_{ou1})	[m]	0.006			
The inner radius of tube 2	(R_{in2})	[m]	0.008	0.01	0.012	0.014
The radius of the shell	(R_{sh})	[m]	0.018			
The length of tube	(L_t)	[m]	1			
The thickness of copper tube 1 and 2		[m]	0.0006			

Table 4 Geometric parameters of the second configuration II.B

The inner radius of tube 1	(R_{in1})	[m]	0.0054			
The outer radius of tube 1	(R_{ou1})	[m]	0.006			
The inner radius of tube 2	(R_{in2})	[m]	0.008	0.01	0.012	0.014
The radius of the shell	(R_{sh})	[m]	0.01902	0.02001	0.02114	0.02239
The length of tube	(L_t)	[m]	1			

range 0.008-0.014m. The variation of the inner radius allows us to obtain several proportions in the volume of the two PCMs, from the case the existence of only the Paraffin wax to the case we obtain the Paraffin wax with RT60 (R_{in2}= 0.014m). The results shown in Fig. 8 indicate a decrease in the time of charging and discharging cycles compared to case of the first thermal storage unit (containing only Paraffin wax), whereas the temperature gradient ΔT_{ch} of the HTF outlet temperature in charging cycle increases in the first time period [0-1500s], then starts to decline. Near the time 4000s, we remark an increase of the outlet temperature and ΔT_{ch}. This is due to the PCMs which have achieved the total phase change from the solid to liquid and we are in sensible phase of heat transfer. In case B (Table 4), we have fixed the volume of Paraffin wax (same volume of the first configuration) and we have varied the inner radius of the second tube R_{in2} from 0.008 to 0.014m, which means the shell radius will vary. In this case the time of charging and discharging cycle also decreases compared to the use of a Paraffin wax alone as presented in Fig. 9. This case is more stable in charging and discharging cycles than case A, as the mass volume of the PCMs of the case B is increased compared to the first case A. However, both cases have a better evolution of the HTF temperature than the paraffin wax alone as shown in Fig. 8 and Fig. 9.

5 Conclusion

As the appropriate choice of the physical and geometric parameters allows to optimize the thermal storage unit, the present study was devoted to examine the effect of these parameters on the shell and tube thermal energy storage unit that investigated previously by Kibria et al. [5]. Moreover, improvements of this storage unit were investigated through new configurations. A two-dimensional numerical method based on the Enthalpy formulation has been used to predict the heat transfer between HTF and PCM. The laminar forced convection inside the tube during charging and discharging process was considered, whereas the natural convection has been ignored inside the PCM enclosure.

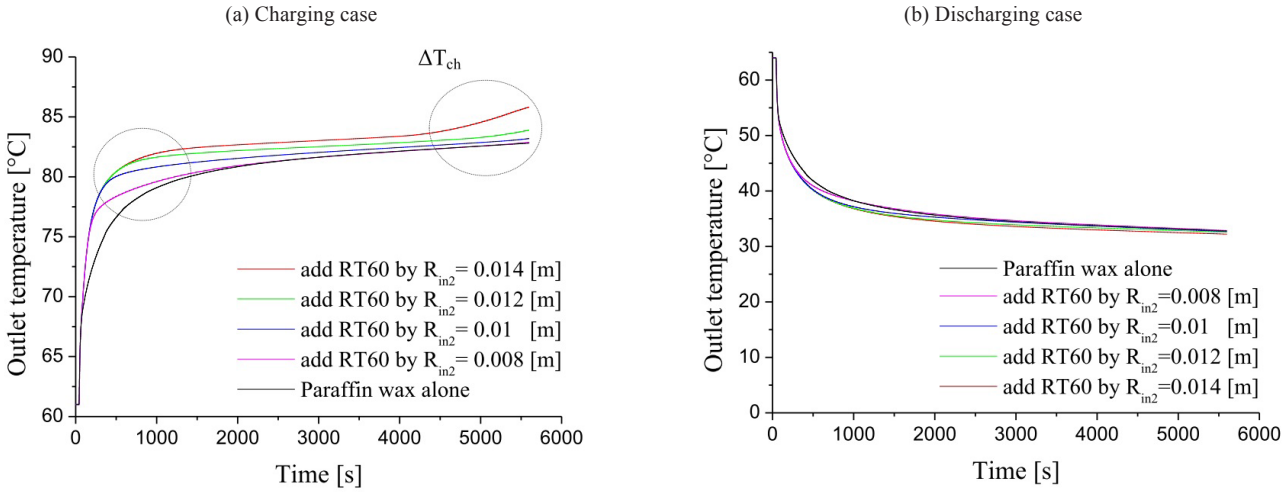

Fig. 8 Charging and discharging cycle of the second configuration II.A

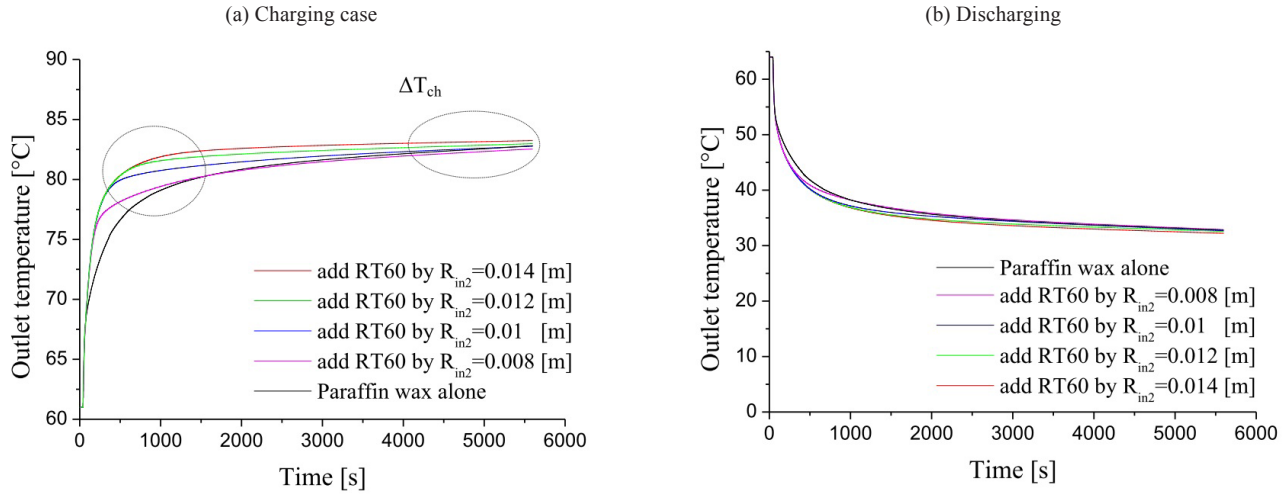

Fig. 9 Charging and discharging cycle of the second configuration II.B

A parametric study has been conducted in order to study the effect of the tube length, shell diameter and Reynolds number. Improvement of the thermal performances of this unit was proposed and investigated.

The results of the parametric study have shown that the tube length and shell diameter have a great effect on the HTF outlet temperature, moreover the Reynolds number is the most influential parameter which has an impact on the time and rate of solidification and melting process.

From the present results, the design parameters should be selected carefully in order to optimize the performance of the storage unit. In addition to that, the new thermal energy storage unit filled by RT60 and Paraffin wax allowed for better efficiency of the rate storage and HTF outlet temperature compared to the unit containing only the Paraffin wax.

Acknowledgments

This work was carried out in the Laboratory of Smart Structure; the authors would like to acknowledge the support of the university center of Ain-Temouchent.

References

[1] Yang, X., Li, Y., Lu, Z., Zhang, L., Zhang, Q., Jin, L. "Thermal and Fluid Characteristics of a Latent Heat Thermal Energy Storage Unit." *Energy Procedia*. 104, pp. 425-430. 2016. https://doi.org/10.1016/j.egypro.2016.12.072

[2] Trp, A., Lenic, K., Frankovic, B. "Analysis of the influence of operating conditions and geometric parameters on heat transfer in water-paraffin shell-and-tube latent thermal energy storage unit." *Applied Thermal Engineering*. 26(16), pp. 1830-1839. 2006. https://doi.org/10.1016/j.applthermaleng.2006.02.004

[3] El Qarnia, H. "Numerical analysis of a coupled solar collector latent heat storage unit using various phase change materials for heating the water." *Energy Conversion and Management*. 50 (2), pp. 247-254. 2009. https://doi.org/10.1016/j.enconman.2008.09.038

[4] Tao, Y. B., Carey, V. P. "Effects of PCM thermophysical properties on thermal storage performance of a shell-and-tube latent heat storage unit." *Applied Energy*. 179, pp. 203-210. 2016. https://doi.org/10.1016/j.apenergy.2016.06.140

[5] Kibria, M. A., Anisur, M. R., Mahfuz, M. H., Saidur, R., Metselaar, I. H. S. C. "Numerical and experimental investigation of heat transfer in a shell and tube thermal energy storage system." *International Communications in Heat and Mass Transfer*. 53, pp. 71-78. 2014. https://doi.org/10.1016/j.icheatmasstransfer.2014.02.023

[6] Hosseini, M. J., Rahimi, M., Bahrampoury, R. "Experimental and computational evolution of a shell and tube heat exchanger as a PCM thermal storage system." *International Communications in Heat and Mass Transfer*. 50, pp. 128-136. 2014. https://doi.org/10.1016/j.icheatmasstransfer.2013.11.008

[7] Wang, Y., Wang, L., Xie, N., Lin, X., Chen, H. "Experimental study on the melting and solidification behavior of erythritol in a vertical shell-and-tube latent heat thermal storage unit." *International Journal of Heat and Mass Transfer*. 99, pp. 770-781. 2016. https://doi.org/10.1016/j.ijheatmasstransfer.2016.03.125

[8] Mosaffa, A. H., Talati, F., Basirat Tabrizi, H., Rosen, M. A. "Analytical modeling of PCM solidification in a shell and tube finned thermal storage for air conditioning systems." *Energy and Buildings*. 49, pp. 356-361. 2012. https://doi.org/10.1016/j.enbuild.2012.02.053

[9] Zhang, Y., Faghri, A. "Heat transfer enhancement in latent heat thermal energy storage system by using the internally finned tube." *International Journal of Heat and Mass Transfer*. 39 (15), pp. 3165-3173. 1996. https://doi.org/10.1016/0017-9310(95)00402-5

[10] Al-Abidi, A. A., Mat, S., Sopian, K., Sulaiman, M. Y., Mohammad, A. T. "Internal and external fin heat transfer enhancement technique for latent heat thermal energy storage in triplex tube heat exchangers." *Applied Thermal Engineering*. 53 (1), pp. 147-156. 2013. https://doi.org/10.1016/j.applthermaleng.2013.01.011

[11] Tao, Y. B., He, Y. L., Qu, Z. G. "Numerical study on performance of molten salt phase change thermal energy storage system with enhanced tubes." *Solar Energy*. 86 (5), pp. 1155-1163. 2012. https://doi.org/10.1016/j.solener.2012.01.004

[12] Regin, A. F., Solanki, S. C., Saini, J. S. "Latent heat thermal energy storage using cylindrical capsule: Numerical and experimental investigations." *Renewable Energy*. 31(13), pp. 2025-2041. 2006. https://doi.org/10.1016/j.renene.2005.10.011

[13] Campos-Celador, Á., Diarce, G., Zubiaga, J. T., Bandos, T. V., García-Romero, A. M., López, L. M., Sala, J. M. "Design of a Finned Plate Latent Heat Thermal Energy Storage System for Domestic Applications." *Energy Procedia*. 48, pp. 300-308. 2014. https://doi.org/10.1016/j.egypro.2014.02.035

[14] Da Veiga, W. R. "Characteristics of a semicircular heat exchanger used in a water heated condenser pump." PhD Thesis, Rand Afrikaans University, South Africa. 2002.